# Eindhoven University of Technology Netherlands

Department of Electrical Engineering

# Spatial Distribution of Traffic in a Cellular Mobile Data Network

by
J.P.M.G. Linnartz

Eindhoven University of Technology Research Reports

EINDHOVEN UNIVERSITY OF TECHNOLOGY

# SPATIAL DISTRIBUTION OF TRAFFIC IN A CELLULAR MOBILE DATA NETWORK

by

J.P.M.G. Linnartz

Eindhoven

February 1987

*This report was accepted as a M.Sc. Thesis by*
*Prof.Dr. J.C. Arnbak, Telecommunications Group,*
*Department of Electrical Engineering,*
*Eindhoven University of Technology, The Netherlands (\*).*
*The work was performed in the period from December 1985*
*to October 1986.*


*(\*) Presently: Telecommunications Laboratory,*
*Department of Electrical Engineering,*
*Delft University of Technology,*
*The Netherlands*

## Abstract

The position of a mobile terminal has a significant influence on
its probability to capture the central receiver in the base station
of a cellular radio system using slotted ALOHA for multiple access.
Integral transforms of the probability density function for the
received power prove a useful tool for analysing the relation
between the spatial distributions of offered and throughput packet
traffic in a mobile radio network with Rayleigh fading channels.

A newly developed method to obtain the spatial distribution of
throughput traffic from a prescribed spatial distribution of
offered traffic is presented and illustrated with examples.
Incoherent and coherent addition of interference signals is
considered. The channel behaviour for heavy traffic loads is
studied. In both the incoherent and coherent case, the spatial
distribution of offered traffic required to ensure a prescribed
spatially uniform throughput is synthesised numerically.

TABLE OF CONTENTS

## LIST OF SYMBOLS

Only frequently used symbols are contained in this list

| symbol | | equation |
|---|---|---|
| $f_X(x)$ | probability density function of random variable X | |
| $F_{z,n}$ | capture probability given $Z_0$ and n | 4.48 |
| $g(v)$ | Laplace image of the area mean power pdf | 4.1 |
| G | total offered traffic (packets per slot= pps) | 1.9 |
| $G(\rho)$ | offered traffic per unit area and per slot | sec 1.4.2 |
| $G_0$ | uniform offered traffic distribution in unit circle | 5.22 |
| | N.B. in some special cases: traffic per unit area | 4.28 |
| $I_{z,n}(\rho)$ | capture probability, given $Z_0$, n and $\rho$ | 4.49 |
| n | number of interferers in the test time slot | 1.1 |
| $P_{-s}$ | actual value of the test packet power | 2.1 |
| $P_s$ | area mean value of the test packet power | 1.8 |
| $P_{-n}$ | actual value of the joint interference power | sec 2.2 |
| $P_n$ | mean value of the joint interference power | sec 2.2 |
| $R_n$ | probability of n contenders in the test time slot | 1.1 |
| $s(v)$ | image of throughput traffic | 6.11 |
| S | total throughput traffic | 1.10 |
| $S(\rho)$ | throughput traffic per slot and per unit area | sec 1.4.2 |
| $S_0$ | uniform traffic throughput distribution per unit area | 3.1 |
| $S_\infty$ | throughput traffic if the total offered traffic is increased without limit | sec 5.5 |
| $t_w$ | synchronisation window | 1.4 |
| v | argument of the image functions $(\text{watt}^{-1})$ | 4.1 |
| $W_z(\cdot)$ | traffic weighting function in incoherent analysis | 5.7 |
| $Z_n$ | receiver threshold in the event of n interferers | 1.4 |
| $Z_0$ | universal receiver threshold | 5.3 |
| $\beta$ | path loss exponent | 1.5 |
| $\epsilon$ | small distance from the base station antenna | 5.32 |
| $\mu_k$ | k-th moment of mean power pdf | 4.9 |
| $\rho$ | normalised distance between terminal and base station | 1.8 |
| $\tau$ | packet duration | sec 1.3 |
| $\upsilon_k$ | k-th moment of instantaneous power pdf | sec 4.2.1 |
| $\phi(v)$ | Laplace image of instantaneous power pdf | 4.36 |

N.B.  $g^n(v)$   n-th power of the function g(v)
       $g^{(k)}(v)$   k-th derivative of the function g(v)

1    INTRODUCTION TO CELLULAR DATA COMMUNICATION

1.1    Mobile data communication

Most of today's mobile radio systems offer analogue (speech)
communication facilities. However, in land-mobile radio, messages
are often short and stereotyped. Most user categories require
message lenghts of approximately 15 seconds, except in the taxi
service (with shorter messages-about 8 sec) and some services with
longer messages [21]. For many of these categories, introduction of
transmission of digital (non-voice) messages is a result of an
increased demand for mobile radio and the need to use the radio
spectrum more efficiently. Data messages can be sent more quickly
and reliably, with less operator involvement. For example, names
and addresses are notoriously difficult to receive correctly with
speech and usually involve the operator in repetitions and errors.
With data communication, new facilities are possible, such as
vehicle printers and automatic repetition of messages if the driver
has been away from the vehicle. Coding and processing of messages
become possible, too.
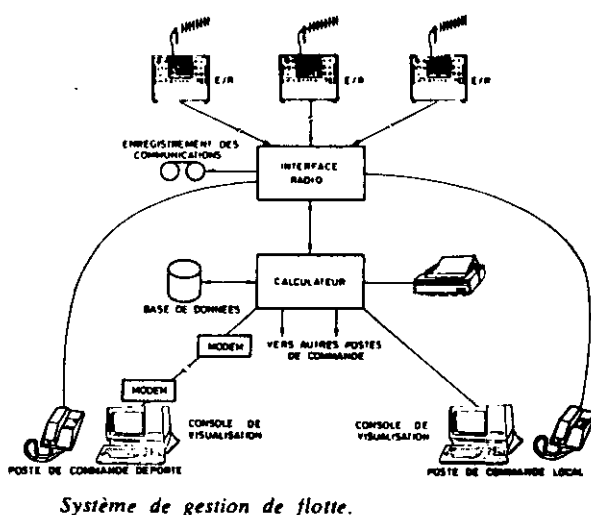


Figure 1.1: Example
of a typical fleet
management system [33].

Système de gestion de flotte.

Direct access to a control computer can enable a fleet of vehicles
to operate more efficiently [33]. Figure 1.1 gives an example of
the fleet management system of the Paris bus service RATP,
installed in 1974. Many mobile users are interested in data stored
in computer files. Radio communication has emerged as a flexible
method for providing remote terminal access to computers.

Packet radio technology [22] [3] offers a highly efficient way of sharing a multiple access radio channel among a potentially large number of mobile subscribers, for instance to support computer communications or to provide local distribution of information. Data from each user is buffered, address and control information is added in a "header", and the resulting bit sequence, or "packet", is transmitted over the shared radio channel.

Although in many cases the more powerful facilities offered by data systems may seem attractive, it is often difficult to make a real case to justify the extra cost. However this picture is changing as an increasing number of users complain about congested channels and so begin to experience a loss in efficiency while waiting for a channel to become available.


## 1.2    Multiple access

In a mobile communication service with many users with "bursty" messages, some kind of collision-type multiple access is unavoidable. The call request and set-up signalling channel of a mobile telephone service is a typical example of such a data channel.   Preller and Koch [20] reported on the MATS-E telephone system, where one control channel is assigned to the base station (BS) on which all functions emanating from (or directed toward) the many mobile stations (MS's) in the cell are handled concurrently. Digital dialogue initiation by a MS leads to one of the most severe problems of control-channel design, because of the vast need for access capacity to serve the randomly occuring, numerous and different service functions initiated by MS's. Message collisions can result in limited channel throughput, and simulation efforts are used to optimise the access capacity.
Channel protocols for packet radio described by Sinha and Gupta [22] reduce the collision problem by carrier-sense methods.
Basic properties of many multiple access schemes can be understood by reducing the collision-type channel to its elementary form: the ALOHA-system.

## 1.2.1   The ALOHA-system

The simplest possible solution to the multiple access problem is
employed. Each user transmits over the packet broadcasting channel
in a completely unsynchronised manner. All active terminals are
assumed to transmit their messages to a single receiver over a
common channel in packets of duration τ, regardless of the activity
of competing terminals. If each individual user of the common
channel is required to have a low activity, the probability of a
packet from one user interfering with a packet from another user is
small as long as the total number of users is not too large.
As the number of users increases, however, the number of packet
overlaps increases and the probability that a packet will be lost
due to an overlap also increases. In figure 1.2 we show a packet
broadcasting channel with two overlapping packets.



Packets from a typical user.

Packets from several users on an ALOHA channel.
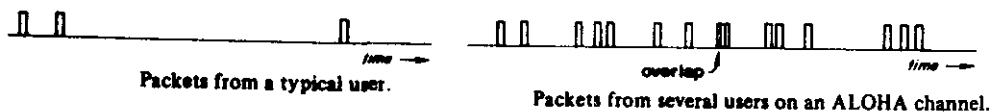
Figure 1.2: Packets offered to the multiple access channel [3].

An unsuccessful packet will be retransmitted after waiting a random
period of time. The multiple-access system is memoryless, i.e., a
retransmitted packet experiences overlaps uncorrelated with its
previous attempts to capture the receiver.

Additional aspects of the ALOHA-system studied in this thesis are
slotted transmission of packets and the fact that a collision of
packets does not always lead to loss of all messages involved.

## 1.3   Slotted ALOHA and capture effect

In slotted ALOHA, the only network discipline imposed on
transmitters is that all dispatched packets must fit into common
timeslots of length τ. If messages conflict they will overlap
completely rather than partially. Compared with unslotted ALOHA,
this strategy thus yields an increased throughput of the channel
[3].

## 1.3.1 Channel throughput

Let the number of packets generated in the network be Poisson distributed. The probability of an arbitrary test packet being overlapped by n other packets is then [43]

$$R_n = \frac{G^n}{n!} \exp\{-G\}, \tag{1.1}$$

with G the mean offered total channel traffic expressed in packets per time slot. The pessimistic assumption made in studies of standard ALOHA [44] networks is that any overlap of packets invariably leads to mutual destruction of all n+1 packets present in that slot. In this event the probability for a test packet to capture the receiver becomes

$$P_{capt} = R_0 = 1 - \sum_{n=1}^{\infty} R_n. \tag{1.2}$$

The total traffic throughput S can be found from [3][44]

$$S = G P_{capt} = G e^{-G}, \tag{1.3}$$

which is illustrated in figure 1.3.
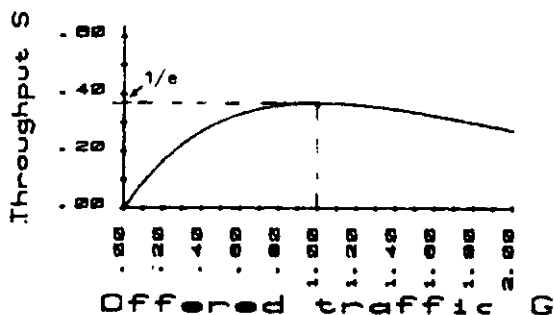


Figure 1.3: Throughput S as a function of the offered traffic G for slotted ALOHA.

Metzner [2] has shown that intentional division of the users in two categories: users transmitting at high power ("loud talkers") and users transmitting at low power ("quiet talkers"), increases the capacity of the multiple access system, as a packet of a loud talker survives a collision with packets from quiet talkers.

Namislo [24] has studied the dynamic behaviour of an ALOHA multiple access system where not all packets experiencing collisions are lost, using a Markov chain model. He demonstrated that the differences in received power between various packets (due to fading and path loss), increase channel capacity and that the system can be very stable under overload. Kuperus and Arnbak [35] studied the throughput properties of the mobile ALOHA channel with the offered traffic distributed in a circular tape centered on the base station receiver. Numerical results show that fading "softens" the channel compared with the contentions of pure ALOHA. The probability of destruction of a packet is modelled as the probability that the signal to interference ratio (SIR) exceeds a certain limit [1] [13] [35].

## 1.3.2    Capture effect

We shall assume a radio receiver which can be captured by a test packet in the presence of n interfering packets, if the power of the former $(P_s)$ sufficiently exceeds the joint interference power $(P_n)$ during a certain section (the sync. window, of duration $t_w$) of the timeslot $\tau$. Consequently, the test packet is considered destroyed in the collision if (and only if)

$$P_s/P_n < Z_n \quad \text{during } t_w, \text{ with } n > 0. \tag{1.4}$$

As the statistic properties of the joint interference signal may depend on the number of interferers n, the receiver threshold $Z_n$ might also depend on n. In chapters 5 and 6 we will assume a universal threshold (i.e., independent of n), which leads to interesting conclusions for the spatial distribution of traffic.

Montomery [36] has given an analytic solution for the performance of a perfect demodulator if the interference behaves like band-limited Gaussian noise.

As the received power will be assumed constant at least during $t_w$, typical values of the receiver threshold will be more optimistic than in many reports on digital mobile communication where usually fading of the signal during the capture period is assumed [39]. Literature on the characteristics of modulation techniques for data communication and their thresholds has been summarised by Oetting [40]. For large numbers of interferers, the resulting signal may resemble band-limited Gaussian noise. The capture performance in this case is illustrated for various modulation schemes in figure 1.4 and expressed in the energy per bit $E_b$ divided by the interference spectral density $N_0$, assuming instant synchronisation ($t_w$=0) and a capture criterion of an error rate of $P_e \leq 10^{-4}$.

| TYPE | MODULATION SCHEME | SPEED (b/s PER Hz) | $E_b/N_0$ (dB)* |
|------|-------------------|--------------------|------------------|
| AM | OOK - COHERENT DETECTION | 0.8 | 12.5 |
| | OOK - ENVELOPE DETECTION | | |
| | QAM | 1.7 | 9.5 |
| | QPR | 2.25 | 11.7 |
| FM | FSK - NONCOHERENT DETECTION (d = 1) | 0.8 | 11.8** |
| | CP-FSK - COHERENT DETECTION (d = .7) | | |
| | CP FSK - NONCOHERENT DETECTION (d = 7) | 1.0 | 10.7 |
| | MSK (d = .5) | 1.9 | 9.4 |
| | MSK - DIFFERENTIAL ENCODING (d = .5) | 1.9 | 10.4 |
| PM | BPSK - COHERENT DETECTION | 0.8 | 9.4 |
| | DE-BPSK | 0.8 | 9.9 |
| | DPSK | 0.8 | 10.6 |
| | QPSK | 1.9 | 9.9 |
| | DQPSK | 1.8 | 11.8 |
| | OK-QPSK | | |
| | 8-ary PSK - COHERENT DETECTION | 2.6 | 12.8 |
| | 16-ary PSK - COHERENT DETECTION | 2.9 | 17.2 |
| AM PM | 16-ary APK | 3.1 | 13.4 |

\* FOR BIT ERROR RATE OF $10^{-4}$
† CALCULATED FROM RESULTS FOR BPSK
\*\* DISCRIMINATOR DETECTION

d = FM MODULATION INDEX

Figure 1.4: Performance of representative modulation schemes [40].

The given $E_b/N_0$ rate can be transferred to signal interference ratios by multiplying by R/W, where R the data rate and W the bandwidth [40].

The receiver threshold becomes

$$Z_\infty = \frac{E_b}{N_0} \frac{R}{W}.$$ 
(1.5)

In this thesis, thermal noise effects will be neglected throughout, corresponding to an "ideal", interference-limited design of the network. In practice, this ideal can be reached by raising all transmit powers of the mobile terminals by a suitable gain factor.

## 1.4    Cell model

Spectrum efficiency is one of the most important aspects in modern radio service planning. The increasing demand for more communication facilities makes effective frequency reuse necessary. Frequencies allocated to the service are reused in a regular pattern of (usually hexagonal) areas called "cells". In figure 1.5 the cell structure for the Dutch radio telephone service at 150 and 450 MHz is depicted [42]. Cellular engineering has become an important discipline of mobile radio system design. It combines traffic engineering, interference management and spectrum conservation [19][29]. Cellular mobile radio differs from previous mobile radio designs in two critical areas: frequency reuse and cell splitting.

With conventional mobile radio systems, the objective is to have each fixed base station cover as large an area as possible by using antennas mounted in high towers and the maximum affordable power. A group of disjoint channels is assigned to the base station and the system configuration does not change for the lifetime of the system.

With cellular systems, the service area is divided in a large number of cells, each with its own base station. Power radiated by the base stations is kept to a minimum and the antennas are located just high enough to achieve the desired coverage.

These procedures enable non-adjacent cells to use the same set of frequencies, which is the frequency reuse feature mentioned above [26].
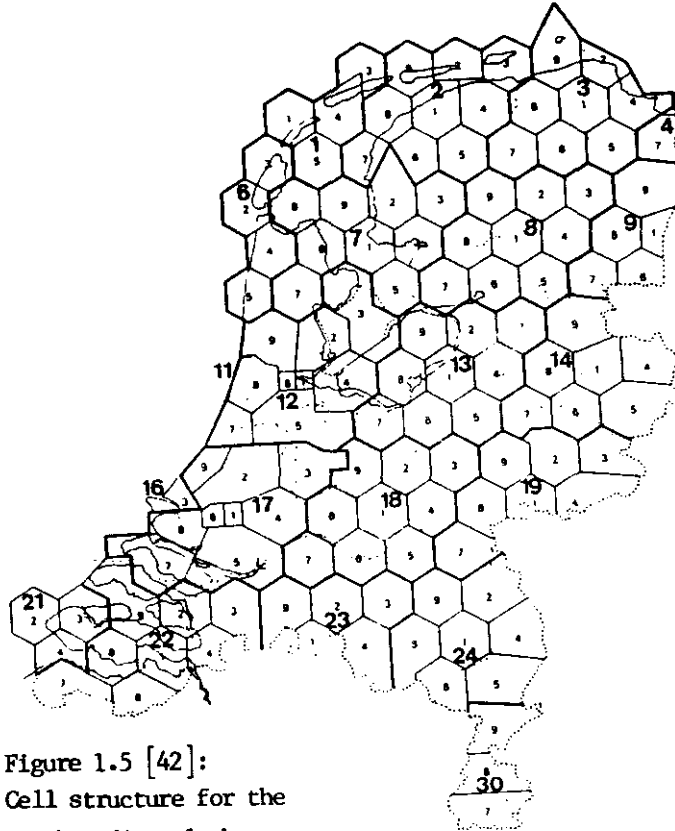


Figure 1.5 [42]:
Cell structure for the
Dutch radio telephone
service at 150 and 450 MHz.

As the demand for services increases, the number of channels assigned to a cell will become insufficient to provide the required grade of service. At this point, cell splitting can be used to increase the number of customers that can be served in a given area without increasing the number of available channels. This process works by subdividing the congested cell into smaller cells (each with its own base station), reducing the antenna height and transmitted power of the new base stations, and reusing the same frequencies in some efficient pattern.

Gosling [23] described the interdependence between frequency reuse distance and required protection ratio, considering only one single co-channel interferer. Diakoku and Ohdate obtained theoretical results for optimal patterns for channel reuse [25]. Many cell structures have been studied. Basic repetition patterns with four, seven and twelve cells are often used [26]. A typical cell radius in a small-cell system can be 3 to 5 km. Improvements can be carried out by using directional antennas, so that cells can be divided in (usually three or six) angular sectors. This makes reuse patterns with only three or four cells possible and increases spectrum efficiency. Reuse partitioning [30] is a technique used to increase capacity. In practical environments with non-uniform data traffic distributions and significant propagation impairments in certain parts of the service area, optimal solutions lead to tailor-made structures with cells of different size. Stocker [28] described the cell structure of the mobile telephone systems in Chicago, Baltimore and Washington D.C., and Tokyo. Often, computer aids have been developed using a topological database [31].

In this thesis the spatial distribution of traffic inside one individual cell will be studied. Initially this distribution will be transformed into the probability density function of the received packet power. The generally accepted propagation model, based on field measurements, will be described in section 2.1 [10] [11] [27] [39] [42].

1.4.1   Attenuation law

The most general propagation aspect in cellular engineering is the attenuation law, for the mean received power as a function of distance.

The area mean power of a packet received from a mobile terminal at a distance r from the receiving base station is of the general form [27]

$$\bar{P}_s = \alpha_i r^{-\beta}.$$  (1.6)

The exponent $\beta$ gives the path attenuation law for the channel considered $(2 \leq \beta < 5)$. In the event of UHF propagation in cellular radio, a typical value is $\beta=4$. The rapid fluctuations of the received power due to fading if the terminal is moved over small distances are introduced in the model at a later stage. In the event of ground-wave propagation without shadowing $[11, (2.1-8)]$

$$\alpha_i \overset{\Delta}{=} P_{T_i}\, G_{T_i}\, G_R\, H_{T_i}^2\, H_R^2,$$  (1.7)

where $P_{T_i}$, $G_{T_i}$ and $H_{T_i}$ are the transmit power, antenna gain and antenna height (above ground), respectively, of the mobile terminal sending slot packet i. $G_R$ and $H_R$ are the gain and height above ground of the base station antenna.
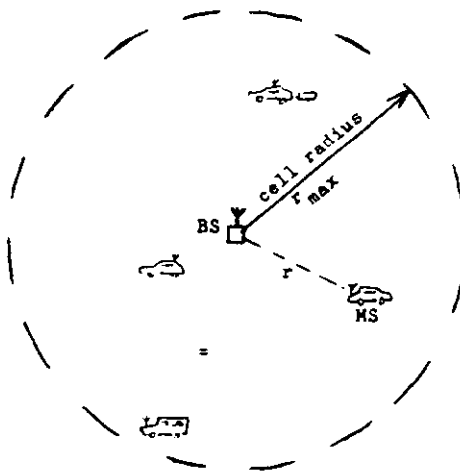


Figure 1.6: A circular cell with radius $r_{max}$. The mobile station MS transmits a packet to the base station BS from a distance r.

If all mobile terminals are assumed identical, and if antennas with omnidirectional radiation patterns in the horizontal plane are used, we may take $\alpha_i$ equal to any suitable normalising constant $\alpha_0$, since the receiver capture is determined by a ratio (1.4) of signal powers.

Take $\alpha_0 = r_{max}^{\beta}$ where $r_{max}$ is the radius of the cellular area in which the associated mobile terminals are expected to move. A circular cell, centered on the base station BS, is depicted in figure 1.6.

Although frequently used in mobile telephone systems, we do not assume adaptive transmitter power control, except perhaps to remove the shadowing effects not accounted for in this thesis. With these assumptions, both power and distance in (1.6) are normalised as

$$\overline{P}_s = \rho^{-\beta}, \tag{1.8}$$

with $0 < \rho \leq 1$, and $\overline{P}_s \geq 1$ for mobile terminals inside the cell.

## 1.4.2 Spatial distribution of traffic

As distinct from [24], we do not assume a discrete number of users, but use a continuous description: a traffic density per unit area at a (normalised) distance $\rho$ from the central receiver is defined analogous to Abramson [3], Kuperus and Arnbak [35] and Arnbak and Van Blitterswijk [1].

> $G(\rho) \triangleq$ offered packet traffic per normalised unit area at a normalised distance $\rho$ .

> $S(\rho) \triangleq$ throughput of (successful) packets sent from a normalised unit area at a normalised distance $\rho$.

Both spatial distributions have the dimension packets per slot per normalised unit area. Here as elsewhere, all distributions are assumed stationary. Consequently, transition and set-up phenomena and the behaviour of the channel in the event of instability cannot be studied from this model. We assume the multiple-access channel to be in equilibrium. In a typical communications environment both distributions will usually be obtained as a time average of the traffic distribution in the memoryless channel. Assuming packet generation to be an ergodic process, in this thesis these distributions will be applied to individual timeslots and thus regarded as the ensemble average.

Considering one circular cell, the total traffic offered to and captured by the receiver, respectively, become

$$G = 2\pi \int_0^\infty G(\rho) \, \rho d\rho \qquad (1.9)$$

and

$$S = 2\pi \int_0^\infty S(\rho) \, \rho d\rho, \qquad (1.10)$$

expressed in packets per slot. (With k-sector cells, the factor $2\pi$ would have to be replaced by $2\pi/k$).

The spatial distribution function for the random generation of packets trying to access the base station considered

$$F_\rho(\rho) \overset{\Delta}{=} \text{Prob}\{\text{the packet is generated within distance } \rho\}$$

$$= \frac{2\pi}{G} \int_0^\rho G(x) \, xdx. \qquad (1.11)$$

The corresponding pdf is

$$f_\rho(\rho) = \frac{2\pi}{G} G(\rho) \, \rho. \qquad (1.12)$$

As packets transmitted from a normalised distance $\rho$ are received with a mean power $\bar{P}_s$, the pdf for the mean received packet power can be found by applying (1.8)

$$f_{\bar{P}_s}(\bar{P}_s = \rho^{-\beta}) = f_\rho(\rho) \left| \frac{d\rho}{d\bar{P}_s} \right| = f_\rho(\rho) \frac{\rho^{\beta+1}}{\beta} \qquad (1.13)$$

Using (1.12) and (1.13), from the traffic density $G(\rho)$ the pdf $f_{\bar{P}_s}(\bar{P}_s)$ of the mean power can be obtained as

$$f_{\bar{P}_s}(\bar{P}_s = \rho^{-\beta}) = \frac{2\pi}{\beta} \rho^{\beta+2} \frac{G(\rho)}{G}. \qquad (1.14)$$

## 1.5   Outline of the thesis

In this thesis, relations between the spatial distributions $G(\rho)$
and $S(\rho)$ will be established. As the receiver capture probability
is expressed in terms of a power ratio, these spatial distributions
will be transformed to appropriate received power pdf's. In chapter
4, integral transforms will be applied to these pdf's to yield
mathematically more tractable equations. Given a certain distri-
bution of the offered traffic $G(\rho)$, the throughput $S(\rho)$ can be
formulated. This will be called "analysis" of the multiple access
channel. Conversely, "synthesis" gives the traffic load $G(\rho)$ to be
offered, if the resulting throughput $S(\rho)$ is prescribed. Both
methods will be presented in chapters 5 and 6, where incoherent and
coherent interference signals are considered, respectively. In
chapter 2 the communication properties of the assumed mobile common
radio channel will be described. In chapter 3, a discussion of the
objectives of this study will be given, and previous studies of the
relation between offered and throughput traffic distributions will
be summarised.

## 2   PROPAGATION AND INTERFERENCE IN THE MOBILE CHANNEL

### 2.1   The mobile data radio channel

When the participants of a network are mobile, communication has to be established under most adverse propagation conditions. A microwave signal transmitted from a moving vehicle to a fixed base station in a typical urban environment exhibits extreme variations in both amplitude and apparent frequency.
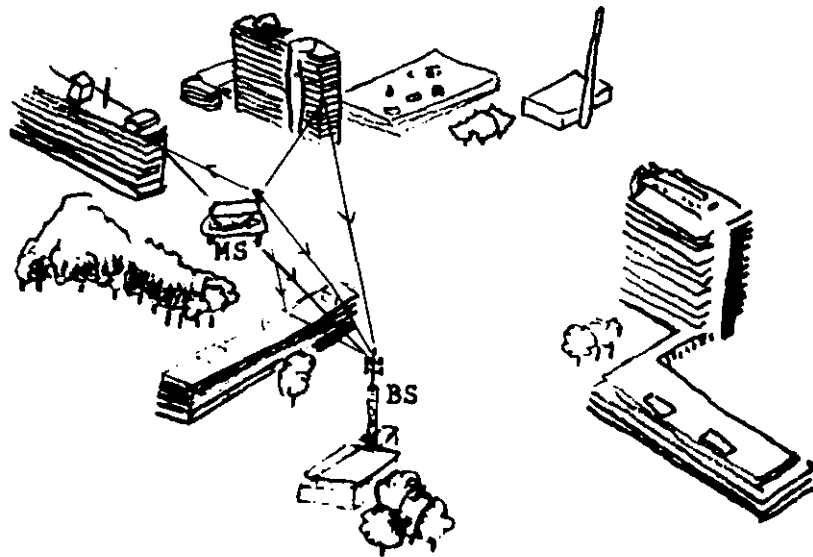


Figure 2.1: Multipath reception from a mobile station MS.

The generally accepted model of mobile radio propagation is based on field experiments and involves three main aspects: path loss, shadowing and multipath fading. The path loss is described in the previous section by equation (1.8) and gives the mean received power level, averaged over an area located at a normalised distance $\rho$ from the base station. This mean power level will be called the area mean power.

The second aspect, shadowing (slow fading) of the radio signal by buildings and hills, leads to gradual changes of the local mean received signal power as the vehicle moves.

This local mean level, averaged over a distance of about 50 m is found to vary with a lognormal distribution about the area mean level. By lognormal is meant that the local mean expressed in dB is normally distributed. The standard deviation σ depends on the topography [42]. This effect, however, is not considered in this thesis, and so area mean power and local mean power are used synonymously. The introduction of shadowing in the propagation model is recommended (Rec. 2 in chapter 7) [10].

The third aspect, (rapid) fading, is caused by multipath propagation (fig. 2.1), which causes the received signal level to fluctuate rapidly as the vehicle moves along the street. The envelope $r_1(t)$ of the received electrical field strength is Rayleigh distributed.
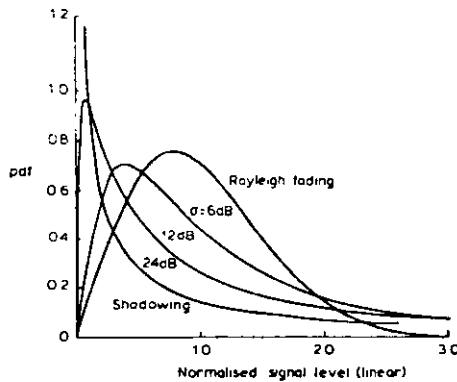


Figure 2.2 [27]:
Signal envelope pdf
with Rayleigh fading
and shadowing.

Figure 2.2 gives the pdf of received signal envelope in a mobile system with both Rayleigh fading and a certain degree σ of shadowing.

In this thesis "(area) mean power $\bar{P}_s$" is used to indicate the expectation value $E(P_s|\rho)$ of the instantaneous power $P_s$, given the distance $\rho$ at which the test packet is transmitted. The mean power thus stands for the (ensemble) mean value of the statistical process of Rayleigh fading

$$E(P_s|\rho) = E(P_s|\bar{P}_s) = \int_0^\infty p_s \, f_{P_s}(p_s|\bar{P}_s) \, dp_s = \bar{P}_s.$$

The unconditional mean power will be written explicitly as

$$\mu_1 \overset{\Delta}{=} E\left(\bar{P}_s\right) \overset{\Delta}{=} \int_0^\infty \bar{P}_s \; f_{\bar{P}_s}\left(\bar{P}_s\right) \; d\bar{P}_s.$$

With the "mean joint interference power" of n packets, which will be introduced later, we assume all n distances $\rho_1 .. \rho_n$ of the n terminals contributing to the interference to be known.

### 2.1.1 The signal received from a mobile station

With a propagation model without shadowing, the pdf's of received powers are now considered in detail. Given a normalised distance $\rho$ between base and mobile station, the pdf of the instantaneous packet power $P_s$ will be exponentially distributed, with area mean $\bar{P}_s$ found from the attenuation law (1.8) [10][11], i.e.

$$f_{P_s}\left(P_s | \bar{P}_s\right) = \frac{1}{\bar{P}_s} \exp\left\{- \frac{P_s}{\bar{P}_s}\right\} \tag{2.1}$$

and so

$$f_{P_s}\left(p_s\right) = \int_{\bar{P}_{s,min}}^{\bar{P}_{s,max}} \frac{1}{\bar{P}_s} \exp\left\{- \frac{P_s}{\bar{P}_s}\right\} f_{\bar{P}_s}\left(\bar{P}_s\right) \; d\bar{P}_s \tag{2.2}$$

The signal of the i-th packet can be written as the real part of

$$X_i(t) = R_i \; \exp\left\{j\omega_c t + \theta_i(t) + \psi_i(t)\right\} \tag{2.3}$$

The phase term $\theta_i(t)$ is due to random carrier phase plus Doppler shifts due to movements of the vehicle. Assuming phase modulation, the baseband data of the i-th packet in the slot is carried by the modulation angle $\psi_i(t)$.

## 2.1.2  Constraints on packet length

During the capture of a packet, the amplitude $R_i$ and the power $P_i$ are assumed to be constant with time. **Consequently,** the sync. window duration $t_w$ has to be restricted, as can be studied from Jakes [11].
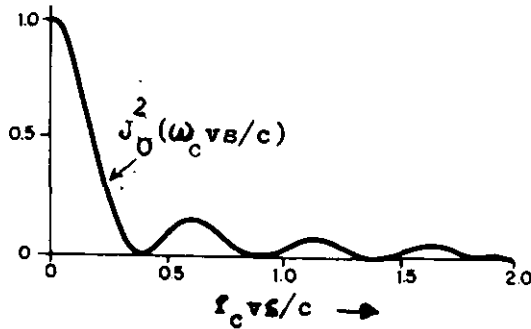


Figure 2.3 [11]:
Normalised envelope
autocorrelation of
the electrical field
strength.

The envelope $r_i(t)$ of the electrical field strength has the autocorrelation

$$R_{r_i}(s) \triangleq E\{r_i(t) \ r_i(t+s)\},$$

where s is the time difference between the sample points. Using the equations [11, (1.3-12) to (1.3-16)], for signals at the frequency of $\omega_c$ radians per second, this can be approximated with good accuracy by

$$R_{r_i}(s) \approx \frac{\pi}{2} \frac{3}{4} E_0^2 \left[1 + \frac{1}{4} J_0^2 (\omega_c \ v \ s/c)\right], \tag{2.4}$$

with c the speed of light, and $J_0(\cdot)$ the zero-order Bessel function of the first kind. The electric field strength corresponding to the area mean power is $E_0$. Removing the constant term in (2.4), one obtains the covariance

$$L(s) \triangleq E\{(r_i(t) - \bar{r}_i)(r_i(t+s) - \bar{r}_i)\} = R_{r_i}(s) - \bar{r}_i^2.$$

This is directly proportional to $J_0^2(\omega_c vs/c)$, which is depicted in figure 2.3. From this figure it can be concluded that, in the 900 MHz band, with vehicle speeds of 20 m/sec (72 km/h), the received power remains nearly constant during the sync. window, if

$$t_w < c / \omega_c v \approx \frac{3 \ 10^8}{2\pi \ 900 \ 10^6 \ 20} \ sec \approx 2.6 \ msec. \qquad (2.5)$$

Consequently one must restrict the distance d the vehicle may move during the sync. window, to be smaller than a fraction of the wavelength [39], say $\lambda/2\pi$, thus

$$d = vt_w < \frac{\lambda}{2\pi} = \frac{c}{\omega_c} \approx 5 \ cm,$$

with $\lambda$ the wavelength ($\lambda \approx 0.3$ m). This result is in agreement with the typical packet duration of about 1 msec proposed by Henry and Glance [32]. Although the packet length $\tau$ can be larger than $t_w$, it is believed that this constraint on packet length leads to shorter packets than proposed by DaSilva et al.[34], where the packets are assumed to be received correctly if (and only if) the whole packet can be contained in a non-fade interval, i.e., the received signal level may fluctuate but must remain above a fixed threshold, determined by the modulation method and the background noise.

Recommendation 1

A study on the interdependence of the sync. window $t_w$, the packet duration $\tau$ and the modulation scheme and the threshold $Z_n$, and application of the results to the equations derived in this thesis is recommended.

## 2.2  Interference signals

The total interference power $P_n$ experienced by the receiver in a particular sync. window is generally not the long-term mean $\bar{P}_n$, but an average taken over the (short) time interval $t_w$.

The joint interference power $P_n$ of n packets is made up of $n^2$ terms, namely

$$P_n = \frac{1}{t_w} \int_{t_0}^{t_0+t_w} \sum_{i=1}^{n} X_i(t) \sum_{j=1}^{n} X_j^*(t) \; dt. \tag{2.6}$$

## 2.2.1 Incoherent addition

In mobile cellular radio where packets are transmitted by many different terminals without any mutual control of carrier signals, the received signals add incoherently. In this event the phase terms of the signals may vary sufficiently fast (e.g. due to differences in carrier frequencies, Doppler shifts or modulation) to assume all crossproducts to vanish. The joint interference power, $P_n^{incoherent}$, now equals

$$P_n^i = \sum_{i=1}^{n} \frac{1}{t_w} \int_{t_0}^{t_0+t_w} X_i(t) \; X_i^*(t) \; dt = \sum_{i=1}^{n} P_i. \tag{2.7}$$

From this equation, the mean joint interference power is found by summing the individual area mean signal powers. The pdf of the joint interference power is then the n-fold convolution of $f_{P_s}$

$$f_{P_n}^i(p_n) = \left\{ f_{P_s}(p_n) \right\}^{*n}. \tag{2.8}$$

The statistical behaviour of the joint interference signal depends on the number of interferers. For n=1, the interference is a phase modulated sine-wave signal, while for n→∞ the interference resembles (bandlimited) Gaussian noise. The latter follows from the central limit theorem.

Boomars [14] reported on the pdf of incoherently interfering signals from different cells, and demonstrated the dependence of the interference pdf on the number of signals.

## 2.2.2    Coherent addition

So far we have assumed incoherent addition of the received signals.
However, mathematical calculation shows [1] that the channel
throughput can be increased if the interfering signals would add
coherently during the packet. For example, in a state-of-art mobile
network, the individual mobile stations could slave their carrier
signal to some signal from the base station by means of a phase
locked loop, so coherent addition of interfering signals may become
more appropriate. If the phase terms $\theta_i(t)$ and $\psi_i(t)$ remain nearly
constant during the capture time $t_w$, the coherent sum

$$X_n = \sum_{i=1}^{n} X_i \qquad (2.9)$$

is also a Rayleigh phasor, with ensemble mean power given by
(2.7). Carrier phases may be random but remain constant during $t_w$.
Achieving coherent addition puts even more emphasis on the
necessity to keep the packet duration $\tau$ short, and also demands
tight control of carrier phase and frequency of packets transmitted
from distinct transmitters. Doppler shifts due to the movements of
vehicles make this control complicated. Furthermore the phase
modulation index needs to be small ($\psi_i(t) \ll 1$).
In this (quasi-static) model, the pdf for $P_n^c$ , given the mean power
$\bar{P}_n$ during the capture window, is the exponential distribution

$$f_{P_n}^c \left( P_n | \bar{P}_n \right) = \frac{1}{\bar{P}_n} \exp\left\{ - \frac{P_n}{\bar{P}_n} \right\}. \qquad (2.10)$$

### 2.2.2.1    Coherent signals compared with one single interferer

In the coherent case, both the signal and interference power during
the packet are assumed to have (comparatively slow) Rayleigh fading
characteristics.

In fact, the model of Rayleigh fading for one moving terminal
assumes the addition of a large number of plane waves with random
amplitudes, phases and angles of departure [39]. This phenomenon is
illustrated in figure 2.1.

As the distance d the transmitting vehicle moves during $t_w$, has been restricted to be much smaller than $\lambda/2\pi$, the fase shift $\Delta\theta_{i,j}$ of the j-th wave from transmitter i will be small [11]:

$$\Delta\theta_{i,j} \leq 2\frac{\pi}{\lambda} d \ll 1 \text{ radian.}$$

Figure 2.4 illustrates the case where these waves are generated by a set of different but coherent transmitters. If none of the vehicles moves more than $\lambda/2\pi$, the fase shift of any of the numerous plane waves from the n different transmitters will be small (much less than one radian). The experienced shift is limited to

$$\Delta\theta_{i,j} \leq 2\frac{\pi}{\lambda} d_{max} \ll 1 \text{ radian,}$$

where $d_{max}$ the distance the fastest moving vehicle moves. Any static spreading of carrier frequencies increases the phase shifts between waves from different terminals. This effect is assumed negligible.
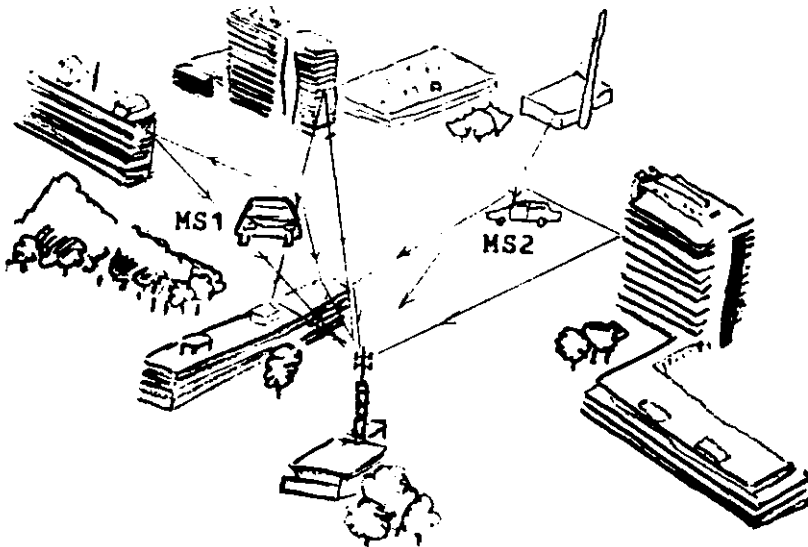


Figure 2.4: Multipath signals from two coherent sources.

It appears that the envelope of the resulting joint interference signal of n coherent transmitters remains highly correlated if none of the vehicles moves more than $\lambda/2\pi$ during $t_w$. The coherent model, assuming coherent reception of signals, thus may be interpreted as adding extra paths to a multipath scenario with one transmitter, if only the interfering carriers are transmitted with sufficient stability within the sync. window $t_w$. This "multi-multipath" model suggests that Doppler shifts need not always be corrected.

## 2.2.2.2 Pdf of joint mean coherent interference

The pdf of the ensemble mean interference power $\bar{P}_n$ is the n-fold convolution of the pdf $f_{\bar{P}_s}(\bar{p}_s)$ of the individual mean packet power $\bar{P}_s$ as given by (1.14):

$$f_{\bar{P}_n}(\bar{p}_n) = \left\{ f_{\bar{P}_s}(\bar{p}_n) \right\}^{*n}. \tag{2.12}$$

Furthermore, removing the area mean power by integration of the conditional pdf (2.10) analogous to (2.2), the unconditional pdf of the coherent joint interference power becomes

$$f_{P_n}^c(p_n) = \int_0^\infty \frac{1}{\lambda} \exp\left\{-\frac{P_n}{\lambda}\right\} f_{\bar{P}_n}(\lambda) \, d\lambda, \tag{2.13}$$

in which (2.12) can be substituted. In general, this equation (2.13) differs from the result (2.8) for incoherent signals [1].

## 3. LITERATURE ON SPATIAL DISTRIBUTIONS IN A CELLULAR AREA

As noted in section 1.4, in many papers optimum cell structures to carry a given traffic distribution have been proposed. The spatial distribution of traffic inside a cell, although affected by unsuccesful attempts of transmitters to capture the base station, received relatively little attention.

### 3.1 The critical circle model [3]

Abramson [3] described the capture probability for a packet transmitted at a certain distance from the central receiver in the base station. His model was very simple and straightforward, ignoring all aspects of fading, shadowing and interference addition. He assumed any packet transmitted at a distance $\rho$ from the central receiver to be lost if at least one other terminal transmits a packet in the same time period from a distance less than $a\rho$, with a a system constant. The circle with radius $a\rho$ will be called the "critical circle" for the test packet.

With this model mathematically tractable results were derived. The throughput $S(\rho)$ of a uniform distribution of offered traffic, $G(\rho)=G_0$, was found to have a Gaussian shape: this will be confirmed by calculations with a more accurate model in this thesis. A uniform throughput distribution $S(\rho)=S_0$ has been synthesised, by finding the corresponding distribution of offered traffic $G(\rho)$ in the event of a perfect-capture receiver (a=1). The shape of the established distribution can be described mathematically as

$$G(\rho) = \frac{S_0}{1-\left(\rho^2/\rho_\sigma^2\right)} \quad \text{and} \quad \rho_\sigma \overset{\Delta}{=} 1/\sqrt{2\pi S_0}. \tag{3.1}$$

The "Sisyphus distance" $\rho_\sigma$, a singularity somewhat outside the cell boundary ($\rho_\sigma \geq 1$), is a distance beyond which no traffic offered would ever capture the receiver in Abramson's model [3].

## 3.2 Traffic distribution in ALOHA networks with fading channels

A perfection of the model, introducing Rayleigh fading and the aspect of interference signal addition, has been presented by Kuperus and Arnbak [35]. The importance of modelling the type of signal addition (coherent or incoherent) has been underlined by Arnbak and Van Blitterswijk [1]. In the latter paper, the throughput arising from traffic offered with the same mean power for all terminals, and the throughput arising from traffic offered with a quasi-uniform spatial distribution over the cell, have been analysed. Verhulst et al. [13] studied the channel capacity by means of characteristic functions of the received power pdf of the dispatched packets.

## 3.3 The image function approach

To study the relations between spatial distributions of offered and throughput traffic in a cellular area, more powerful mathematical tools are necessary than used in e.g. [1]. In this thesis, the image function approach in [13] is extended and the characteristic functions are interpreted as integral transforms, describing the spatial distribution of the traffic. These three equivalent manners to describe the distribution of the traffic are illustrated in figure 3.1.
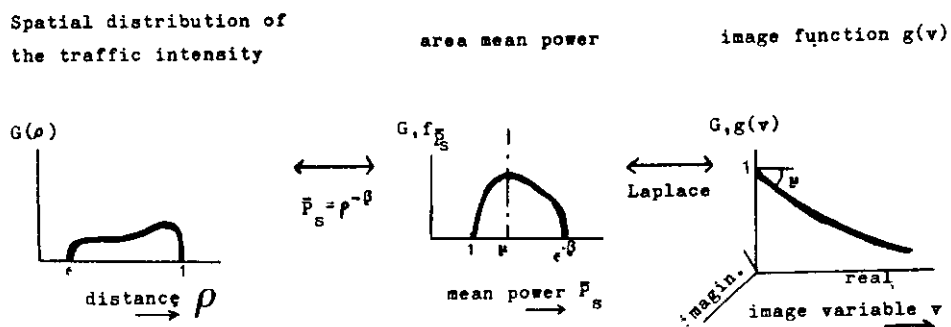


Figure 3.1: The spatial distribution, the mean power pdf and its image g(v), form three equivalent manners to specify the distribution of the traffic (to within a multiplicative factor G for the total traffic).

In chapter 4, the images will be defined and their properties described. In section 4.3, the capture probability will be expressed in terms of image functions. Subsequently, expressions for the traffic throughput of the mobile radio channel will be derived from the appropriate pdf's of the packet power. By using image functions of these pdf's, these expressions can be written in a mathematically more convenient form. For instance, in contrast with [1], summing over the number of interferers will no longer be necessary.

## 3.4 New methods and their application

To establish a relation between the distribution of the offered and throughput traffic, we will distinguish the analysis and the synthesis problem. An offered traffic distribution $G(\rho)$ can be analysed, giving the throughput distribution. If the offered traffic is known, the statistical properties of the interference are uniquely determined. This gives the capture propability and thus the throughput.

| OFFERED TRAFFIC | analysis | THROUGHPUT TRAFFIC |
|---|---|---|
| G, $G(\rho)$ | → → →<br>← ← ←<br>synthesis | S, $S(\rho)$ |
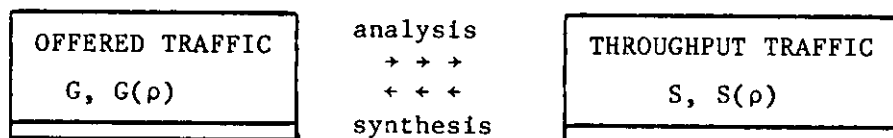
Figure 3.2: Methods to derive the relation between
offered traffic and throughput traffic.

Conversely, the synthesis problem is much harder to solve analytically. We are interested in the offered traffic if the throughput is prescribed. This corresponds to the pratical situation where a certain amount of traffic, S, has to be transferred to the base station. In this case both the offered traffic distribution and the resulting interference have to be found simultaneously from the throughput.

For both analysis and synthesis, the prescribed traffic and the traffic to be obtained are shown in figure 3.2.

Even in slotted ALOHA (1.3), finding the offered traffic G to
synthesise a certain throughput S from $S=G \exp\{-G\}$ can only be done
numerically. In this thesis, the relation between throughput and
offered traffic is more complicated than this exponential function.
Furthermore, beside the total traffic, we are also interested in
the spatial distribution.

Synthesis might be of interest to control the multiple access
channel. The control system can measure the instantaneous power of
the received packets, giving the spatial distribution of throughput
traffic. A method for this will be given in section 4.1 (see the
Taylor expansion (4.42) and figure 3.1). With this throughput
distribution, the offered traffic can be synthesised. In this way
indications of the saturation of the channel can be derived (or
predicted).

The aim of this thesis is to describe a newly developed analysis
method. From the capture propability in section 4.3, analysis
equations will be derived for incoherent and coherent addition.
Examples for specific distributions will be given. General
statements on the channel behaviour will be made; more
specifically, the behaviour of the mobile ALOHA-channel under high
traffic loads will be studied. Methods will be indicated to
synthesise the traffic to be offered if the throughput is
prescribed. Numerical synthesis results will be obtained for
constant throughput per unit area.

The way the analysis equations were originally derived during the
preparation of this thesis will be described in appendix C. In the
main body of the text, a more elegant and straightforward approach
is given.

# 4. IMAGE FUNCTION EXPRESSION FOR THE CAPTURE PROBABILITY

## 4.1 Image functions of mean power pdf's

Similar to characteristic functions used by Verhulst et al. [13] to calculate channel capacity, interpretation of these image functions as Laplace transforms proves useful in finding spatial distributions. The advantage of transformation is also observed in [14]. The pdf of the joint interference power is quite easy to find from the pdf of the power of one single transmitter. The problem of reverse transformations is avoided as the actual throughput expressions can be written directly in terms of the image functions. In the last part of this chapter, the receiver capture probability is expressed in terms of image functions.

### 4.1.1  Laplace transformation

Initially, we will discuss several of the model aspects described in the previous sections by using image functions. First we introduce the Laplace transform pair

$$g(v) \quad \xleftarrow{L_I^I} \quad f_{\bar{P}_s}(\bar{P}_s). \tag{4.1}$$

Another notation used is

$$g(v) \overset{\Delta}{=} L_I^I \{ f_{\bar{P}_s}, v \}, \tag{4.2}$$

where $g(v)$ is defined as the one-dimensional, one-sided image of the mean power pdf $f_{\bar{P}_s}$

$$g(v) \overset{\Delta}{=} \int_0^\infty e^{-vy} f_{\bar{P}_s}(y)\, dy. \tag{4.3}$$

The image $g(v)$, together with the multiplicative factor G for the total offered traffic, uniquely describes the spatial distribution of the traffic offered to the channel from the mobile packet transmitters.

The defining integral in (4.3) converges (at least) for Re(v) $\geq$ 0. Moreover

$$\left| g(v) \right| \leq g(0) = 1 \quad \text{for } Re(v) \geq 0. \tag{4.4}$$

From (4.3) it is also clear that the image and all even derivatives of the image of a pdf of a positive random variable are real, positive, and decreasing functions of their argument v along the positive real axis (v>0), since all odd derivatives are negative and increasing with v (v>0). For k a natural number and v>0:

$$
\left.
\begin{aligned}
0 \quad &< g^{(2k)}(v) \quad < g^{(2k)}(0) \qquad v>0 \quad k \in \mathbb{N} \\
g^{(2k+1)}(0) \quad &< g^{(2k+1)}(v) \quad < 0 \qquad\qquad v>0 \quad k \in \mathbb{N}
\end{aligned}
\right\} \tag{4.5}
$$

Furthermore $[5,(3.6)]$, $\quad \lim_{v \to \infty} g(v) = 0$ $\hspace{3cm}$ (4.6)

shows the image g(v) to vanish for real v tending to infinity. More detailed information on the behaviour of Laplace images in the limit v→∞ can been found in $[5]$. A summary of properties of the Laplace transform can be found in appendix A. Furthermore, we refer to $[4][5][6][7,(29)]$.
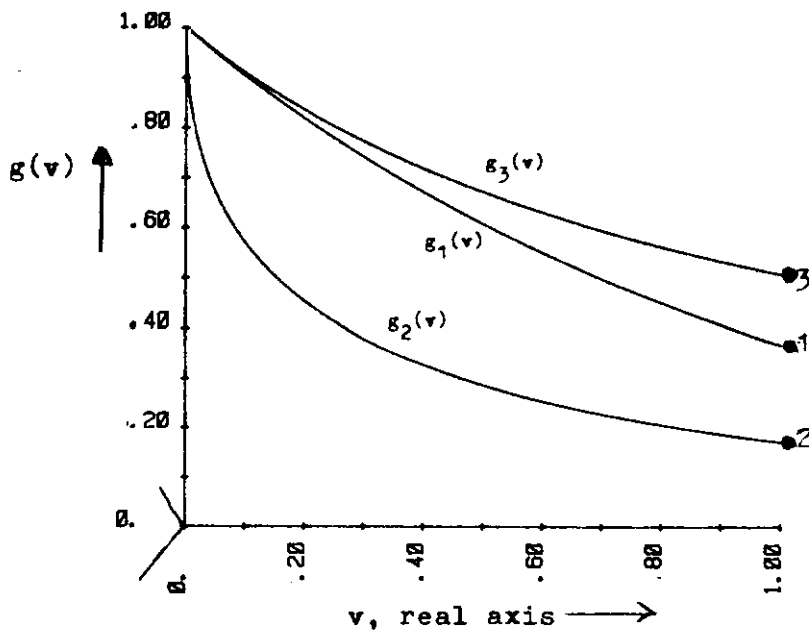


figure 4.1: Examples of image functions for
●1 a ring model
●2 quasi-constant traffic
●3 a "belt" traffic model
For v real, g(v) is also real.

## 4.1.2    Characteristic functions

To gain more insight in the image functions, we also refer to the theory of characteristic functions (cf) in statistical mathematics [14][15][16]. The cf is the expectation of $(\exp\{jvx\})$, with j the imaginary unit $\sqrt{-1}$, i.e.,

$$cf(v) \triangleq E\left(e^{jxv}\right) \triangleq \int_{x_{min}}^{x_{max}} e^{jxv} \, f_X(x) \, dx. \qquad (4.7)$$

The cf is thus the Fourier transform of the pdf and can also be written as a Laplace transform, namely, in our case

$$cf_{\bar{P}_s}(jv) = \int_0^\infty e^{-vx} \, f_{\bar{P}_s}(x) \, dx \triangleq L\{f_{\bar{P}_s}, v\} \triangleq g(v). \qquad (4.8)$$

The k-th derivative of g(v) in the point v=0 equals $(-1)^k$-times the k-th moment $\mu_k$ of the original pdf [15, p225]

$$g^{(k)}(0) = \int_0^\infty (-x)^k \, e^0 \, f_{\bar{P}_s}(x) \, dx = (-1)^k \, E(\bar{P}_s^k) \triangleq (-1)^k \mu_k. \qquad (4.9)$$

All image functions equal unity for v=0:

$$g(0) = \mu_0 = \int_0^\infty f_{\bar{P}_s}(\bar{P}_s) d\bar{P}_s = 1. \qquad (4.10)$$

The function g(v) can be obtained directly from the spatial distribution of the offered traffic G(ρ) by substituting (1.14) in the definition (4.3) of the image function g(v):

$$G \, g(v) = \int_0^\infty 2\pi\rho \, G(\rho) \, e^{-v\rho^{-\beta}} d\rho. \qquad (4.11)$$

## 4.1.3    Examples

Three examples of possible image functions are shown in figure 4.1, for real and positive v. The throughput of the first and second distributions has been studied extensively in [1], while Fronczak [17] obtained analytical and numerical results with the distribution of the third example.

## Example 1

A spatial distribution with all mobile terminals transmitting from a circular ring centered on the base station, can be modelled by

$$G(\rho) = \frac{G}{2\pi} \delta(\rho-1), \quad \text{or, equivalently} \quad G \, f_{\overline{p}_s}(\overline{p}_s) = G \, \delta(\overline{p}_s - 1). \quad (4.12)$$

The corresponding image $g_1(v) = e^{-v}$ is found by Laplace transformation of the latter and is exhibited in figure 4.1, curve ●1. The first derivative $g'(v)$ equals $-1$ for $v=0$, corresponding to a mean received signal power of $E(\overline{p}_s) = 1$. The higher order moments are all equal to unity, so the higher order central moments (about the mean $\mu_1$) are all zero, which is in agreement with the fact that a fluctuating behaviour is ruled out by the $\delta$-distribution of mean power.

## Example 2

In this example traffic distributed uniformly over the cell is considered. Two distributions are considered. The first, a quasi-constant distribution, yields an image with an simple analytical form, while the second distribution of a truly uniform traffic has a somewhat more complicated form.

### Quasi-constant offered traffic

A virtually constant traffic [1] in the area $0 < \rho < 1$ modelled by

$$G(\rho) = \frac{G}{\pi} \exp\left\{- \frac{\pi}{4}\rho^4\right\} \quad (4.13)$$

has, if $\beta=4$, the mean power pdf $\left(\text{see } (1.14)\right)$

$$f_{\overline{p}_s}(\overline{p}_s) = \frac{1}{2} \, \overline{p}_s^{-1\frac{1}{2}} \exp\left\{-\frac{\pi}{4\overline{p}_s}\right\}, \quad (4.14)$$

which has the transform $\left[7,(29.3.82)\right]$

$$g_2(v) = \exp\left\{-\sqrt{\pi v}\right\}. \quad (4.15)$$

As can also be seen from figure 4.1, the image $g_2(v)$ has an unbounded derivative $g'(0)$.

$$g_2'(0) = \frac{-\frac{1}{2}\sqrt{\pi}}{\sqrt{\varepsilon}} \, e^{-\sqrt{\pi\varepsilon}} \Big|_{\varepsilon \to 0} \to \infty. \quad (4.16)$$

According to (4.9), this indicates that the expectation value $\mu_1$ of the received power is unbounded. The spatial distribution $G(\rho)$ has non-zero values for $\rho$ arbitrarily close to zero. As shown by the attenuation law (1.8), the received power from this area tends to infinity. This phenomenon is responsible for the unbounded moments $\mu_k$. General statements on the rate of increase of moments will be made in section 4.1.4.

## Truly-constant offered traffic

Beside this simple form of a quasi-constant distribution, a truly-constant distribution is of interest. The image of this will now be derived. To avoid unbounded moments we shall assume a mobile station to be at a distance $\rho$ of at least $\rho_1$ from the base station:

$$G(\rho) = \begin{cases} \dfrac{G_*}{\pi} = \dfrac{G}{\pi(\rho_2^2-\rho_1^2)} & \text{for } \rho_1 < \rho < \rho_2 \\ 0 & \text{elsewhere} \end{cases} \qquad (4.17)$$

$G_*$ is introduced for convenience of notation. A constant throughput for $0 < \rho < 1$ can be regarded as the limit for

$$\rho_1 \to 0 \quad \text{and} \quad \rho_2 \to 1. \qquad (4.18)$$

In this limit $G_* \to G$. The derivative $g'(v)$ can be found from (4.11)

$$G\,g'(v) = \frac{G_*}{\pi} \int_{\rho_1}^{\rho_2} 2\pi\rho^{1-\beta} \exp\{-v\rho^{-\beta}\}\, d\rho. \qquad (4.19)$$

In the case $\beta=4$ this becomes

$$G\,g'(v) = G_* \int_{\rho=\rho_1}^{\rho_2} \exp\{-v\rho^{-4}\}\, d\rho^{-2}. \qquad (4.20)$$

Substitution of $v\rho^{-4} = \lambda^2$ gives

$$G\,g'(v) = \frac{G_*}{\sqrt{v}} \int_{\rho_1^{-2}\sqrt{v}}^{\rho_2^{-2}\sqrt{v}} e^{-\lambda^2}\, d\lambda = \frac{\sqrt{\pi}\, G_*}{\sqrt{v}}\left[\text{erf}\left(\frac{\sqrt{v}}{\rho_2^2}\right)-\text{erf}\left(\frac{\sqrt{v}}{\rho_1^2}\right)\right]$$

using the error function $\text{erf}(z) \overset{\Delta}{=} \dfrac{2}{\sqrt{\pi}} \int_0^z e^{-t^2}dt$, described in

$[7,(7.11)]$ and $[8,(8.250)]$. The image function can be found by integration and imposing the boundary condition $g(\infty) = 0$, so

$$G\ g(v) = \lim_{\zeta \to \infty} -\int_v^\zeta Gg'(\lambda)d\lambda = \lim_{\zeta \to \infty} -\sqrt{\pi}\ G_*\int_v^\zeta \frac{1}{\sqrt{\lambda}}[\mathrm{erf}(\frac{\sqrt{\lambda}}{\rho_1^2})-\mathrm{erf}(\frac{\sqrt{\lambda}}{\rho_2^2})]\ d\lambda$$

Substitution of $\sqrt{\lambda} \overset{\Delta}{=} \kappa$ yields

$$G\ g(v) = \lim_{\zeta \to \infty} -\sqrt{\pi}\ G\int_{\sqrt{v}}^{\sqrt{\zeta}} \mathrm{erf}(\frac{\kappa}{\rho_1^2})-\mathrm{erf}(\frac{\kappa}{\rho_2^2})\ d\kappa, \qquad (4.21)$$

which is given in $[8,(5.41)]$

$$G\ g(v) = \lim_{\zeta \to \infty} \sqrt{\pi}\ G\ [-\sqrt{\zeta}\ \mathrm{erf}(\frac{\sqrt{\zeta}}{\rho_2^2}) - \frac{\rho_2^2}{\sqrt{\pi}}e^{-\zeta\rho_2^{-4}} + \sqrt{v}\ \mathrm{erf}(\frac{\sqrt{v}}{\rho_2^2}) + \frac{\rho_2^2}{\sqrt{\pi}}e^{-v\rho_2^{-4}}$$

$$+\sqrt{\zeta}\ \mathrm{erf}(\frac{\sqrt{\zeta}}{\rho_1^2}) + \frac{\rho_1^2}{\sqrt{\pi}}e^{-\zeta\rho_1^{-4}} - \sqrt{v}\ \mathrm{erf}(\frac{\sqrt{v}}{\rho_1^2}) - \frac{\rho_1^2}{\sqrt{\pi}}e^{-v\rho_1^{-4}}\ ]$$

Inserting $\mathrm{erf}(\infty) = 1$ , this yields the image function $\qquad (4.22)$

$$G\ g(v) = G\ [\ \sqrt{\pi v}\ \{\mathrm{erf}(\frac{\sqrt{v}}{\rho_2^2}) - \mathrm{erf}(\frac{\sqrt{v}}{\rho_1^2})\} + \rho_2^2\ e^{-v\rho_2^{-4}} - \rho_1^2\ e^{-v\rho_1^{-4}}\ ].$$

Taking the limit $\rho_1 \to 0$, and inserting $\rho_2 = 1$, yields

$$G\ g(v) = G\ [-\sqrt{\pi v}\ \mathrm{erfc}(\sqrt{v}) + e^{-v}], \qquad (4.23)$$

where $\mathrm{erfc}(z) \overset{\Delta}{=} 1 - \mathrm{erf}(z)$. An unbounded derivative in $v=0$ cannot be avoided if $\rho_1 = 0$.

## Example 3

A third case is the exponential pdf

$$f_{\bar{P}_s}(\bar{p}_s) = \exp\{-\bar{p}_s\}, \qquad (4.24)$$

corresponding to a spatial distribution of the form

$$G(\rho) = \frac{2G}{\pi\rho^6}\exp\{-\rho^{-4}\}, \qquad (4.25)$$

where the traffic is concentrated in a circular belt near the ring with radius $\rho=1$ $[17]$. The image function

$$g_3(v) = \frac{1}{v+1} \qquad (4.26)$$

is depicted in figure 4.1•3. The k-th derivative in v=0 yields the k-th order moment of the pdf

$$\mu_k = (-1)^k g^{(k)}(0) = k!. \tag{4.27}$$

Comparing $g_1(.)$ with $g_3(.)$ in figure 4.1, we note that spreading the distribution of received packet power around a constant $\mu_1$ yields a larger image function (for $\rho > 0$). This agrees with the increase of higher even order moments $\mu_{2k}$. Formal statements on the behaviour of image functions in the event of spreading the power pdf about mean $\mu_1$ are believed to be of interest, but have not been established as the odd moments put obstacles to the derivation.

## 4.1.4    Bounds on the moments $\mu_k$

The above examples suggest that the moments $\mu_k$ of the mean power pdf's may easily become infinite (ex.2) or may increase very rapidly (ex.3: $\mu_k \therefore k!$). The rate of increase of the moments as a function of their order k is a great importance for the convergence of series expansions which will be derived in chapter 6.

From (4.11) it follows that any distribution with non-zero traffic $G(\rho) \approx G_0$ for $\rho \to 0$, has unbounded moments $\mu_k$, since

$$\mu_k = (-1)^k g^{(k)}(v) = \int_0^\infty 2\pi\rho^{1-k\beta} \frac{G(\rho)}{G} d\rho > 2\pi \frac{G_0}{G} \int_0^\varepsilon \rho^{1-k\beta} d\rho, \tag{4.28}$$

where $\varepsilon$ is sufficiently small to assume $G(\rho)$ to be constant. This integral diverges for $k \geq 1$ if $\beta \geq 2$, a problem also indicated in $[13,(7)]$.

On the other hand, assuming all traffic to be generated beyond a distance of at least $\varepsilon$, with $\varepsilon$ a small number, we can prove the moments to increase no faster than exponentially with k. Taking the k-th derivative of g(v) in (4.11), we find the moments $\mu_k$, as

$$\mu_k = \int_\varepsilon^\infty 2\pi\lambda^{1-k\beta} \frac{G(\lambda)}{G} d\lambda. \tag{4.29}$$

Inserting the inequality $\lambda \geq \varepsilon$, this can be bounded as

$$\mu_k \leq \varepsilon^{-k\beta} \int_\varepsilon^\infty 2\pi\lambda \frac{G(\lambda)}{G} d\lambda = (\frac{1}{\varepsilon})^{k\beta} \tag{4.30}$$

## 4.1.5   Interpretation of the image function

A second and less abstract interpretation of the image function might be useful for intuitive assessments of results derived later. The integral in (4.11) can be estimated by using the step approximation

$$\exp\{-v\rho^{-\beta}\} \approx \begin{cases} 0 \text{ if } \rho < {}^{\beta}\!\sqrt{v} & \text{i.e. if } v\rho^{-\beta} \text{ is large} \\ 1 \text{ if } \rho > {}^{\beta}\!\sqrt{v} & \text{i.e. if } v\rho^{-\beta} \text{ is small} \end{cases} \qquad (4.31)$$

Thus, equation (4.20) now can be approximated as

$$Gg(v) \approx \int_{{}^{\beta}\!\sqrt{v}}^{\infty} 2\pi\rho \; G(\rho) \; d\rho \; \overset{\Delta}{=} \; G - G_{cr}({}^{\beta}\!\sqrt{v}), \qquad (4.32)$$

where we have introduced the critical traffic $G_{cr}(\rho_*)$, being the total traffic generated inside a critical circle of radius $\rho_*$. Thus, the image function $g(v)$ can be approximated by the part of the traffic generated outside the critical circle of radius ${}^{\beta}\!\sqrt{v}$.
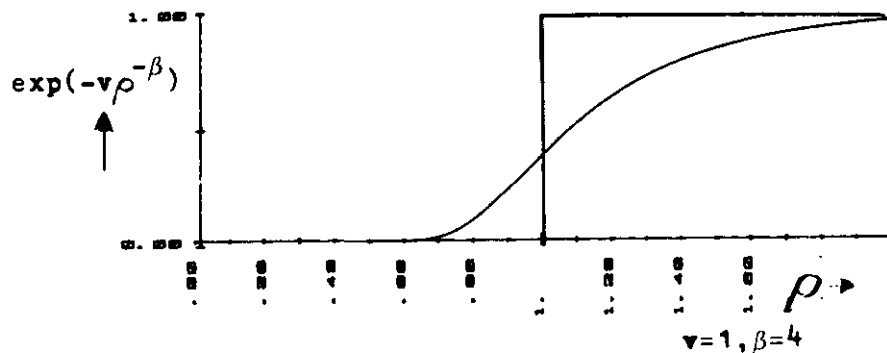


Fig.4.2: The factor $\exp\{-v\rho^{-\beta}\}$ can be interpreted as step function

The factor $\exp\{-v\rho^{-\beta}\}$ depicted in figure 4.2 is an increasing function of $\rho$ for real and positive $v$. When moving transmitters closer to the base station, $g(v)$ is reduced (if $v>0$). For real and positive arguments $v$, it can be concluded that any distribution of traffic within the cell with unity radius $(0 < \rho < 1)$, will yield an image function smaller than $\exp\{-v\}$,

which is the image of the $\delta$-distribution with all transmitters
concentrated on the outer cell boundary. This bound is valid for
the truly-constant throughput of example 2, which can be seen from
(4.23), but not for the quasi-constant distrubution (see (4.15) or
figure 4.1•2). In example 3, a very large part of all traffic is
generated outside the unity circle, and $g_3(v) \geq \exp\{-v\}$.

If, in addition, one demands all terminals to be at a distance
greater than a small number $\epsilon$ from the central receiver, the
following bounds are valid:

$$\exp\{-v\epsilon^{-\beta}\} \leq g(v) \leq \exp\{-v\}, \quad \text{for any real and positive } v. \quad (4.33)$$

Stronger bounds $\left(\text{e.g. } g(v) \geq \exp\{-\mu_1 v\}\right)$ probably exist, but have
not been found. The inequalities presented in $[16, \text{par } 13.4]$ are
recommended as starting point for further study.

## 4.1.6 Image of the mean coherent interference power pdf

While $g(v)$ is the image of the received power pdf of an individual
transmitter, we are also interested in the joint interference power
distribution. As stated before (in (2.7)), the ensemble mean
interference power $\bar{P}_n$ is the sum of n stochastic independent powers
$\bar{P}_i$, so the pdf of $\bar{P}_n$ equals the n-fold convolution of the pdf of
$\bar{P}_s$. Due to the properties of the Laplace transform, the n-th power
of $g(v)$ then maps the image of the mean interference power pdf $\bar{f}_{P_n}$
(see (A.1.3)).

$$g^n(u) \quad \xleftarrow{L^I_I} \quad \{f_{\bar{P}_s}(\bar{P}_n)\}^{*n} = f_{\bar{P}_n}(\bar{P}_n). \quad (4.34)$$

In the event of coherent addition, the Laplace transform of the
interference power pdf is found by applying the lemma of appendix A
(A.2.2) to the pdf of the coherent interference power (2.13).

We find $\quad L\{f^c_{P_n}, v\} = \dfrac{1}{v} \displaystyle\int_0^\infty \exp\{-\dfrac{\lambda}{v}\} \, g^n(\lambda) \, d\lambda. \quad (4.35)$

## 4.2    Image of the instantaneous power pdf

### 4.2.1    Definition and relation with other images

We also introduce an image function $\phi(v)$, which is the Laplace transform of the instantaneous packet power pdf $f_{P_s}$ (rather than the transform of the area mean power pdf $f_{\bar{P}_s}$). As distinct from $g(v)$, $\phi(v)$ thus incorporates the effect of Rayleigh fading.

$$\phi(v) \overset{\Delta}{=} \int_0^\infty f_{P_s}(w)\ e^{-vw}dw = \int_0^\infty \int_0^\infty f_{P_s}(w|x)f_{\bar{P}_s}(x)\ e^{-vw}dxdw. \quad (4.36)$$

Here the effects of Rayleigh fading are contained in $f_P\left(p_s|\bar{p}_s\right)$, which gives the conditional pdf of packet power $P_s$, given an area mean power $\bar{P}_s$ dependant on $\rho$ via the power attenuation law (1.8). More explicitly we insert the exponential distribution (2.1)

$$\phi(v) = \int_0^\infty \int_0^\infty \frac{1}{x}\ \exp\left\{-\frac{w}{x}-wv\right\}\ f_{\bar{P}_s}(x)\ dx\ dw. \quad (4.37)$$

Analogous to the derivation of (4.35), we find the image of the instantaneous power pdf of a Rayleigh fading signal by applying the lemma of appendix A (A.2.2). Thus the relation between $f_{P_s}$ and $f_{\bar{P}_s}$, can be expressed in the Laplace v-domain as

$$\phi(v) = \frac{1}{v}\ \int_0^\infty \exp\left\{-\frac{\lambda}{v}\right\}\ g(\lambda)\ d\lambda. \quad (4.38)$$

As fading tends to spread out the pdf of received packet power, the function $\phi(v)$ is the image of a smoother pdf than is the case with $g(v)$. In agreement with this, the moments $\upsilon_k$ of $f_{P_s}$ can be proved to be substantially larger than the moments $\mu_k$ of $f_{\bar{P}_s}$.

After substituting $\lambda/v \overset{\Delta}{=} x$ in (4.38), one finds

$$\phi(v) = \int_0^\infty g(vx)\ e^{-x}\ dx \quad \left(\text{if } v \neq 0\right). \quad (4.39)$$

The k-th derivative of $\phi(v)$ now becomes

$$\phi^{(k)}(v) = \int_0^\infty x^k e^{-x} g^{(k)}(xv) \, dx. \qquad (4.40)$$

In the limit $v \to 0$ and by applying $[8,(3.351.3)]$, this becomes

$$\phi^{(k)}(0) = g^{(k)}(0) \int_0^\infty x^k e^{-x} \, dx = k! \, g^{(k)}(0). \qquad (4.41)$$

A formal proof of the existance of the limit is not given as the same result can be obtained by comparing derivatives $g^{(k)}(0)$ obtained from (4.11) and $\phi^{(k)}(0)$ from (4.44). The latter equation will be obtained from the definition (4.36) of $\phi(v)$, written in terms of the spatial distribution of the offered traffic. Equation (4.41) is a trivial result for $k=0$ and $k=1$, but shows that higher order moments $\upsilon_k$ of the instantaneous power pdf equal $k!$ times the higher order moments $\mu_k$ of the mean power pdf. Furthermore, we conclude that $\phi(v)$, which at first glance might appear only "an unfocussed picture" of $g(v)$, uniquely specifies all moments of the mean power pdf. Moreover, as seen via a Taylor expansion of $g(v)$, $\phi(v)$ also uniquely specifies the spatial distribution $G(\rho)$ except the multiplicative factor of total traffic $G$. $[41,(\text{Th } 6.10.1)]$:

$$g(v) = \sum_{k=0}^\infty \mu_k \frac{(-v)^k}{k!} = \sum_{i=0}^\infty \frac{\upsilon_k (-v)^k}{(k!)^2}. \qquad (4.42)$$

In practice this means that the spatial distribution of the (offered) traffic can uniquely be found from the statistical properties of the power of the individual packets. Rayleigh fading does not destroy the unique correspondance.

The definition of $\phi(v)$ as an integral transform (4.36) can be stated in terms of $G(\rho)$ by inserting (1.14)

$$\phi(v) = \int_0^\infty \int_0^\infty 2\pi \, \lambda^{\beta+1} \exp\{-(\lambda^\beta + v)w\} \frac{G(\lambda)}{G} \, d\lambda \, dw. \qquad (4.43)$$

Interchanging the order of integration, yields

$$\phi(v) = \int_0^\infty \frac{2\pi\lambda^{\beta+1}}{\lambda^\beta + v} \frac{G(\lambda)}{G} \, d\lambda. \tag{4.44}$$

Many of the properties of $g(v)$ are valid also for $\phi(v)$, e.g.

$$\phi(0) = 1 \quad \text{and} \quad \phi'(v) < 0 \text{ for } v \text{ real and positive.} \tag{4.45}$$

Example 4

As an example, we give the image $\phi_1(v)$ of the $\delta$-distribution in example 1. Applying the sampling property to (4.44) yields

$$\phi_1(v) = \frac{1}{1+v}, \tag{4.46}$$

which happens to be equal to $g_3(v)$ of example 3 in section 4.1.3. Thus Rayleigh fading appears to spread the power pdf in the same way as the spatial spreading of example 3.

4.2.2  Images of instantaneous interference power pdf's

The addition (2.7) of stochastic independent powers gives the pdf of the incoherent joint interference power $P_n^i$ (during each slot), as the n-fold convolution (2.8) of the instantaneous signal power pdf $f_{P_s}$. After Laplace transformation of $f_{P_s}$ this convolution corresponds to the n-th power of the image function $\phi(v)$.

$$\phi^n(v) = L_I^I\left(\{f_{P_s}(w)\}^{*n}\right) = L_I^I\{f_{P_n}^i(w)\} \overset{\Delta}{=} \int_0^\infty f_{P_n}^i(w) e^{-vw} dw \tag{4.47}$$

The image $\phi^n(v)$ will prove very useful for the model corresponding to incoherent addition of interferers.

4.3  Capture probability and spatial distribution

Corresponding to [1] we introduce the conditional probability of loss for a packet, given the presence of n other packets:

$$F_{z,n} \overset{\Delta}{=} \text{Prob}\{\text{loss}|n,Z_n\}. \tag{4.48}$$

Furthermore, the conditional probability of loss for a packet transmitted from a normalised distance $\rho$, in the presence of n other packets is defined as

$$I_{z,n}(\rho) \triangleq \text{Prob}\{\text{loss}|n, Z_n, \rho\}. \tag{4.49}$$

To derive expressions for $F_{z,n}$ and $I_{z,n}(\rho)$, we define the stochastic variables $[1, (15) \text{ to } (20)]$

$$z \triangleq \frac{P_s}{P_n}, \qquad 0 \leq z < \infty \tag{4.50}$$

and $\quad w \triangleq P_n, \qquad 0 \leq w < \infty \tag{4.51}$

We may write the two-dimensional pdf

$$f_{z,w}(z,w) = f_{P_s,P_n}(P_s,P_n) \left| \frac{\partial(P_s,P_n)}{\partial(z,w)} \right| \tag{4.52}$$

By virtue of the stochastic independence of $P_s$ and $P_n$, this becomes for a given type of interference addition (index a)

$$f_{z,w}(z,w) = f_{P_s}(zw) \, f_{P_n}^a(w) \, w, \tag{4.53}$$

from which the pdf for z

$$f_z(z) = \int_0^\infty f_{P_s}(zw) \, f_{P_n}^a(w) \, w dw \tag{4.54}$$

and the corresponding distribution function

$$F_z(Z) = \int_0^Z dz \int_0^\infty f_{P_s}(zw) \, f_{P_n}^a(w) \, w dw \tag{4.55}$$

can be calculated.

Distribution (4.55) gives the probability of satisfying the loss condition of (1.4). The choice of $f_{P_n}^a(p_n)$ is determined by the type of addition (index a) assumed for the interfering signals. The alternatives considered here are (2.8) for incoherent and (2.13) for coherent addition. The pdf $f_{P_s}$ can be replaced by a suitable conditional pdf if constraints are imposed on the test packet.

## 4.3.1 Capture probability

For the probability of packet loss (4.48), we maintain the unconditional $f_{P_s}$

$$F_{z,n} = \int_0^{Z_n} dz \int_0^\infty f_{P_s}(zw) \, f_{P_n}^a(w) \, w \, dw \qquad (4.56)$$

Although the equation could be written in the form of a convolution after Mellin transformation (Appendix C) from $Z_n$ to the image domain, Laplace transformation yields a more useful result. In Appendix C it will be shown that in the coherent case, probability (4.56) can be written in terms of the image function $g(v)$, namely, as (C.14)

$$F_{z,n} = 1 + \int_0^\infty g^n(Z_n\lambda) \, g'(\lambda) \, d\lambda. \qquad (4.57)$$

This probability is less than unity as the derivative $g'(v)$, and hence the integral, is negative (see (4.5)).

## 4.3.2 Capture probability conditioned on distance ρ

To obtain a similar expression for the conditional probability of loss $I_{z,n}(\rho)$ we consider a test packet transmitted from the normalised distance $\rho$, so the pdf of the mean packet power is the $\delta$-distribution

$$f_{\overline{P}_s}^{test}(\overline{p}_s|\rho) = \delta(\overline{p}_s - \rho^{-\beta}). \qquad (4.58)$$

Introducing Rayleigh fading (2.2), we find the instantaneous packet power pdf to be

$$f_{P_s}^{test}(p_s|\rho) = \int_0^\infty \frac{1}{\bar{p}_s} \exp\{\frac{-p_s}{\bar{p}_s}\} \; \delta(\bar{p}_s - \rho^{-\beta}) \; d\bar{p}_s = \rho^\beta \; \exp\{-\rho^\beta p_s\}. \quad (4.59)$$

Inserting this in distribution (4.55) gives

$$I_{z,n}(\rho) = \int_0^{Z_n} dz \int_0^\infty f_{P_s}^{test}(zw|\rho) \; f_{P_n}^a(w) \quad w dw, \quad (4.60)$$

or

$$I_{z,n}(\rho) = \int_0^{Z_n} dz \int_0^\infty \rho^\beta \exp\{-zw\rho^\beta\} \; f_{P_n}^a(w) \quad w dw. \quad (4.61)$$

Integration over $Z_n$ yields

$$I_{z,n}(\rho) = \int_0^\infty [1 - \exp\{-Z_n w \rho^\beta\}] \; f_{P_n}^a(w) \; dw. \quad (4.62)$$

We divide this into two integrals. The first, being a pdf integrated over its domain, equals unity, the second equals the Laplace transform of the pdf in the image point $v=Z_n\rho^\beta$.

Thus,

$$I_{z,n}(\rho) = 1 - L\{f_{P_n}^a, \; v=Z_n\rho^\beta\}, \quad (4.63)$$

in which either the interference image (4.47) or (4.35) should be inserted, depending on whether the interference adds incoherently or coherently.

Rayleigh fading of the test packet signal is incorporated in (4.63), while the fading of the interference signals is incorporated in (4.47) and (4.35). The Poisson character of the traffic will be introduced later. The probability (4.63) thus applies generally for any statistical behaviour of the traffic. It can for instance also be used to analyse slow-frequency hopping CDMA [13].

Example 5

Assume a test packet transmitted from a normalised distance $\rho_s$, and one contender transmitting a packet in the same time slot from a

normalised distance $\rho_i$. Both experience uncorrelated Rayleigh fading. The image function $\phi_i(v)$ of the received interference power is

$$\phi_i(v) = \frac{\rho_i^\beta}{v + \rho_i^\beta}.$$ (4.64)

Using (4.63), the probability of loss of the test packet becomes

$$I_{z,n}(\rho_s) = \frac{z_1 \rho_s^\beta}{z_1 \rho_s^\beta + \rho_i^\beta},$$ (4.65)

which is in agreement with a result by Diakoku and Ohdate [25,p219].

## 4.3.3  Spatial distribution of traffic throughput

The probability of packet loss can be found by summing the conditional probability of loss $F_{z,n}$ over the number of interferers n, weighted by the probability of n contenders in the same time slot [1]. Considering Poisson distributed traffic [43], the probability of being able to capture the receiver in an arbitrary time slot is, using (1.1),

$$P_{capt} = 1 - \sum_{n=1}^{\infty} R_n F_{z,n},$$ (4.66)

The total traffic throughput S is [1]

$$S = G \ P_{capt} = G \left[ 1 - \sum_{n=1}^{\infty} R_n F_{z,n} \right].$$ (4.67)

The channel throughput $S(\rho)$ for the packets transmitted from a distance $\rho$ can be written similarly as

$$S(\rho) = G(\rho) \left[ 1 - \sum_{n=1}^{\infty} R_n I_{z,n}(\rho) \right],$$ (4.68)

The standard slotted-ALOHA case can be found by inserting a receiver threshold which never allows capture for $n > 0$ ($Z_n \to \infty$), so $F_{z,n} = 1$ and $I_{z,n} = 1$. For finite receiver thresholds, overlaps will not always destroy all n+1 packets involved, so $F_{z,n}$ and $I_{z,n}$ may be less than one.

## 5    INCOHERENT ADDITION

### 5.1  Spatial distribution of traffic throughput.

In this chapter an analysis method for incoherent signals will be derived. Main aspects of the "incoherent model" leading to this equation are: the incoherent addition of interfering signals as described in section 2.2.1, uncorrelated fading for all packets and a universal receiver threshold, independent of the number of interferers n.

In the special case of incoherent addition, the interference power pdf needed in the conditional capture probability (4.63) is given by (4.47). The conditional probability of packet loss $I_{z,n}(\rho)$ becomes

$$I_{z,n}(\rho) = 1 - \phi^n(Z_n\rho^\beta).\tag{5.1}$$

To find the spatial distribution of the traffic throughput we insert $I_{z,n}(\rho)$ of (5.1) in the throughput equation (4.68)

$$S(\rho) = G(\rho)\left[1 - \sum_{n=1}^{\infty} \frac{G^n}{n!} e^{-G} + \sum_{n=1}^{\infty} \frac{G^n\phi^n(Z_n\rho^\beta)\, e^{-G}}{n!}\right].\tag{5.2}$$

Interesting results can be obtained if we assume the receiver threshold $Z_n$ to be no longer a function of n:

$$Z_n \equiv Z_0 \text{ for all n.}\tag{5.3}$$

Packets now capture the receiver if their power exceeds the joint interference power, averaged over $t_w$, by at least a factor $Z_0$. The receiver threshold is assumed to be independent of the statistical behaviour of the interference signal.

Recommendation 1

   Further study of the characteristics of the receiver threshold $Z_n$ and application of the results in the throughput calculation, is recommended [40].

Series expansion of the exponential function [7,(4.2.1)] applied in (5.2) gives

$$S(\rho)= G(\rho) \; \exp\{G\phi(Z_0\rho^\beta)-G\}. \tag{5.4}$$

Using $\phi(v)$ as given by (4.44) and writing the total traffic G as an integral (1.9) gives

$$S(\rho)= G(\rho) \; \exp\{- \int_0^\infty [1- \frac{\lambda^\beta}{\lambda^\beta+Z_0\rho^\beta}] \; 2\pi\lambda \; G(\lambda) \; d\lambda\}. \tag{5.5}$$

This can be written as

$$S(\rho)= G(\rho) \; \exp\{ -\int_0^\infty W_{Z_0}(\frac{\lambda}{\rho}) \quad 2\pi\lambda \; G(\lambda) \; d\lambda\}, \tag{5.6}$$

which we shall call the incoherent analysis equation. We have introduced the weighting function $W_Z$ $(0 \le W_Z \le 1)$

$$W_{Z_0}(\frac{\lambda}{\rho}) \;\triangleq\; \frac{Z_0\rho^\beta}{\lambda^\beta+Z_0\rho^\beta} \;=\; \frac{Z_0}{(\frac{\lambda}{\rho})^\beta + Z_0}. \tag{5.7}$$

$W_1$ is shown in figure 5.1. Various values of $Z_0$ correspond to scaling the argument of the weighting function. It is believed that the throughput for other propagation models can also be described by (5.6), but with a distinct weighting function. The incoherent analysis equation (5.6) is very useful for evaluating the spatial traffic distribution, and several examples will be treated later in this chapter. First, we give an interpretation of this result by distinguishing two different roles of the offered traffic $G(\rho)$ in (5.6). This approach is also used in [2] and [3]. Assume the (partial) traffic

$$S_p = G_p \; \exp\{-G_{int}\}, \tag{5.8}$$

with $G_p$ the (part of the) traffic being candidate to capture the receiver and contribute to S, while $G_{int}$ is the traffic causing harmful interference.

The probability of being able to capture the receiver thus equals $\exp\{-G_{int}\}$. We see in the analysis equation (5.6) that the $G_{int}$ equals the offered traffic weighted by $W_z$ and integrated over the total area.

## 5.2   The critical circle model [3]

An approximation of $G_1$ can be made by replacing the soft weighting function by a step function:

$$W_{Z_0}\left(\frac{\lambda}{\rho}\right) \approx \begin{cases} 1 \text{ for } Z_0\rho^\beta > \lambda^\beta \\ 0 \text{ for } Z_0\rho^\beta < \lambda^\beta \end{cases} . \qquad (5.10)$$

$W_1(\frac{\lambda}{\rho})$ is shown in figure 5.1.
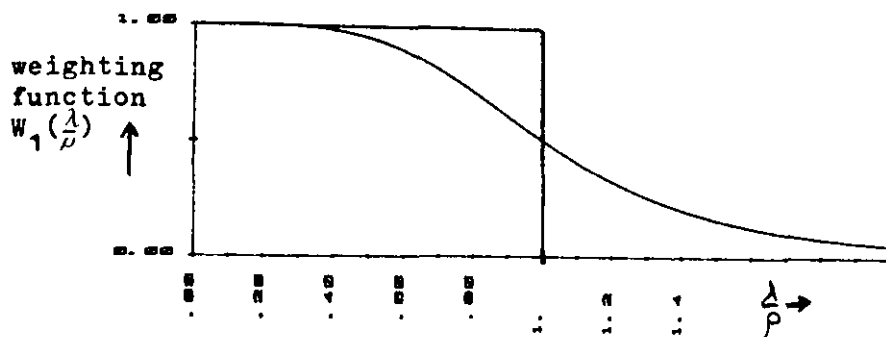


Figure 5.1: Weighting function in the incoherent analysis equation

We now find the simple throughput relation

$$S(\rho) = G(\rho) \exp\left\{ -\int_0^{a\rho} 2\pi x\, G(x)\, dx\right\}, \quad \text{with } a \triangleq \sqrt[\beta]{Z_0}, \qquad (5.11)$$

which will be called the critical circle analysis equation. This result has been derived by Abramson in [3]. A factor 4 in his formula [3,(36)] is due to his consideration of unslotted ALOHA. His model assumes that a test packet transmitted at a distance $\rho$ can capture the receiver if no other packet is generated inside a critical circle of radius $a\rho$ (see fig. 5.2), whereas the competition from one or more packet signals generated outside the circle is not taken into account.

Extra interference, due to active terminals outside the critical circle, introduces an influence of the traffic $G(x)$ outside the circle ($a\rho < x < \infty$).

Accordingly, the integral in our model (5.6) has its upper limit at infinity, and Rayleigh fading changes the critical circle adopted by Abramson into the softer transition region described by $W_z(\frac{\lambda}{\rho})$ in the incoherent analysis equation (5.6).

### 5.2.1 The critical circle model applied to perfect capture

As a special case of the critical surface model, we consider the perfect-capture receiver with $Z_0=1$, and thus $a=1$. Using integration (1.10) with (5.6), the total throughput S becomes

$$S = \int_0^\infty 2\pi\rho \ G(\rho) \ \exp\left\{-\int_0^\rho 2\pi x \ G(x) \ dx\right\} \ d\rho. \qquad (5.12)$$

A solution for the integrals can be found immediately if we introduce the distribution function

$$F(\rho) \triangleq \int_0^\rho 2\pi\lambda \ G(\lambda) \ d\lambda, \qquad (5.13)$$

with $F(0) = 0$ and $F(\infty)= G$. We find

$$S = \int_{\rho=0}^\infty F'(\rho) \ \exp\left\{-F(\rho)\right\} \ d\rho = -\exp\left\{-F(\rho)\right\}\Big|_{\rho=0}^\infty = 1-e^{-G} \qquad (5.14)$$

In the event of unslotted ALOHA, using Abramson's version $[3,(36)]$ of the analysis equation, one finds a corresponding

$$S = \tfrac{1}{2} - \tfrac{1}{2}\exp\left\{-2G\right\}. \qquad (5.15)$$

According to equations (5.14) and (1.1), the perfect-capture receiver accepts on average one packet in every slot occupied by at least one packet. The packet selected will, with the critical circle model, be the one transmitted from the terminal nearest to the base station, as there is no contender in its critical region. From this simple consideration we can conclude that the restriction "on average" may here be replaced by "exactly". In the limit $G\rightarrow\infty$, we find $S_\infty=1$ for slotted ALOHA, and $S_\infty=\tfrac{1}{2}$ for unslotted ALOHA. Abramson $[3]$ has given two particular examples of the latter limit.

For receiver thresholds near or below $Z_0=1$, the traffic loads may become relatively heavy before throughput losses due to collisions start to play an important role. In this event the possibility of more than one contender in the same slot will be relatively high and addition of interfering signals can no longer be neglected.

The critical circle model is then believed to yield too optimistic throughputs. As a striking example it will be shown that for perfect capture ($Z_0=1$), $S_\infty$ must equal zero (and not unity) for most realistic spatial distributions.
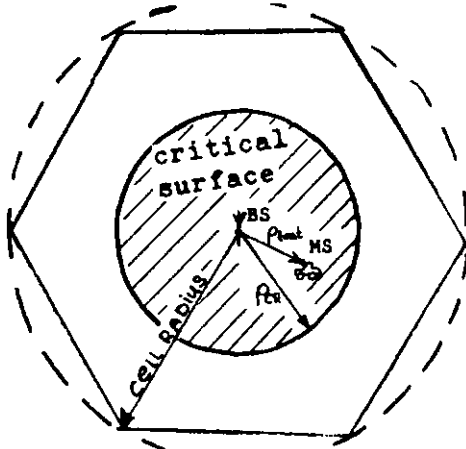


Figure 5.2: The critical circle for a test packet transmitted by the mobile station MS has the radius a$\rho$.

On the other hand, for high receiver thresholds ($Z_0>4$), the fading modelled in this thesis will significantly increase throughput while the critical circle model is believed to yield too pessimistic results. This will be confirmed in the examples of synthesis in section 5.11.

## 5.2.2 Spatial distribution near the cell boundary

From the critical circle model, one can draw a qualitative conclusion on the behaviour of the traffic distribution near the boundary ($\rho \to 1$) of the cell if non-perfect capture ($Z_0>1$) is assumed:

For non-perfect capture receiver thresholds ($Z_0 > 1$) and for large $\rho$ ($\rho \to 1$), the capture probability becomes independent of the distance at which the test packet is transmitted, and the analysis equation may be approximated with

$$S(\rho) = G(\rho) \ \exp\{-G\}.$$

(5.16)

This means that the spatial distribution of the throughput traffic
has the same shape as the offered traffic, but is reduced by the
loss factor $\exp\{-G\}$ for standard ALOHA, where all packets
experiencing overlaps are lost. The main reason for this is the
cellular approach in this thesis. No traffic is generated outside
the unit circle. For $\rho > 1/a$, the integral in the critical circle
analysis equation (5.11) is taken over the entire cell surface, and
equals the total offered traffic G found from (1.9). For test
packets generated in this area, any interfering packet has a power
$P_{int}$ high enough to satisfy the loss condition (1.4):

$$P_{test} < a^\beta P_{int}, \quad \text{since } P_{test} = \rho^{-\beta} < a^\beta \quad \text{and} \quad P_{int} \geq 1 \quad (5.17)$$

With the incoherent model, the above inequality is valid as far as
area mean powers are concerned. Rayleigh fading will make this
effect less pronounced.
The effect described by (5.16) will be confirmed by examples of
synthesis in section 5.11 using the critical circle model.
Appropriate examples using the incoherent model will be given in
sections 5.9 and 5.11.

We now consider several examples of spatial traffic distributions.

5.3  The ring model [1] [13].

In this example we assume all terminals to be located on the
circular ring with radius $\rho=1$. Thus, the packets are received with
the same mean power.

$$G(\rho) = \frac{G}{2\pi} \delta(\rho-1) \qquad (5.18)$$

The sampling property of the $\delta$-function applied in the analysis
equation (5.6) gives

$$S(\rho) = G(\rho) \exp\left\{-G\left(\frac{z_0}{z_0+1}\right)\right\} \qquad (5.19)$$

and so, by using integrations (1.9) and (1.10) for total traffic,

$$S = G \exp\left\{-G\left(\frac{Z_0}{Z_0+1}\right)\right\}. \tag{5.20}$$

The extremum of this throughput curve is found for

$$G = \frac{Z_0+1}{Z_0} \quad \text{and} \quad S = \frac{Z_0+1}{Z_0} \frac{1}{e}, \tag{5.21}$$

which equals 2/e (0.76) in case of perfect capture ($Z_0 = 1$).
Thus, if packet signals add incoherently, the effect of fading simply gives an increase of channel capacity in slotted ALOHA by a factor of $\frac{Z_0+1}{Z_0}$.

This result has been derived by Verhulst et al. in [13]. Equations (5.19) and (5.20) also describe the throughput if an adaptive power control mechanism compensates for the path loss and shadowing, but not for Rayleigh fading.

The total traffic throughput S tends to zero for G increasing. We shall see in chapter 6 that in the coherent case, a spatial ring-distribution of the traffic leads to non-zero throughput if G increases without limit.

## 5.4 Homogeneous offered traffic

In this example we drop the idea of a cellular structure and assume a traffic which is constant with distance.

$$G(\rho) = \frac{G_0}{\pi} \quad \text{for any } \rho > 0. \tag{5.22}$$

The traffic offered within the unit circle ($0 < \rho < 1$) is $G_0$.
The total traffic G (found from (1.9)) is unbounded.

The traffic throughput can be found from the incoherent analysis equation (5.6)

$$S(\rho) = \frac{G_0}{\pi} \exp\left\{-2G_0 \int_0^\infty \frac{Z_0\rho^\beta x}{x^\beta+Z_0\rho^\beta} dx\right\}. \tag{5.23}$$

The Gaussian shape of this spatial distribution, which has been shown by Abramson $[3,(42)]$, appears after substitution of $x \stackrel{\Delta}{=} t\rho \ z_0^{1/\beta}$.

$$S(\rho) = \frac{G_0}{\pi} \exp\left\{ -2G_0 \ z_0^{2/\beta} \ \rho^2 \int_0^\infty \frac{t \ dt}{t^\beta+1} \right\} \qquad (5.24)$$

The integral is solved in $[8,(3.241.2)]$

$$S(\rho) = \frac{G_0}{\pi} \exp\left\{ -\frac{2}{\beta} \ \pi \ z_0^{2/\beta} \ G_0 \ \rho^2 \ \operatorname{cosec} \ 2\frac{\pi}{\beta} \right\} \qquad (5.25)$$

In the event of the propagation law $\beta=4$ we find

$$S(\rho) = \frac{G_0}{\pi} \exp\left\{ -\frac{\pi}{2}G_0 \ \sqrt{z_0} \ \rho^2 \right\}, \qquad (5.26)$$

which is depicted in figure 5.3 for different traffic loads $G_0$.



Figure 5.3:
Throughput $S(\rho)$ (in packets per slot and per area) of a uniform offered traffic distribution.
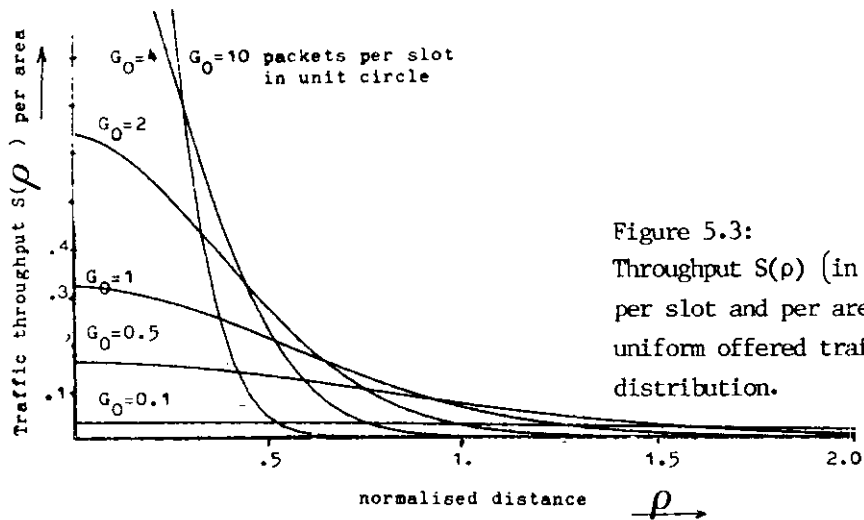
Although the total offered traffic $G$ is unbounded for any $G_0$, the total traffic throughput does not tend to zero by collision effects.

$$S_\infty = \int_0^\infty 2\pi\rho \ S(\rho) \ d\rho = \frac{2}{\pi\sqrt{z_0}} \approx \frac{0.64}{\sqrt{z_0}} \quad \text{for any } G_0 > 0. \qquad (5.27)$$

## 5.4.1   Throughput for other propagation models

Recommendation 2.1

If a weighting factor $W_z^*(\nu)$ exists for other propagation models, the Gaussian shape will now be shown to apply also for these models. The propagation model must at least contain the attenuation law (1.8) for area mean power.

Assuming a constant $G(\rho)$ = $G_0/\pi$, substitution of the integration variable $\lambda \overset{\Delta}{=} \nu\rho$ yields

$$S(\rho) = \frac{G_0}{\pi} \exp\{-\rho^2 \frac{G_0}{\pi} \int_0^\infty W_z(\nu) \, 2\pi\nu \, d\nu\}. \tag{5.28}$$

This clearly demonstrates the Gaussian shape of the throughput distribution. Convergence of the integral can be studied from

$$\text{integral} = \lim_{\substack{\epsilon \to 0 \\ \eta \to \infty}} \int_\epsilon^\eta W_z(\nu) \, 2\pi\nu \, d\nu. \tag{5.29}$$

The integral converges for $\epsilon \to 0$ as the weighting function is less than unity, while the convergence for large $\eta$ is guaranteed if the weighting function decreases more rapidly than inversely proporitional with the square of its argument $\nu$.

Derivation of the throughput for Rician fading and/or shadowing is recommended.


## 5.4.2   Success rate

In a well-functioning multiple access system, one may demand the average probability of capture within a range of transmitter distances $(0 < \rho < 1)$, to be larger than a minimum value q. The parameter q $(0 \le q \le 1)$ is called the "minimum succes rate". In the event of homogeneous offered traffic,

$$P\{\text{succes}|\rho\} = \frac{S(\rho)}{G(\rho)} = \exp\{- \frac{\pi}{2} G_0 \sqrt{z_0} \, \rho^2\} \ge q. \tag{5.30}$$

So, to meet the specification, the total offered traffic $G_0$ inside the cell with unity radius must be bounded by

$$G_0 < -\frac{2}{\pi}\frac{\ln q}{\sqrt{Z_0}} = G_{0,max}. \qquad (5.31)$$

This is depicted in figure 5.4, where the maximum permitted traffic $G_0$ is given as a function of the minimum succes rate q, with receiver threshold $Z_0$ as a parameter.
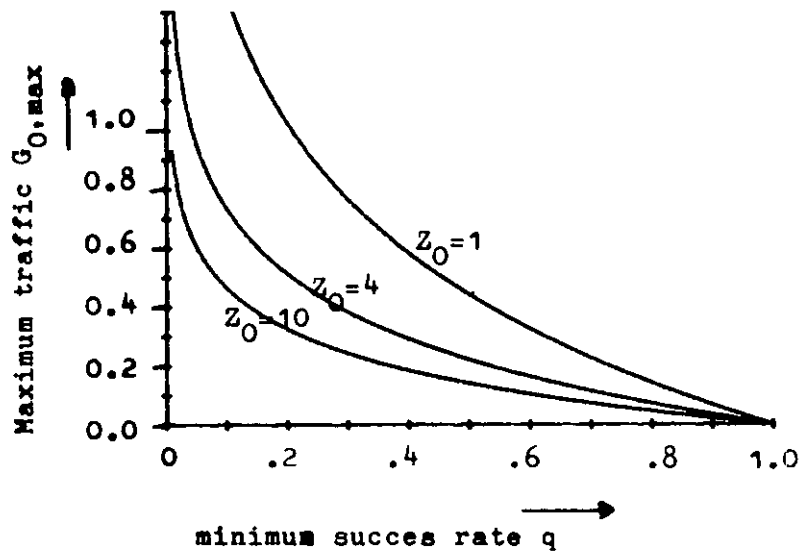


Figure 5.4: The maximum traffic load $G_{0,max}$ inside the unit circle expressed in packets per slot as a function of the minimum succes rate q.

Traffic generated outside the unit circle does not necessarily meet the minimum succes-rate specification. In a practical situation this extra-cellular traffic can represent interference from other cells.

## 5.5  Behaviour under heavy traffic loads.

Throughput equation (5.27) states that $S_\infty$ remains finite even for $G_0 \to \infty$. However, a weak point in the physical modelling of the previous example is the convenient mathematical assumption that packets can be transmitted from distances arbitrarily close to the base station, and thus, according to the attenuation law of (1.8), are received with arbitrarily high mean power $\bar{P}_s$.

We assume the results (5.25), (5.27) and (5.31) valid if the amount of traffic $G_\epsilon$ contributed by terminals located very close ($\rho < \epsilon \ll 1$) to the receiver is relatively small, i.e., if

$$G_\epsilon \ll S. \tag{5.32}$$

In this case the influence of $G_\epsilon$ to both candidate traffic $G_p$ and interfering traffic $G_{int}$ in (5.8) is negligible. To satisfy this condition in the example of uniform offered traffic, the maximum traffic load has to be bounded by

$$\pi \frac{\epsilon^2}{\pi} G_0 \ll \frac{0.64}{\sqrt{Z_0}}. \tag{5.33}$$

Inserting typical values $Z_0=10$ and $\epsilon=0.01$, the traffic $G$ offered inside the unity circle can be increased to more than one thousand packets per slot before (5.33) is violated. If (5.33) is satisfied, we may conclude that packets need not have unlimited power to capture the receiver. Two possible models to cope with the case that the offered traffic exceeds this bound are either [1]) to keep the <u>received</u> mean power constant with distance for transmitters close to the base station $\left(\rho < \epsilon_1, \epsilon_1 \text{ small but constant}\right)$, or [2]) to prevent terminals from being closer than a minimum distance $\epsilon_2$ to the receiving base station.

**Ad** [1]) This model, suggested in [13], can be regarded as a further elaboration of the propagation power law of (1.8), but the unique correspondance between $G(\rho)$ and $Gg(v)$ must then be dropped.

In terms of a traffic distribution we can model this with the spatial distribution

$$G(\rho) = \epsilon_1^2 G_0 \delta(\rho-\epsilon_1) + \frac{G_0}{\pi} U(\rho-\epsilon_1), \tag{5.34}$$

with $U(.)$ the unit step function.

In contrast to the previous result (5.27), the throughput now has
the behaviour of a ring model with the traffic on the ring
increasing without limit ($\varepsilon_1^2 G_0 \to \infty$). As shown in (5.19) this has zero
throughput $S_\infty$. Additional interference by the traffic $G_0 U(\rho-\varepsilon_1)$ can
only decrease the capture probability. Consequently, the throughput
of packets from the ring and further away tends to zero. The
channel has zero throughput if $G_0 \to \infty$.

**Ad** [2]) Under this realistic assumption we do not allow mobile
stations "to climb up the base station tower". The spatial
distribution of offered traffic is simply

$$G(\rho) = \frac{G_0}{\pi} U(\rho-\varepsilon_2). \qquad (5.35)$$

In a small-cell network with a cell radius $r_{max}$ = 5 km and an
antenna height $H_R$ = 50 meter, $\varepsilon_2$ will indeed be in the order of
0.01.

In the discrete Markov-chain model presented by Namislo, the limit
$S_\infty$ greater than zero is no longer achievable if the received power
is bounded [24,p588]. With the above model we find a similar result
which states that the throughput limit $S_\infty$ has to be zero. However,
it is believed that the offered traffic G has to be raised to
extreme values before the channel is completely destroyed by mutual
collisions.

## 5.6    Traffic distributed in a circular band

In this example we deal with spatial distributions constrained by
the condition that all traffic is concentrated in a circular band.
Thus, the offered traffic per unit area $G(\rho)$ is zero for $\rho < \rho_1$ and
$\rho > \rho_2$. The contributing cell now has inner and outer boundaries
$\rho_1$ and $\rho_2$.

In this case, the total traffic throughput S theoretically tends to
zero, if the total offered traffic increases without limit. This
can be concluded from the observation that

$$S \le G \exp\left\{\frac{-Z_0 G}{\alpha^\beta + Z_0}\right\}, \qquad \text{with } \alpha \overset{\Delta}{=} \frac{\rho 2}{\rho 1}. \qquad (5.36)$$

We prove this result by inserting the analysis equation (5.6) in
the integral (1.10) and bounding the resulting S. The integral

$$S = \int_{\rho 1}^{\rho 2} 2\pi\rho \; G(\rho) \; \exp\left\{- \int_{\rho 1}^{\rho 2} W_{Z_0}\left(\frac{\lambda}{\rho}\right) \; 2\pi\lambda \; G(\lambda) \; d\lambda\right\} \; d\rho \qquad (5.37)$$

can be overbounded by inserting the most favourable value in the
weighting function $W_z$. By doing so, one finds

$$S \le G \exp\left\{-W_{Z_0}\left(\frac{\rho 2}{\rho 1}\right) G\right\} = G \exp\left\{\frac{-Z_0}{\alpha^\beta + Z_0} G\right\}. \qquad (5.38)$$

This result can be understood by the (physically unrealistic)
insertion in the analysis equation (5.6), interpreted as (5.8), of
the traffic $G_p$ as if it were concentrated at $\rho_1$ (strong candida-
tes), and the traffic in $G_{int}$ as if it were concentrated at $\rho_2$
(weak interference). Stronger bounds appear to be possible, but the
desired conclusion can be drawn from this result.

An implication of the bound (5.36) is that achieving a non-zero
throughput limit $S_\infty$ will be possible only by assuming $\rho_1$ to be zero
or by assuming $\rho_2$ to tend to infinity. The former can lead to
infinitely strong received packet signals, while the latter allows
the ineffective traffic by terminals far outside the cell to be
unbounded without catastrophic results for the traffic closer by.

However, with typical cellular distributions ($\rho_1 = \varepsilon \sim 0.01$ and $\rho_2 = 1$),
the bound (5.36) becomes

$$S \le G \exp\left\{-10^{-8} Z_0 G\right\}, \qquad (5.39)$$

so it no longer is a practical problem, even for high G.

This is in agreement with observations by Namislo [24], who stated that the mobile slotted ALOHA radio network will remain very stable under overload: only for very large numbers of contenders the throughput will eventually tend to zero ("graceful degradation"). This is in sharp contrast to the situation in pure slotted ALOHA.

Recommendation 3

Formal statements on the throughput behaviour under large traffic
loads might be obtained by inserting the intermediate result (5.4)
in the integral for total throughput traffic (1.10) and applying
the asymptotic expansion for Laplace integrals [38].

## 5.7 Offered traffic distributed homogeneously in a circular band

In this example we assume an offered traffic distributed uniformly with intensity $G_0$ per unit area between radii $\rho_1$ and $\rho_2$.

$$G(\rho) = \begin{cases} \dfrac{G}{\pi\left(\rho_2^2-\rho_1^2\right)} \triangleq \dfrac{G_*}{\pi} & (\rho_1 < \rho < \rho_2) \\[2mm] 0 & \text{elsewhere} \end{cases} \tag{5.40}$$

The parameter $G_*$ is introduced for convenience of notation. The traffic throughput now becomes

$$S(\rho) = \frac{G_*}{\pi} \exp\left\{-G_* \int_{\lambda=\rho_1}^{\rho_2} \frac{Z_0\rho^4 \, d\lambda^2}{\lambda^4 + Z_0\rho^4}\right\}. \tag{5.41}$$

After solving the integral and using [8,(1.625.9)] to substract both arctan terms, we find

$$S(\rho) = \frac{G_*}{\pi} \exp\left\{- \sqrt{Z_0}\,\rho^2\,G_*\,\arctan\left(\frac{\sqrt{Z_0}\,\rho^2(\rho_2^2-\rho_1^2)}{\sqrt{Z_0}\rho^4 + \rho_1^2\,\rho_2^2}\right)\right\}. \tag{5.42}$$

Inserting $\rho_2=1$ and taking the limit $\rho_1\to 0$ (thus $G=G_*$), the throughput distribution from a homogeneous offered traffic within the cell is found on the form

$$S(\rho) = \frac{G}{\pi} \exp\left\{-\sqrt{Z_0}\,\rho^2\,G\,\arctan\left(\frac{1}{\rho^2}\right)\right\}. \tag{5.43}$$

For a minimum succes rate q, the total traffic G offered in the unity cell must be bounded by

$$G < \frac{-4}{\pi} \frac{\ln q}{\sqrt{Z_0}} ,\qquad (5.44)$$

which is twice the maximum allowed traffic in the event of uniform spatial distribution (with infinite extension (5.27)).

## 5.8   Offered traffic increasing linearly with distance

We next assume unbounded traffic with the spatial distribution

$$G(\rho)= \frac{3}{2\pi}\, \rho\, G_0, \quad \text{for any } \rho > 0. \qquad (5.45)$$

The traffic transmitted from inside the unit circle is $G_0$. Assuming $\beta=4$, we find a traffic throughput of

$$S(\rho)= \frac{3}{2\pi}\, \rho\, G_0\, \exp\!\left\{ -3G_0 \int_0^\infty \frac{Z_0\rho^4\,\lambda^2}{\lambda^4+Z_0\rho^4}\, d\lambda \right\}. \qquad (5.46)$$

We substitute $\lambda \stackrel{\Delta}{=} t\,\rho\; \sqrt[4]{Z_0}$. The integral is $\left[8,(3.241.2)\right]$

$$S(\rho)= \frac{3}{2\pi}\, \rho\, G_0\, \exp\!\left\{ - \frac{3}{4}\pi\, G_0\, Z_0^{3/4}\, \rho^3\; \operatorname{cosec} \frac{3}{4}\pi \right\}. \qquad (5.47)$$

The total traffic throughput S now equals, using (1.10),

$$S_\infty = \int_0^\infty G_0\, \exp\!\left\{ - \frac{3}{4}\pi\, G_0\, \rho^3\, Z_0^{3/4}\; \operatorname{cosec} \frac{3\pi}{4} \right\}\, d\rho^3 \qquad (5.48)$$

$$= \frac{2\sqrt2}{3\,\pi}\; Z_0^{-3/4} \approx 0.300\; Z_0^{-3/4}\; \text{for any } G_0 > 0. \qquad (5.49)$$

A perfect-capture receiver will be captured by an average of about 0.300 packets per timeslot, independent of the intensity of traffic. We have thus obtained a constant throughput, independent of the offered traffic per unit area (the dependence on the total traffic G is indefinite as G is infinite for any $G_0>0$).

In the above result, only a fraction $S_\epsilon$, with

$$S_\epsilon \overset{\Delta}{=} \int_0^\epsilon 2\pi\rho \; S(\rho) \; d\rho \quad < \quad \int_0^\epsilon 2\pi\rho \; G(\rho)d\rho = \epsilon^2 \; G_0, \qquad (5.50)$$

is contributed by traffic offered inside a small circle of radius $\epsilon$. This traffic is received with unacceptable high packet power. We may assume the result valid if $S_\epsilon \ll S$, i.e. for

$$G_0 \ll \frac{0.300}{\epsilon^2} \; Z_0^{-3/4}, \qquad (5.51)$$

which will normally be the case in practical situations.

## 5.9   Offered traffic increasing quadraticly with distance

$$G(\rho) = \begin{cases} \rho^2 \; \frac{2}{\pi} \; G & \text{for } \rho < 1 \\ \\ 0 & \text{for } \rho > 1 \end{cases} \qquad (5.52)$$

The throughput distribution becomes

$$S(\rho) = \frac{2}{\pi} \rho^2 \; G \; \exp\left\{ -G \; Z_0 \; \rho^4 \int_0^1 \frac{4x^3}{x^4+Z_0\rho^4} \; dx \right\} \qquad (5.53)$$

$$= \frac{2}{\pi} \rho^2 \; G \; \exp\left\{ -GZ_0\rho^4 \; \ln\left[ \frac{1+Z_0\rho^4}{Z_0\rho^4} \right] \right\}$$

$$= G(\rho) \; \left[ 1 + \frac{1}{Z_0\rho^4} \right]^{-G \; Z_0\rho^4}. \qquad (5.54)$$

Examples of this spatial distribution have been computed and are illustrated in the three figures 5.5, 5.6 and 5.7. The independent variable is $\rho$ ($0<\rho<1$). In the first figure the offered traffic $G$ is fixed at an average of one packet per slot;  the channel is below saturation. The spatial distribution of the offered traffic $G(\rho)$ is also given in this figure, as it has the same dimension as $S(\rho)$: packets per slot per unit area. $G(\rho)$ can be interpreted as $S(\rho)$ for the special receiver that is captured by all packets regardless of overlap ($Z_0=0$).

Figure 5.5 shows that the influence of $Z_0$ $(1 < Z_0 < 10)$ is not very large if the channel is below saturation. This can be noted also in the throughput relation for total traffic, given in figure 5.8.
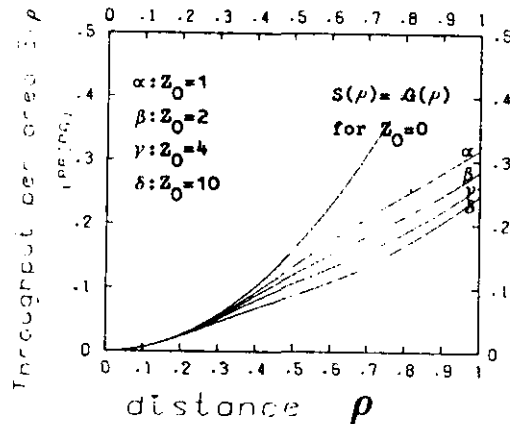


figure 5.5: Quadratic offered traffic throughput by various $Z_0$ for G=1.

In the next figure (5.6), $S(\rho)$ is given for a perfect capture receiver $(Z_0=1)$, when the total traffic load G is increased in steps $(G=1 \rightarrow 2 \rightarrow 4 \rightarrow 10)$. The quadratic shape of the curves is clear for small $\rho$, but for larger $\rho$ the effect of loss due to collisions becomes significant. With a total traffic approaching the average of 10 packets per timeslot, the packet throughput from the boundary $(\rho \approx 1)$ of the cell tends to zero, even though the traffic offered from this region is very large.
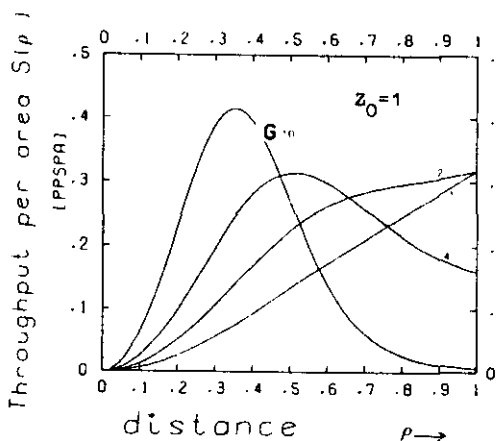


Figure 5.6: Quadratic offered traffic throughput by a $Z_0=1$ receiver with total traffic G as a parameter.
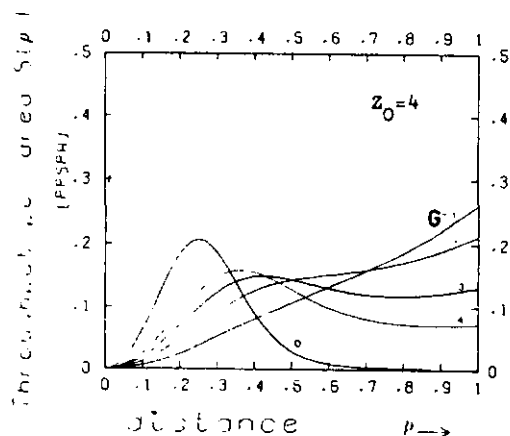
Figure 5.7: Quadratic offered traffic throughput by a $Z_0=4$ receiver with total traffic G as a parameter.

In figure 5.7, the throughput curves are given for a radio receiver with threshold $Z_0=4$ (6dB). For terminals close to the base station

($\rho < 0.2$), the throughput figures do not show much difference from the previous case where $Z_0=1$. For more distant terminals the saturation effect becomes evident far earlier, and the increase with distance of the traffic throughput is weakened. In some cases ($G>2$), the curve even decreases with distance.

For terminals near the boundary of the cell ($\rho \to 1$) and for $Z_0=4$, we recognise the saturation effect described by (5.16). The numerical value of the loss factor in (5.54)

$$\left[ 1 + \frac{1}{Z_0\rho^4}\right]^{-GZ_0\rho^4} \approx \left( \frac{5}{4} \right)^{-4G} \approx (2.44)^{-G} \tag{5.55}$$

approaches the limit of $e^{-G}$ [7,(4.2.21)]. In this region, nearly all packets experiencing overlaps are lost. Thus, for larger G ($2 < G < 4$), we see another increase with $\rho$, caused by $G(\rho)$, of the throughput $S(\rho)$. Combining these opposite effects the throughput curve becomes quite constant in the area $0.3 < \rho < 1$, especially for a traffic load of $G \approx 3$ packets per slot.

For higher traffic loads ($G>3$), the throughput of packets transmitted relatively far from the base station drops quickly due to collisions. Compared with this, the increase of the throughput of packets from terminals close to the central receiver is relatively small.
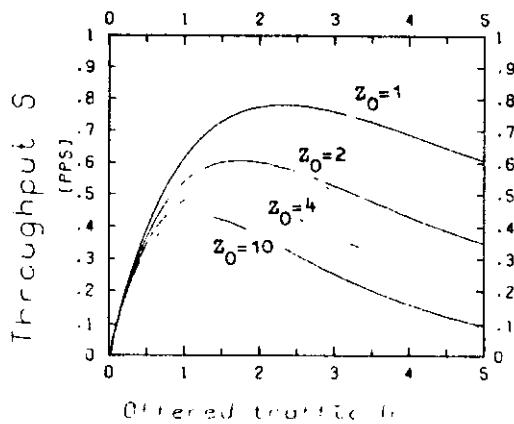


Figure 5.8: Total throughput S as a function of the offered traffic G for various receiver thresholds $Z_0$.

In this comparison it should be remembered that in the integral for S (1.10), the throughput per unit area $S(\rho)$ is weighted with $\rho d\rho$.

As a result, the total traffic S is believed to tend to zero for G increasing without limit. The total throughput S is depicted in figure 5.8 as a function of the offered traffic G. As previously noted the influence of the receiver threshold $Z_0$ becomes more significant, when the total traffic G increases towards saturation of the channel.


Recommendation 3.1

> The S versus G relation giving the throughput, can be assessed by inserting $S(\rho)$ in (1.10). A numerical value of the limit S has not been found (see recommendation 3 in section 5.6). We find bounds for S using $[7,(4.2.36)]$
>
> $$G\, e^{-G} < \quad S = G \int_0^1 \left[1 + \frac{1}{Z_0\rho^4}\right]^{-GZ_0\rho^4} d\rho^4 \quad < \quad G \int_0^1 \exp\left\{\frac{-GZ_0y}{Z_0y+1}\right\}\, dy,$$
>
> with $y \overset{\Delta}{=} \rho^4$ substituted. It can be shown by using the asymptotic expansion for Laplace integrals $[38]$ that this bound only yields $0 < S_\infty < 1/Z_0$.


## 5.10    Synthesis methods

In our analysis so far, the traffic $G(\rho)$ offered to the channel was assumed to be known. From this the traffic throughput could be calculated. In most practical communications environments, however, a certain transfer of data S has to be guaranteed at the receiver. Packets lost in collisions do not contribute to S and have to be retransmitted. Thus we must address the problem of synthesis of a distribution of $G(\rho)$ resulting in a specified $S(\rho)$, taking account of these retransmissions.


### 5.10.1    Numerical method of increasing sample distance $\rho$

In the critical circle model, the special case of uniform throughput has been derived for the perfect-capture receiver in $[3]$. In this event ($Z_0=1$), the critical circle has a radius equal to the distance $\rho_{test}$ traversed by the test packet, so a method to calculate the offered traffic required to achieve any prescribed

throughput $S(\rho)$ can be obtained from (5.8). The competing traffic $G_{int}$ is derived by integrating $G(\rho)$ for traffic originating closer to the base station:

$$G_{int} = \int_0^\rho 2\pi\lambda \ G(\lambda) \ d\lambda. \qquad (5.56)$$

As it is illustrated in figure 5.9, from $G_{int}$ and $S(\rho)$, the traffic $G_p$ to be offered from the normalised distance $\rho_{test}$ can be found as

$$G(\rho) = S(\rho) \ \exp\{G_{int}\} \qquad (5.57)$$

This numerical synthesis approach starts near the base station ($\rho=0$), where $G(0)$ equals $S(0)$. By increasing $\rho_{test}$ step by step, the traffic to be offered can be found for any distance $\rho$ ($0<\rho<1$).
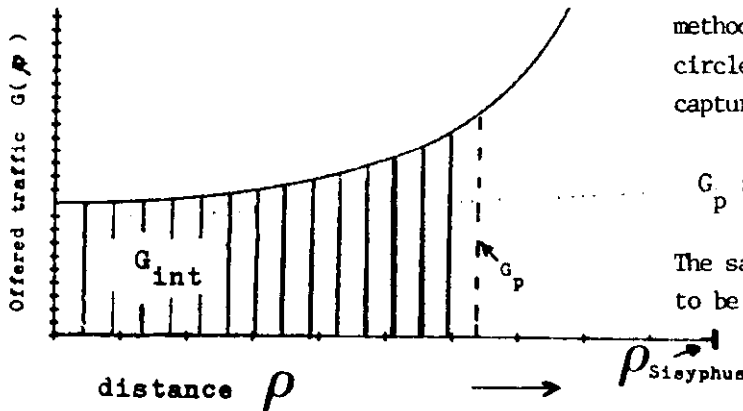


Figure 5.9: Illustration of a numerical synthesis method using the critical circle model for perfect capture.

$$G_p := S_0 \ \exp\{+G_{int}\}$$

The sample distance $\rho$ is to be increased step by step.

This method can only be used for $Z_0 \leq 1$: for higher receiver thresholds the required traffic $G(\rho)$ for $\rho$ larger than $\rho_{test}$ has to be known before it can be calculated.

Abramson derived the analytic solution (3.1) for a uniform throughput $S_0$ and perfect capture $(Z_0=1)$.

## 5.10.2 Iterative numerical method

A general explicit solution for $G(\rho)$, given $S(\rho)$, has not been found, neither with the critical circle model nor with the incoherent model. However, the analysis equation (5.6) is amendable to iterative numerical solution, by rewriting it in the form

$$G_{i+1}(\rho) = S(\rho) \exp\left\{+ \int_0^\infty W_Z\left(\frac{\lambda}{\rho}\right) 2\pi\lambda \, G_i(\lambda) \, d\lambda\right\}, \qquad (5.58)$$

where $S(\rho)$ is a prescribed (desired) traffic throughput. Using the i-th trial version $G_i(\rho)$, the next (and hopefully better) estimate $G_{i+1}(\rho)$ can be found.

A simple choice of the starting function is taking $G_0(\rho)$ equal to the desired throughput density $S(\rho)$. In general, it can be stated that if the starting function satisfies

$$0 \leq G_0(\rho) \leq G(\rho) \qquad \text{for all } \rho, \qquad (5.59)$$

then all estimates $G_i(\rho)$ have values between $S(\rho)$ and the solution $G(\rho)$. This can be proved by induction, as follows:

The lower bound is based on the simple recognition that all estimates are greater than $S(\rho)$ for any $\rho$, as the integrand in (5.58) is non-negative. The upper bound is derived from the induction step that

$$\text{if } G_i(\rho) \leq G(\rho), \qquad \text{then } G_{i+1} \leq G(\rho), \qquad (5.60)$$

which follows from

$$G_{i+1}(\rho) = S(\rho) \exp\left\{ \int W_Z\left(\frac{\lambda}{\rho}\right) 2\pi\lambda \, G_i(\lambda) \, d\lambda\right\}$$

$$\leq S(\rho) \exp\left\{ \int W_Z\left(\frac{\lambda}{\rho}\right) 2\pi\lambda \, G(\lambda) \, d\lambda\right\} = G(\rho).$$

An immediate consequence of (5.59) is that a bounded solution $G(\rho)$ can not exist if the sequence of estimates $G_i(\rho)$ diverges. However, in practice this observation is of limited value, as it does not consider the numerical (quantisation) problems of digital computing, which may also be the cause of divergent steps.

### 5.10.2.1   The computer program

A synthesis computer program has been written to find $G(\rho)$, given $S(\rho)$. It has been applied to both the critical circle and the incoherent model. A very appropriate case is uniform traffic throughput: we assume $S(\rho)$ to be constant within the circular cell of normalised radius $\rho=1$, i.e.

$$S(\rho) = \begin{cases} S_0 = \dfrac{S}{\pi} & 0 < \rho < 1 \\ \\ 0 & \text{elsewhere} \end{cases} \qquad (5.61)$$

The spatial distributions are sampled in N points (typical values are between 10 and 50). The iteration is terminated when the integrated relative changes ER in the distribution $G(\rho)$ drops below a certain threshold (e.g. $10^{-4} = 0.01\%$)

$$ER_{i+1} \triangleq \int_0^{\infty} \left| \frac{G_{i+1}(\rho) - G_i(\rho)}{G_i(\rho)} \right| d\rho \quad < \quad \text{THRESHOLD.} \qquad (5.62)$$

The maximum number of iterations is limited to M. The total offered traffic G $\left(\text{found from } (1.9)\right)$ is monitored to indicate possible divergence of the equation. The starting function $G_0(\rho)$ is taken equal to $S(\rho)$. Convergence is quick ($ER_{i+1} \ll ER_i$) as long as the channel is well below saturation: only four or five iterations are needed. With higher traffic loads the convergence becomes slower. Numerical results will be presented in section 5.11.

5.10.2.2   Simulation of the dynamic behaviour of the channel

The rate and the manner of convergence have a very useful practical interpretation. In the standard ALOHA equation $S = G\,e^{-G}$, we may distinguish two roles of the offered traffic, namely the candidate and the interference role of the traffic variable G, described by equation (5.8). In our iterations:

$$G_p \stackrel{\Delta}{=} G_{i+1}(\rho) \quad \text{and} \quad G_{int} \stackrel{\Delta}{=} \int_0^1 W_Z\left(\frac{\lambda}{\rho}\right) 2\pi\lambda\, G_i(\lambda)\, d\lambda. \qquad (5.63)$$

In a quasi-static description, assume the momentary value at instant i of interference to be $G_{int}$. To achieve a throughput $S_p$, a certain number of packets has to be retransmitted resulting in the offered traffic load

$$G_p = S_p \, \exp\{-G_{int}\}. \qquad (5.64)$$

The increased traffic $G_p$ results in more interference

$$G_{int}^{new}(G_p) > G_{int} \qquad (5.65)$$

and a new estimate $G_p^{new}$ has to be made.

Slow convergence indicates that the retransmissions result in a significant increase in interference, again causing a substantial increase in additional retransmissions. The channel is thus approaching saturation. The iterative computer programme appears to simulate the modelled dynamic behavior of the channel, as a sequence of steps modelled by quasi-static offered traffic estimates $G_p$. It should be noted that this interpretation is at odds with the assumption of stationary distributions made in section 1.4.2.

## 5.11    Uniform throughput

The program described in the previous section is contained in appendix B. The offered traffic distributions are depicted in figures 5.10a, 5.11a and 5.12a. Results by the incoherent model are indicated with solid lines, while the results by the critical circle model are marked.

The first figure (5.10) applies for receiver threshold $Z_0 = 1$ (perfect capture). The traffic $G(\rho)$ to be offered according to the incoherent model is given for various throughput intensities S=0.1, 0.2, up to 0.8. The number of retransmissions, and thus $G(\rho)$, increases rapidly for terminals near the boundary of the cell ($\rho \to 1$) as soon as the total traffic S exceeds some 0.6 packets per slot (pps). The program then has to execute nine or more iterations before reaching the ER-criterion in (5.62). A total traffic as high as 0.8 pps can be received, but distant terminals must offer a traffic more than four times higher (more than one pps per normalised unit of area, ppspa) than is successfully received ($0.8/\pi \sim 0.25$ ppspa).

Calculations for S=0.9 (and higher) no longer converge and seem near or beyond the channel capacity. The total offered traffic G is given as a function of S in figure 5.10b.

The results are compared with

- the standard slotted ALOHA curve $S = G \exp\{-G\}$
- $S = G \exp\left\{ \dfrac{-Z_0 G}{Z_0 + 1} \right\}$ of section 5.1
- $S = 1 - \exp\{-G\}$ for a receiver that can be captured on average by one packet per occupied slot,
- the bound $S \leq G$ for any receiver.

Calculations using the critical circle model confirm the analytic results derived by Abramson for $Z_0 = 1$. Furthermore, in this event the total offered traffic G closely follows the relation

$$S = 1 - \exp\{-G\},$$

which was predicted in (5.14).

Information on the convergence rate can be found in appendix B by means of computer tables of the variables ER and the total traffic G.

The traffic to be offered if the receiver has a threshold of $Z_0=4$ and $Z_0=10$ is given in figures 5.11 and 5.12. Near the cell boundary ($\rho\to1$) the number of retransmissions increases rapidly with the traffic load if S is larger than S=0.4 pps resp. S=0.3 pps. The channel appears to reach its capacity limit for

$$0.5 < S < 0.6 \text{ pps} \quad \text{resp.} \quad 0.4 < S < 0.5 \text{ pps.}$$

As confirmed by the curves for higher receiver thresholds ($Z_0 > 4$), the offered traffic can be constant with distance when $\rho \to 1$. The effect has been explained by (5.18), predicting the existence of a constant $G(\rho) = S_0 \exp\{G\}$ for $\rho > \left(^\beta\sqrt{Z_0}\right)^{-1} = \tfrac{1}{2}\sqrt{2}$.

Comparing the plots using the critical circle model with the plots using the incoherent model, we note the following:

For low receiver thresholds $\left(Z_0=1\right)$, the critical circle model is more optimistic, while for median to large thresholds $\left(Z_0=4 \text{ and } 10\right)$ the incoherent model is more optimistic.

For intermediate values of $\rho$ ($\rho\approx0.5$), high thresholds and large traffic loads, the effect of interference generated outside a circle of radius $a\rho$ is apparent: the incoherent model requires more traffic per area to be offered than according to the critical circle model. On the other hand for the much larger area of relatively large $\rho$ ($\rho>0.5$) the effect of fading is very favourable.

Traffic G(ρ) to be offered to give a homogeneous
spatial distribution of the traffic troughput S(ρ)

Incoherent addition

receiver threshold: 1.0 ( 0.0 dB )



Figure 5.10a(↑) and 5.11a(↓):

Spatial distribution of required
offered traffic G(ρ) for uniform
throughput S(ρ)=S/π with S=0.1, 0.2,
etc, for a receiver threshold of $Z_0=1$
and $Z_0=4$, respectively.

Figure 5.10b(↑) and 5.11b(↓):
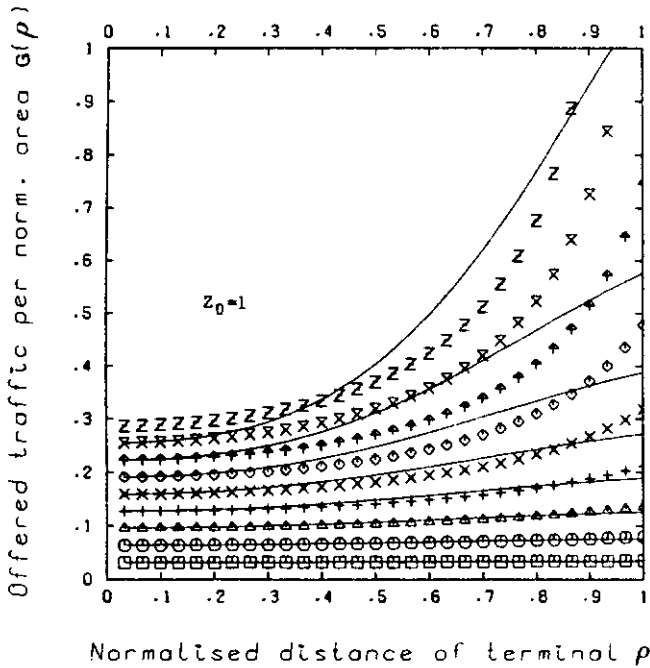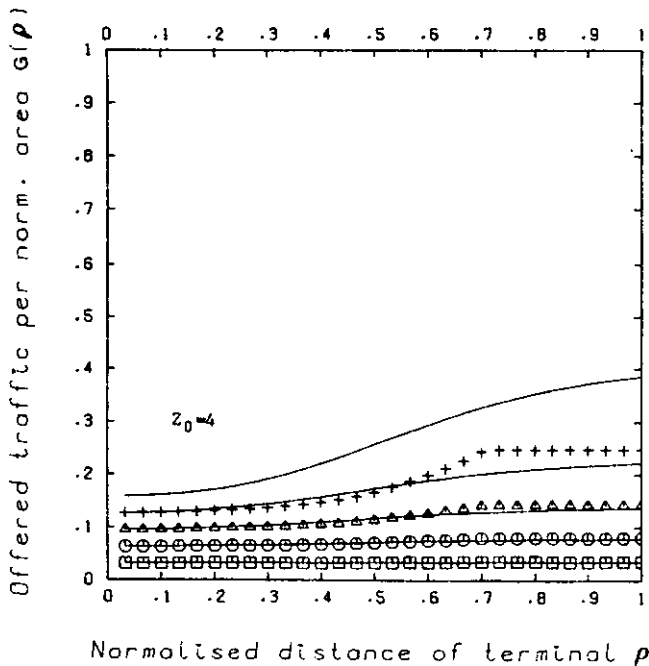
Total required offered traffic G
for a receiver threshold of $Z_0=1$ and
$Z_0=4$, respectively, as function of
the throughput S, compared with
•1 standard slotted ALOHA: $S=G \, e^{-G}$
•2 ring model (section 5.3)
•3 capture of one packet every
occupied slot: $S=1-R_0$
•4 capture of all packets: $S=G$

Traffic G(ρ) to be offered to give a homogeneous
spatial distribution of the traffic troughput S(ρ)

Incoherent addition

receiver threshold: 4.0 ( 6.0 dB )

Troffic G(ρ) to be offereᵈ to give a homogeneous
spatial distribution of the traffic troughput S(ρ)

Incoherent addition
receiver threshold:10.0 ( 10.0 dB)



Normalised distance of terminal ρ
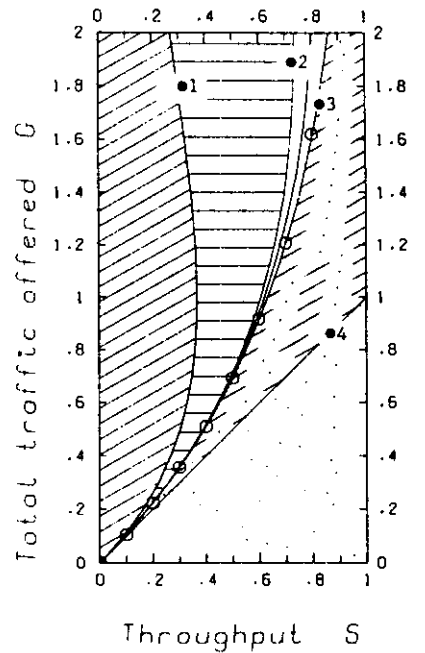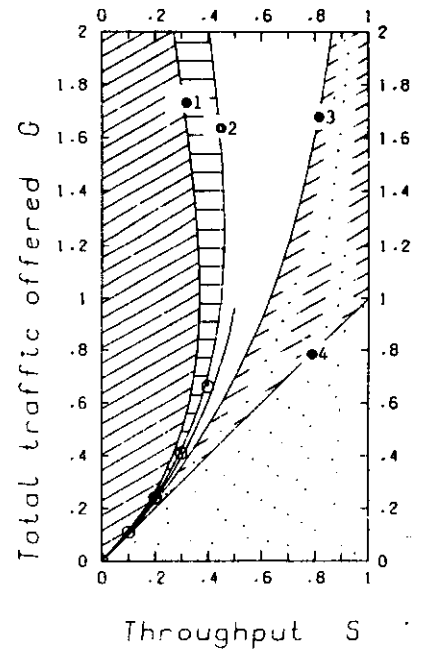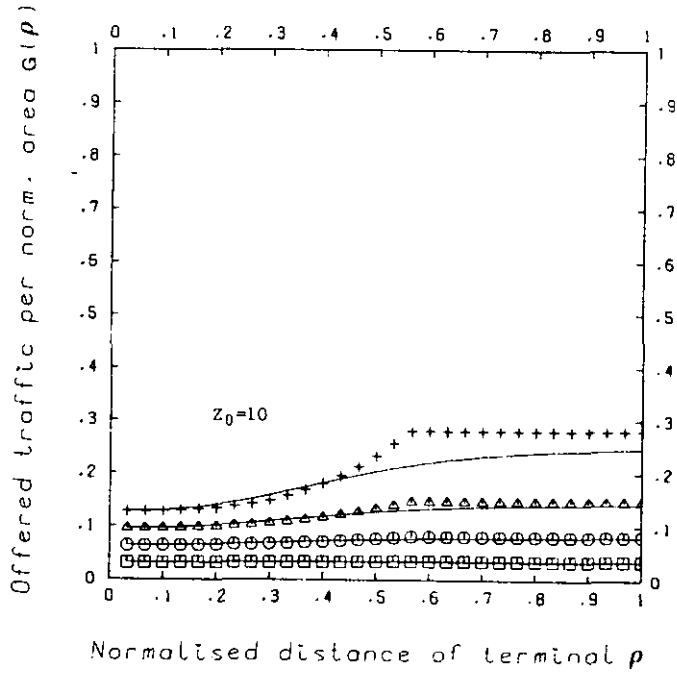
Throughput S

**Figure 5.12a:**

Spatial distribution of required
offered traffic G(ρ) for uniform
throughput S(ρ)=S/π with S=0.1, 0.2, ...
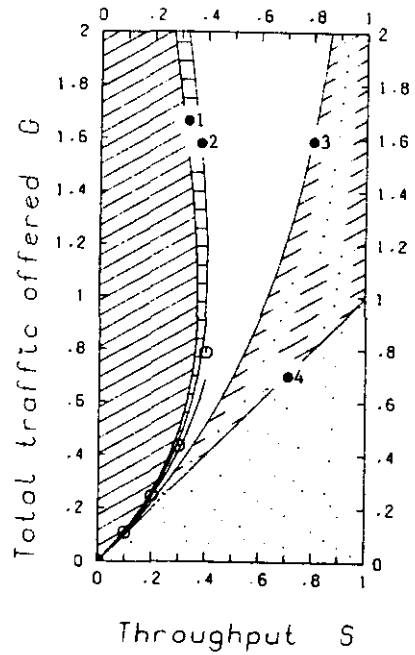
**Figure 5.12b:**

Total required offered traffic G
as function of throughput S, compared
with

●1 standard slotted ALOHA: $S = G \, e^{-G}$

●2 ring model (section 5.3)

●3 capture of one packet every
   occupied slot: $S = 1 - R_0$

●4 capture of all packets: $S = G$

## 6    COHERENT ADDITION

### 6.1    Spatial distribution of the traffic throughput

Coherent signal addition has been described in section 2.2.2. These results are now used to study the channel throughput behaviour. Arnbak and Van Blitterswijk [1] concluded that, compared with incoherent addition, the coherent addition of interfering signals promises a higher channel capacity. The model of propagation (section 2.1) and addition of interference signals will be referred to as the "coherent model". In analogy with the incoherent case we also assume a universal threshold $Z_0$ independent of n (5.3). The validity of this assumption requires further study.

In this section the spatial distribution is found by inserting the image of the joint mean power pdf (4.35) in the conditional capture probability (4.63)

$$I_{z,n}(\rho) = 1 - \rho^{-\beta} \int_0^\infty \exp\{-\rho^{-\beta}\lambda\} g^n(Z_0\lambda)d\lambda, \qquad (6.1)$$

where we have replaced the integration variable $\lambda$ by $Z_0\lambda$. With (4.68) and (6.1) the channel throughput per normalised unit area, $S(\rho)$, can be written as

$$S(\rho) = G(\rho)\left[1 - \sum_{n=1}^\infty R_n + \sum_{n=1}^\infty \{R_n\rho^{-\beta} \int_0^\infty \exp\{-\lambda\rho^{-\beta}\} g^n(Z_0\lambda)d\lambda\}\right], \qquad (6.2)$$

or, after interchanging integration and summation and using the series expansion of the exponential function

$$S(\rho) = G(\rho) e^{-G}\left[1 + \rho^{-\beta} \int_0^\infty \exp\{-\lambda\rho^{-\beta}\} \left(\exp\{G\, g(Z_0\lambda)\}-1\right) d\lambda\right]$$

$$= G(\rho)e^{-G}\rho^{-\beta} \int_0^\infty \exp\{-\lambda\rho^{-\beta} + Gg(Z_0\lambda)\}d\lambda. \qquad (6.3)$$

Three methods to analyse the spatial distribution of traffic in a mobile ALOHA network with this equation will be proposed. First, $S(\rho)$ can be found using the Gauss-Laguerre numerical integration method; a second method is provided by a formal series expansion, and the third possibility is given by Laplace transformation of the throughput density. For large traffic loads G, an asymptotic expansion of the Laplace integrals may be useful.

## 6.2 The Gauss-Laguerre numerical integration method

A substitution of $\lambda\rho^{-\beta} \overset{\Delta}{=} x$ in (6.3) yields

$$S(\rho) = G(\rho) \int_0^\infty e^{-x} \exp\{-G + Gg(Z_0\rho^\beta x)\}\, dx. \tag{6.4}$$

Integrals of this form can be calculated numerically from the Gauss-Laguerre integration method [7,(25.4.45) and table (25.9)]

$$\int_0^\infty e^{-x} f(x)\, dx = \sum_{j=1}^{m} w_j f(x_j) + R_m \tag{6.5}$$

for an m-point integration, where $w_j$ are weight factors in the sampling in the points $x_j$ and $R_m$ is the residual error.
An example of the set $(w_j, x_j)$ for a 6-point integration is given in figure 6.1 [7].

**ABSCISSAS AND WEIGHT FACTORS**

**FOR LAGUERRE INTEGRATION**

$$\int_0^\infty e^{-x} f(x)\, dx = \sum_{i=1}^{n} w_i f(x_i)$$

Abscissas = $x_i$ (Zeros of Laguerre Polynomials)
Weight Factors = $w_i$

**n=6**

| $x_i$ | $w_i$ |
|---|---|
| 0.22284 66041 79 | (-1)4.58964 673950 |
| 1.18893 21016 73 | (-1)4.17000 830772 |
| 2.99273 63260 59 | (-1)1.13373 382074 |
| 5.77514 35691 05 | (-2)1.03991 974531 |
| 9.83746 74183 83 | (-4)2.61017 202815 |
| 15.98287 39806 02 | (-7)8.98547 906430 |

Figure 6.1 [7]

Applied to (6.3) one finds

$$S(\rho) \approx G(\rho) \sum_{j=1}^{m} w_j \exp\{-G+Gg(Z_0\rho^\beta x_j)\} \qquad (6.6)$$

## 6.3 Series expansion

A formal series expansion of $S(\rho)$ can be found from

$$S(\rho) = -G(\rho) e^{-G} \int_{\lambda=0}^{\infty} \exp\{Gg(Z_0\lambda)\} \, d\, \exp\{-\rho^{-\beta}\lambda\}. \qquad (6.7)$$

After integrating by parts we can write

$$S(\rho) = G(\rho)\left[1-Z_0 e^{-G} \rho^\beta \int_{\lambda=0}^{\infty} Gg'(Z_0\lambda) \exp\{Gg(Z_0\lambda)\} \, d\, \exp\{-\rho^{-\beta}\lambda\}\right].$$

Partial integration can be repeated with integrals of the form

$$S(\rho) = G(\rho)\left[1+\ldots\ldots + \int_{\lambda=0}^{\infty} \ldots\ldots \, d\, \exp\{-\rho^{-\beta}\lambda\}\right].$$

This results in the expansion

$$S(\rho) = G(\rho)\left[1+Z_0\rho^\beta Gg'(0) + Z_0^2\rho^{2\beta}\{Gg''(0)+(Gg'(0))^2\} + \ldots\right], \qquad (6.8)$$

provided the expansion converges and $g^{(k)}(0)$ exists for all $k$. Writing the expansion (6.8) in terms of the moments $\mu_k$, we find

$$S(\rho) = G(\rho)\left[1-Z_0\rho^\beta G\mu_1 + Z_0^2\rho^{2\beta}(G\mu_2+G^2\mu_1^2) + \cdots \right.$$
$$\left. Z_0^3\rho^{3\beta}(G\mu_3-3G^2\mu_1\mu_2-G^3\mu_1^3) + \ldots\ldots \right], \qquad (6.9)$$

if all moments $\mu_k$ exist. From the normalisation (1.8) of $\bar{P}_s$, it will be clear that the moments $\mu_k$ increase with $k$, so the expansion must be restricted to sufficiently small values of $\rho$. Bounds on the moments are described by (4.28) and (4.30).

Recommendations 4.1 and 4.2

The form of the throughput per unit area $S(\rho)$ written in terms of the statistical properties (i.e., the moments $\mu_k$) of the unconditional packet power pdf, suggests that Mellin transformation of the mean power pdf might be useful. The Mellin transformation is described in Appendix C.

Writing the expansion (6.9) in terms of central moments $m_k$ (about the mean $\mu_1$) is also recommended for further study. The central moments are defined as

$$m_k \triangleq E\left((\bar{P}_s - \mu_1)^k\right) \tag{6.10}$$

and for instance $m_2 = \mu_2 - \mu_1^2$. The second central moment $m_2$ is better known as the variance $\sigma^2$.

## 6.4 The image of the spatial throughput distribution

Analogous to $g(v)$, a Laplace-transformed image function $s(v)$ of the spatial distribution of the traffic throughput can be defined as

$$s(v) \triangleq L_I^I\{S_{\bar{P}_s}(\bar{P}_s)\} = \int_0^\infty 2\pi\rho \ S(\rho) \ e^{-v\rho^{-\beta}} \ d\rho \tag{6.11}$$

This function is the Laplace image of the traffic throughput per unit of mean packet power given by

$$S_{\bar{P}_s}(\bar{P}_s = \rho^{-\beta}) \triangleq 2\pi\rho \ S(\rho) \left| \frac{d\rho}{d\bar{P}_s} \right| = \frac{2\pi}{\beta}\rho^{\beta+2} \ S(\rho). \tag{6.12}$$

As distinct from $g(v)$ and $f_{\bar{P}_s}$, the functions $s(v)$ and $S_{\bar{P}_s}$ are not normalised to unity, but to S. So, using integration (1.10),

$$s(0) = S \quad \text{and} \quad \int_0^\infty S_{\bar{P}_s}(x) \ dx = S. \tag{6.13}$$

Inserting (6.3) in definition (6.11) of the image $s(v)$, we find

$$s(v) = \int_0^\infty 2\pi\rho \; G(\rho) \; e^{-G} \; \rho^{-\beta} \int_0^\infty \exp\left\{-(\lambda+v)\rho^{-\beta} + Gg(Z_0\lambda)\right\} \; d\lambda \; d\rho.$$

By substitution of $\rho^{-\beta} = x$, using (1.14) and interchanging the order of integration

$$s(v) = Ge^{-G} \int_0^\infty \int_0^\infty f_{\frac{1}{P}_s}(x) \; x \; e^{-(\lambda+v)x} dx \quad e^{Gg(Z_0\lambda)} d\lambda.$$

The inner integral equals the derivative of the translated Laplace image $-g'(\lambda+v)$, so

$$s(v) = -Ge^{-G} \int_0^\infty g'(\lambda+v) \; \exp\left\{Gg(Z_0\lambda)\right\} \; d\lambda, \tag{6.14}$$

which gives the image function of the spatial distribution of the traffic throughput. We shall call equation (6.14) the coherent analysis equation as it provides an expression for the traffic throughput, given the traffic offered.

Recommendation 4.3

We have not found a general solution for the integral equation (6.14). A substitution of $Gg(v) \triangleq \ln\{h(v)\}$ may be useful. We then find

$$s(v) = -\int_0^\infty \frac{h'(v+\kappa)}{h(v+\kappa)} \frac{h(Z_0\kappa)}{h(0)} \; d\kappa. \tag{6.15}$$

Boundary conditions are $h(0) = e^G$ and $h(\infty) = 1$ (see (4.4) and (4.6)).

- 75 -

## 6.4.1 Special cases of the coherent analysis equation

Although general solutions are difficult to derive, some special cases of the coherent analysis equation are interesting (and easy) to derive.

In case of a light (offered) traffic load (G→0), we find

$$s(v) \to G\ g(v), \tag{6.16}$$

confirming that the effect of collisions can be neglected in this case. A similar case can be derived from $Z_0 \to 0$. In this event all packets can capture the receiver, irrespective of any overlap.

With high receiver thresholds ($Z_0 \to \infty$), we find from the analysis equation (6.14)

$$s(v) = -\int_0^\infty Ge^{-G}g'(\lambda+v)\ e^0\ d\lambda$$

$$= -Ge^{-G}\int_v^\infty g'(\kappa)\ d\kappa \qquad = G\ g(v)\ \exp\{-G\} \tag{6.17}$$

With the high-threshold receiver, an overlap will destroy all involved n+1 packets. Only packets transmitted in slots with no interfering packets (n=0) capture the receiver. The probability $R_0$ of no interference is equal for all transmitters (i.e., independant of distance $\rho$). So for $Z_0 \to \infty$ the spatial distribution of $S(\rho)$ has the same shape as $G(\rho)$, but is reduced by the loss factor $\exp\{-G\}$ for slotted ALOHA.

Recommendation 4.4

This effect has already been noticed in the incoherent case, where it is of particular influence for traffic from the boundaries of the cell, as packets generated in this region often satisfy the loss criterion (1.4) even with moderate $Z_0$. Derivation of a similar observation in the coherent case is recommended. The approximation (4.32) may be useful.

## 6.5 Asymptotic integral expansion for high traffic loads

An asymptotic expansion for high traffic loads $(G \to \infty)$ of (6.14) can be obtained by integration by parts of the Laplace integrals [38,p258]. The analysis equation is rewritten as

$$s(v) = \frac{-Ge^{-G}}{Z_0 G} \int_0^\infty \frac{g'(\lambda+v)}{g'(Z_0\lambda)} \frac{d}{d\lambda} \exp\{Gg(Z_0\lambda)\} \, d\lambda, \qquad (6.18)$$

with which the partial integration is carried out: (6.19)

$$s(v) = \frac{-e^{-G}}{Z_0} \frac{g'(\lambda+v)}{g'(Z_0\lambda)} \exp\{Gg(Z_0\lambda)\}\Big|_0^\infty + e^{-G} \int_0^\infty \exp\{Gg(Z_0\lambda)\}\frac{d}{d\lambda} \frac{g'(\lambda+v)}{g'(Z_0\lambda)} \, d\lambda.$$

This is permissible if the image function $g(v)$ is at least twice differentiable, i.e., according to (4.5) and (4.9), if at least the first and second moments $\mu_1$ and $\mu_2$ exist. (As can be seen from (4.28), this will be the case for realistic distributions, but for instance not for the (quasi-) constant distribution of example 2 in section 4.1.3.) From (4.5) and (4.9) it then follows that the conditions (3) in [38,p259] are satisfied:

$$g(Z_0\lambda) < 1 \; \big(\text{for } 0 \leq \lambda < \infty\big), \quad Z_0 \neq 0, \quad \mu_1 \neq 0 \text{ and } g'(v) \neq 0. \qquad (6.20)$$

These conditions are insufficient to ensure that the integral on the right hand of side (6.19) exists, but they can be shown [38] strong enough to ensure that

$$s(v) \approx \frac{g'(v)}{Z_0 g'(0)} = \frac{-g'(v)}{Z_0 \mu_1} \qquad \text{for } G \to \infty. \quad (6.21)$$

Reverse transformation of both sides and applying (A.1.5) yields the distribution of the mean power of the received packets

$$S_{\bar{P}_s}(\bar{P}_s) \approx \frac{\bar{P}_s}{Z_0 \mu_1} f_{\bar{P}_s}(\bar{P}_s) \qquad \text{for } G \to \infty. \quad (6.22)$$

The spatial distribution of throughput traffic can now be obtained
from (1.14) and (6.12)

$$S(\rho) \approx \frac{\rho^{-\beta}}{Z_0 \mu_1} \frac{G(\rho)}{G} \qquad \text{for } G \to \infty. \quad (6.23)$$

Integration by parts may be continued to obtain higher-order terms.
Each step introduces a new factor of $1/G$. After some algebra, which
is contained in appendix E, we find

$$s(v) = -\frac{g'(v)}{Z_0 \mu_1} - \frac{1}{G}\left[ \frac{g''(v)}{Z_0^2 \mu_1^2} + \frac{\mu_2}{\mu_1^3} \frac{g'(v)}{Z_0} \right]$$

$$+ \frac{1}{G^2}\left[ \left( \frac{-\mu_3}{\mu_1^4} + 3\frac{\mu_2^2}{\mu_1^5} \right) \frac{g'(v)}{Z_0} - \frac{\mu_2}{\mu_1^4} \frac{g''(v)}{Z_0^2} - \frac{1}{\mu_1^3} \frac{g'''(v)}{Z_0^3} \right] + \ldots$$

$$(6.24)$$

After reverse transformation to the $\rho$ domain, the spatial
distribution of throughput traffic can be found on the form

$$S_\rho(\rho) = G(\rho)\left[ a_1 \rho^{-\beta} + a_2 \rho^{-2\beta} + a_3 \rho^{-3\beta} + \ldots \right], \qquad (6.25)$$

with $a_i$ an expansion in terms of $G^{-j}$:

$$a_1 \overset{\Delta}{=} \frac{1}{Z_0 G \mu_1}\left[ 1 + \frac{1}{G}\frac{\mu_2}{\mu_1^2} + \frac{1}{G^2}\left(-3\frac{\mu_2^2}{\mu_1^4} + \frac{\mu_3}{\mu_1^3}\right) + \ldots \right]$$

$$a_2 \overset{\Delta}{=} \frac{1}{Z_0^2 G^2 \mu_1^2}\left[ -1 - \frac{1}{G}\frac{\mu_2}{\mu_1^2} + \ldots \right]$$

$$a_3 \overset{\Delta}{=} \frac{1}{Z_0^3 G^3 \mu_1^3}\left[ 1 + \ldots \right].$$

Recommendation 4.5

> The above asymptotic expansion was only derived a few weeks before
> finishing this thesis. A more detailed study is recommended.
> Derivation of a general form of the factors $a_i$ in (6.25) is
> recommended. Expansion (6.24) appears to incorporate a factor $\mu_i$ in
> its i-th term. As $\mu_i$ can increase exponentially with i,
> convergence of (6.24) remains to be shown.

## 6.6 Total traffic throughput S

We now study the special case $v=0$ in the analysis equation (6.14)

$$s(0) = -Ge^{-G} \int_0^\infty g'(\lambda) \exp\{Gg(Z_0\lambda)\} d\lambda = S, \qquad (6.26)$$

where the last equality follows from (6.13). We have thus found an expression for the total traffic throughput S. In appendix C this equation will be derived in a different way by transformation of formulas in [1].

Comparing (6.26) with the standard ALOHA throughput relation, the improvement factor of the channel throughput can be defined as

$$\eta(G,Z_0) = \int_0^\infty -g'(\lambda)\exp\{Gg(Z_0\lambda)\} d\lambda > 1 \qquad (6.27)$$

The improvement factor $\eta$ increases with G and decreases if the receiver threshold $Z_0$ increases.

Three special values of the receiver threshold have been found for which the S-G relation is independant of the spatial distribution of the traffic. Moreover, for large traffic loads ($G \to \infty$) all realistic distributions will be shown to result in the limit

$$S_\infty = \frac{1}{Z_0}.$$

Spatial distributions with unbounded moments may give other limits [1]. It will be shown that with most thresholds $Z_0$, the total throughput S depends not only on $Z_0$ and the total offered traffic G, but also on the shape of the spatial distribution of traffic.

## 6.6.1 Spatial cases of the total traffic throughput equation

- High receiver thresholds: $Z_0 \to +\infty$

   In this case formula (6.26) correctly returns to the pure ALOHA case as

$$S = G\ e^{-G}\ \int_0^{\infty} -g'(\lambda)d\lambda\ = G\ \exp(-G) \qquad (6.28)$$

   All packets experiencing overlap are lost.

- The perfect-capture receiver: $Z_0 = 1$

   We find

$$S = -\exp\{-G\}\ \exp\{Gg(\lambda)\}\Big|_{\lambda=0}^{\infty} = 1 - \exp(-G) \qquad (6.29)$$

   The Poisson character of the offered traffic gives an interpretation of this result, as precisely the part $1 - e^{-G}$ of all time slots is occupied by one or more packets. Thus all occupied slots contribute, on average, one successful packet. This is an interesting result as it means that, given perfect capture in the coherent case, increasing traffic G never leads to a decrease in channel throughput. Remarkably, the throughput S also equals the throughput (5.14) for the critical circle model. However in (6.29) we may not assume that every occupied slot contributes exactly one received packet. Some occupied slots will contribute none, while other slots may contribute, in principle, more than one packet!

- special case $Z_0 = 0$

$$S = -Ge^{-G}\ \int_0^{\infty} g'(\lambda)\ e^{G}\ d\lambda\ = G \qquad (6.30)$$

   All packets capture the receiver.

These three cases apply for any spatial distribution of the offered traffic.

## 6.6.2 Series expansion for heavy traffic loads

For other receiver thresholds, results will now be obtained by inserting $v=0$ in the formal asymptotic expansion (6.24)

$$S = \frac{1}{Z_0} + \frac{1}{G}\frac{\mu_2}{\mu_1^2}\frac{Z_0-1}{Z_0^2} - \frac{1}{G^2}\left[\frac{\mu_3 Z_0^2-1}{\mu_1^3 Z_0^3} + \frac{\mu_2^2(3Z_0+1)}{\mu_1^4 Z_0^2}\right]\ldots \quad (6.31)$$

Apparently, any spatial distribution with bounded moments has, in the coherent case, the non-zero throughput limit

$$S_\infty = \frac{1}{Z_0} \quad \text{for } G \to \infty. \quad (6.32)$$

This has been found in a special case in [1].
Writing (6.31) in terms of central moments (6.10) yields

$$S = \frac{1}{Z_0} + \frac{1}{G}\left[\frac{Z_0-1}{Z_0^2}\left(1+\frac{m_2}{\mu_1^2}\right)\right] + \ldots \quad (6.33)$$

The first-order term clearly confirms an increase in traffic throughput if the differences in received packet power are increased [2] [24].
For non-perfect capture $(Z_0 > 1)$ saturation effects occur, since $S$ decreases with $G$ for large $G$. Thus, the S-G throughput curve has an extremum $S_{max}$ with

$$S_{max} > S_\infty = \frac{1}{Z_0}. \quad (6.34)$$

Recommendation 4.6

Derivation of the general form of the i-th term of the expansion is recommended.

We now continue with some specific examples of spatial distributions of the offered traffic.

## 6.7. Ring model

In the ring model the spatial distribution of the traffic is a $\delta$-distribution [1]. All packets are received with the same mean power.

$$G(\rho) = \frac{G}{2\pi} \, \delta(\rho-1) \qquad \text{and} \qquad f_{\bar{P}_s}(\bar{P}_s) = \delta(\bar{P}_s-1).  \qquad (6.35)$$

The Laplace transform of the latter is $g(v) = \exp\{-v\}$.

### 6.7.1 Capture probability

Although the intermediate results of the probabilities $F_{z,n}$ and $I_{z,n}$ are no longer necessary to obtain the desired throughput S and its spatial distribution $S(\rho)$, these probabilities are given as an illustration. We apply the formulas (4.57) and (4.63) to find

$$F_{z,n} = 1 + \int_0^{\infty} \exp\{-(nZ_0+1)\lambda\} \; d\lambda \;=\; \frac{nZ_0}{nZ_0+1}  \qquad (6.36)$$

$$\begin{aligned} I_{z,n}(\rho) &= F_{z,n} \qquad \text{for } \rho=1 \\ \left(I_{z,n}(\rho)\right. & \qquad\qquad \text{for } \rho \neq 1 \text{ is of no interest}\big). \end{aligned}$$

These results agree with [1].

### 6.7.2 Traffic throughput

The traffic throughput image can be derived by applying the coherent analysis equation (6.14)

$$s(v) = -Ge^{-G} \int_0^{\infty} \exp\{-\lambda-v+Ge^{-Z_0\lambda}\} \; d\lambda.  \qquad (6.37)$$

The integral is given in $[8,(3.331.1)$ on p308$]$

$$s(v) = -e^{-v} \frac{Ge^{-G}}{Z_0} \; (-G)^{-Z_0^{-1}} \; \gamma(Z_0^{-1}, -G) \tag{6.38}$$

using the incomplete $\gamma$-function $\gamma(a,x) \stackrel{\Delta}{=} \int_0^x e^{-t} \, t^{a-1} \, dt.$

As might be expected we find a spatial ring distribution of the traffic throughput

$$s(v) = S \, e^{-v} \qquad \text{and thus} \quad S(\rho) = \frac{S}{2\pi} \delta(\rho-1). \tag{6.39}$$

The total throughput of the channel now becomes

$$S \stackrel{\Delta}{=} G \, e^{-G} \, \eta(G,Z_0) = \frac{-G \, e^{-G}}{Z_0} \; (-G)^{Z_0^{-1}} \; \gamma(Z_0^{-1}, -G) \tag{6.40}$$

Another standard-form solution is found by substituting $g(\lambda) \stackrel{\Delta}{=} t$ in the expression (6.26) for the total throughput:

$$S = -G \int_{t=0}^{1} t \, \exp\{G(t^{Z_0}-1)\} \, d \ln t, \tag{6.41}$$

which can be written as the integral representation $[7,(13.2.1)]$ of Kummer's function $[7,(13.1.2)]$, after substituting $t^{Z_0}-1 \stackrel{\Delta}{=} -x$

$$S = G \int_0^1 e^{-Gx} \frac{dt}{dx} \, dx = G \int_0^1 e^{-Gx} \frac{d}{dx}\left[(1-x)^{Z_0^{-1}}\right] dx. \tag{6.42}$$

One finds

$$S = G \, M(1, Z_0^{-1}+1, -G), \tag{6.43}$$

where Kummer's function can be represented by $[7,(13.1.2)]$

$$M(1, Z_0^{-1}+1, -G) \stackrel{\Delta}{=} \int_0^1 e^{-Gx} \, x^0 \, (1-x)^{Z_0^{-1}-1} \, dx.$$

A series expansion for the total traffic can be found from the slightly different substitution $G(t^{Z_0}-1) \overset{\Delta}{=} -x$ in (6.41). Partial integration then yields

$$S = G - G \int_0^G e^{-x} \left(1- \frac{x}{G}\right)^{Z_0^{-1}} dx = G - G \int_0^G e^{-x} d\left[\frac{-G}{Z_0+1} \left(1- \frac{x}{G}\right)^{Z_0^{-1}-1}\right]$$

Repeating the integration by parts leads to the series expansion

$$S= G - \frac{G^2}{Z_0^{-1}+1} + \frac{G^3}{\left(Z_0^{-1}+1\right)\left(Z_0^{-1}+2\right)} - \cdots . \tag{6.44}$$

which is the same as $[7,(13.1.2)]$. The limit $S_\infty = 1/Z_0$ is confirmed by $[7,(13.1.15)]$

$$S = \frac{1}{Z_0} \left(1 + O(G^{-1})\right). \tag{6.45}$$

The expansion has the correct limits $S=1-e^{-G}$ for $Z_0=1$ and $S=Ge^{-G}$ for $Z_0\to\infty$. As can be seen from figures 6.2 and 6.3, the first terms of the series expansion give a good approximation for G not too large. Other properties of the total throughput traffic S(G) curve, e.g. the extremum, may be found by applying the theory of confluent hypergeometric functions $[7,(13)]$.
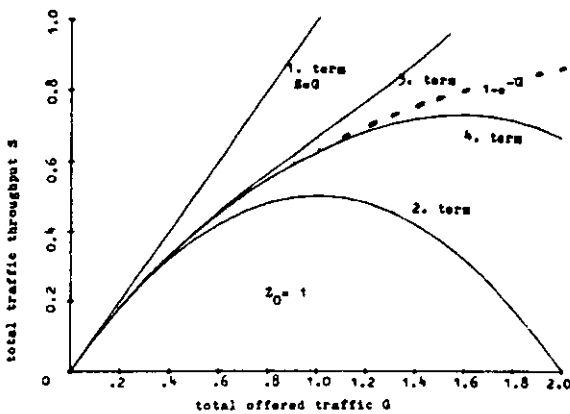


Figure 6.2: Expansion for the total traffic throughput S as a function of the offered traffic G for a perfect-capture receiver.
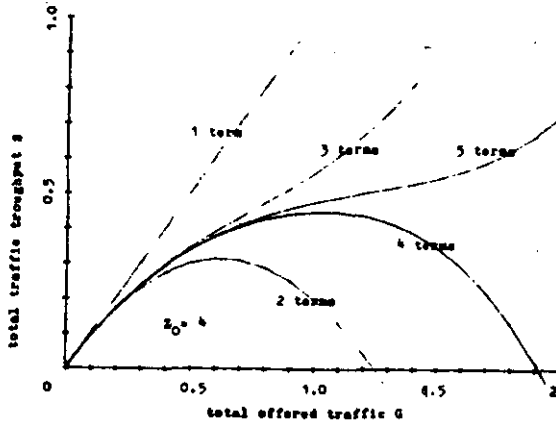
Figure 6.3: Expansion for the total traffic throughput S as a function of the offered traffic G for a receiver with threshold $Z_0 = 4$.

For large G the expansion by partial integration (6.24) is valid

$$S(\rho) = \frac{S}{2\pi}\delta(\rho-1) = \frac{\delta(\rho-1)}{2\pi}\left[\frac{1}{Z_0} + \frac{1}{G}\frac{Z_0-1}{Z_0^2} - \frac{1}{G^2}\frac{(Z_0+1)(2Z_0-1)}{Z_0^3} + ..\right]. \quad (6.46)$$

The limit $S_\infty$ is in accordance with results in $[1]$.

## 6.8  Quasi-constant traffic density

The quasi-constant traffic density $G(\rho) = \frac{G}{\pi}\exp\left\{-\frac{\pi}{4}\rho^4\right\}$, described in $[1]$ and example 1 in section 4.1.3, for $\beta=4$ has the area mean power pdf

$$f_{\bar{P}_s}(\bar{p}_s) = \frac{1}{2}\bar{p}_s^{-\frac{3}{2}}\exp\left\{\frac{-\pi}{4\bar{p}_s}\right\}, \quad (=4.13)$$

and its Laplace image has the form $[7,(29.3.82)]$

$$g(v) = \exp\left\{-\sqrt{\pi v}\right\}. \quad (=4.14)$$

Although the behaviour of a distribution with unbounded expected received power ($\mu_1 \to \infty$) has to be regarded with caution, this example does yield instructive results $[1]$.

6.8.1  Capture_probability [1]

Using the formula of the capture probability (4.57) we find

$$F_{z,n} = 1 - \int_0^\infty \sqrt{\pi} \, \exp\{-\sqrt{\pi} \, (n\sqrt{Z_0}+1) \, \sqrt{\lambda}\} \, d\lambda$$

$$= 1 - \frac{\exp\{t\}}{n\sqrt{Z_0}+1} \Big|_{t=0}^\infty = \frac{n\sqrt{Z_0}}{n\sqrt{Z_0}+1} \cdot \tag{6.47}$$

$F_{z,n}$ here has the same form as in the ring-model, if $Z_0$ in the
latter is replaced by $\sqrt{Z_0}$. This confirms the observation that only
in the events $Z_0 = 0$, 1 or $\infty$, the throughput relation (S-G) becomes
independant of the spatial distribution involved.

6.8.2  Total_traffic_throughput

The correspondance $Z_0 \rightarrow \sqrt{Z_0}$ can also be established for the total
throughput S. Applying formula (6.24), we find                     (6.48)

$$S = G \int_0^1 \exp\{G[t^{\sqrt{Z_0}}-1]\} \, dt = \frac{-G}{G^{Z_0^{-\frac{1}{2}}} Z_0^{\frac{1}{2}}} \int_0^G e^{-x}(G-x)^{Z_0^{-\frac{1}{2}}-1} dx$$

where we have substituted $\exp\{-\sqrt{\pi s}\} \triangleq t$ and $G[1-t^{Z_0^{\frac{1}{2}}}] \triangleq x$.
Erdélyi gives the solution for the integral [9,(6) p137 vol.I], so

$$S = Z_0^{-\frac{1}{2}} \, Ge^{-G} \, (-G)^{-Z_0^{-\frac{1}{2}}} \, \gamma(Z_0^{-\frac{1}{2}},-G), \tag{6.49}$$

confirming the correspondence with the ring distribution. The above
equation, using Kummer's function, thus equals

$$S = G \, M(1,Z_0^{-\frac{1}{2}}+1,-G). \tag{6.50}$$

The expansion suggested in (6.9) can not yield results due to the unbounded moments $\mu_k$. In this case, however, application of the expansion method in the previous example yields a valid result, corresponding to (6.44) with $Z_0$ replaced by $\sqrt{Z_0}$.

$$S = G - \frac{G^2}{Z_0^{-\frac{1}{2}}+1} + \frac{G^3}{\left(Z_0^{-\frac{1}{2}}+1\right)\left(Z_0^{-\frac{1}{2}}+2\right)} - \ldots]. \qquad (6.51)$$

Consequently figures 6.2 and 6.3 correspond to the cases $Z_0=1$ and $Z_0=16$, respectively, when the offered traffic has the quasi-constant density of example 1.

The expansion for large traffic loads (6.24) is not valid as $\mu_1$ is unbounded. But according to the $Z_0 \to \sqrt{Z_0}$ correspondance, this distribution has the throughput limit [1]

$$S_\infty = 1/\sqrt{Z_0}. \qquad (6.52)$$

### 6.8.3 Conditional capture probability

Spatial properties of the throughput can be derived from (4.63)

$$I_{z,n}(\rho) = 1 - \int_0^\infty \exp\left\{-\lambda - n\sqrt{\pi Z_0}\ \rho^2\sqrt{\lambda}\right\}d\lambda. \qquad (6.53)$$

We now substitute $\gamma_n \triangleq \frac{1}{2}n\sqrt{\pi Z_0}\rho^2$ and $q \triangleq \sqrt{\lambda} + \gamma_n$

$$I_{z,n}(\rho) = 1 - \int_0^\infty \exp\left\{\gamma_n^2 - q^2\right\} 2\left\{q-\gamma_n\right\} dq. \qquad (6.54)$$

By separating this into two integrals the first cancels with unity, and only the second integral remains: $\qquad\qquad (6.55)$

$$I_{z,n}(\rho) = 2\gamma_n \exp\left\{\gamma_n^2\right\} \int_{\gamma_n}^\infty \exp\left\{-q^2\right\} dq = \sqrt{\pi}\ \gamma_n \exp\left\{\gamma_n^2\right\} \mathrm{erfc}\left\{\gamma_n\right\},$$

where erfc(x) $\overset{\Delta}{=}$ 1- $\frac{2}{\sqrt{\pi}}$ $\int\limits_{x}^{\infty}$ exp$\{-t^2\}$dt $[7,(7)]$.

These results are similar to those in $[1]$, which were obtained in another way.

## 6.8.4 Spatial distribution of throughput traffic

Although the image functions have proved convenient to derive $I_{z,n}$, a closed-form solution for the spatial distribution of traffic has not been found, because

$$S(\rho)= G(\rho)\ e^{-G}\ \rho^{-4}\ \int\limits_{0}^{\infty} 2t\ \exp\{-\rho^{-4}t^2 + G\ e^{-\sqrt{\pi Z_0}t}\ \}\ dt \qquad (6.56)$$

has not been solved. Analytic calculations are difficult, as the image function g(v) has unbounded derivatives for v=0.

## 6.9 Coherent synthesis

### 6.9.1 Synthesis using the Gauss-Laguerre method

In the event of coherent addition, a synthesis method using iterative numerical computing with the Gauss-Laguerre analysis method will now be proposed. Results will be presented and discussed for perfect capture ($Z_0$=1) and for a receiver with threshold $Z_0$=4. The iteration scheme is obtained from the Gauss-Laguerre integration method described by (6.6). Analogous to the synthesis scheme for incoherent signals, the loss factor is obtained from the i-th estimate. Together with the required throughput, this gives the new estimate

$$G_{i+1}(\rho) = S(\rho)\ \frac{1}{\sum\limits_{j=1}^{m} w_j\ \exp\{-G_i+G_ig_i(Z_0\rho^\beta x_j)\}}, \qquad (6.57)$$

where, using (4.11) and (1.9), the image function expression can be written as

$$-G_i + G_i \ g_i(v) = \int_0^1 2\pi\lambda \ G_i(\lambda) \left( e^{-v\lambda^{-\beta}} - 1 \right) d\lambda \qquad (6.58)$$

The starting function is chosen as

$$G_0(\rho) \quad = \quad S(\rho).$$

The spatial distributions are sampled in N points, and from an N-point integration, the argument

$$-G_i + G_i g(Z_0\rho \ x_j)$$

of the exponent in (6.57) is obtained for each specific distance $\rho$ and summation index j. An m-term summation gives the loss factor in (6.57). As the loss factor depends on distance $\rho$, this has to be executed for all N samples to yield a new estimate $G_{i+1}(\rho)$.

Sufficiently accurate results have been obtained with an 8-term summation, 25 samples of the spatial distributions and up to 30 iteration steps. Synthesising light traffic loads required far less iterations. As in the incoherent synthesis, the iteration is terminated when the required accuracy is reached (see (5.62)); if the sequence of estimates diverges; if the total traffic to be offered $G_i$ becomes too large ($G_i > 30$ pps); or if the maximum number of M (M=30) iterations is exceeded. Processing time for coherent synthesis is approximately twenty times larger than for incoherent synthesis, partly due to the extra summation.

## 6.9.2     Uniform throughput

The programme used to synthesise uniform throughput is contained in appendix B. In figure 6.4a, the offered traffic distribution in the event of perfect capture is depicted for various throughputs

$$S(\rho) = \begin{cases} S/\pi & \text{for } 0 < \rho < 1 \\ 0 & \text{elsewhere} \end{cases},$$

with S= 0.1, 0.2, .... 0.9 packets per slot.

Comparing this figure with figure 5.10, one can -not surprisingly- conclude that coherent addition requires less traffic to be offered to yield a certain throughput than is required with incoherent addition. In figure 6.6 the required offered traffic distributions for the three models are compared in the event of perfect capture and a uniform throughput S = 0.6 packets per slot.

As can be seen in figure 6.4b, the numerically obtained total traffic relation closely follows

$$S = 1 - \exp\{-G\},$$

which was predicted by (6.29). As far as total traffic is concerned, the results of coherent modelling are the same as results from the critical circle model.

However, as can be seen in figure 6.6, the spatial distributions differ for the two models. With coherent addition, for intermediate distances $(0.3 < \rho < 0.7)$, more traffic per unit area has to be offered. This is due to signal addition in the event of more than one interferer outside the critical circle of the test packet. On the other hand, for larger distances $(\rho \rightarrow 1)$, the offered traffic required by the coherent model is less: in this area the effect of Rayleigh fading appears to have a favourable influence on the capture probability.
Information on the rate of convergence can be found in appendix B.

Results for a receiver threshold of $Z_0=4$ are depicted in figure 6.5. As can be seen in figure 6.5a, near the cell boundary $(\rho \rightarrow 1)$, the required offered traffic $G(\rho)$ becomes rather constant with disctance. Comparing this distribution with $G(\rho)$ in the event of incoherent uniform throughput in section 5.11, coherent addition yields slightly more optimistic results.

Traffic S(ρ) to be offered to give a homogeneous
spatial distribution of the traffic throughput S(ρ)

coherent addition
receiver threshold: 1.0 ( 0.0 dB)



Normalised distance of terminal ρ

Throughput  S

**Figure 6.4a(†) and 6.5a(+):**
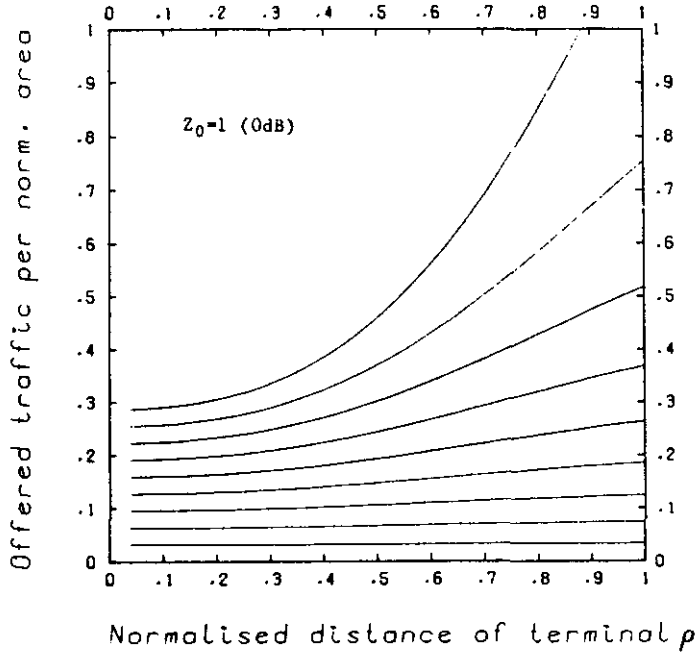
Spatial distribution of required
offered traffic G(ρ) for uniform
throughput S(ρ)=6/π with S=0.1, 0.2,
etc, for a receiver with threshold
$Z_0$=1 and $Z_0$=4, respectively.

**Figure 6.4b(†) and 6.5b(+):**
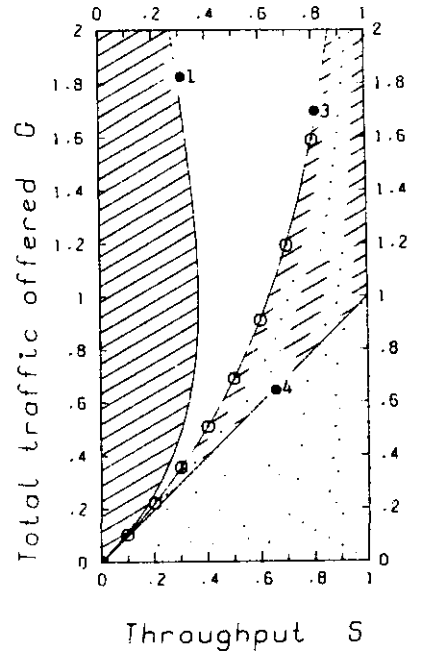
Total required offered traffic G for
receiver thresholds $Z_0$=1 and $Z_0$=4,
respectively, as function of
throughput S, compared with
●1 standard slotted ALOHA: $S=G \, e^{-G}$
●3 capture of one packet every
   occupied slot: $S=1-R_0$
●4 capture of all packets: $S=G$

Traffic G(ρ) to be offered to give a homogeneous
spatial distribution of the traffic throughput S(ρ)

coherent addition
receiver threshold: 4.0 ( 6.0 dB)



Normalised distance of terminal ρ

Throughput  S

Traffic G(ρ) to be offered to give a homogeneous
spatial distribution of the traffic troughput S(ρ)



Normalised distance of terminal ρ
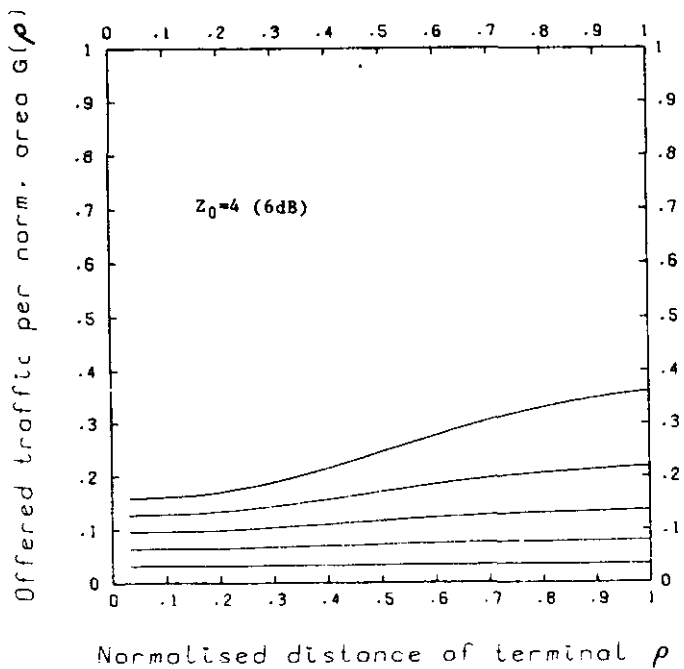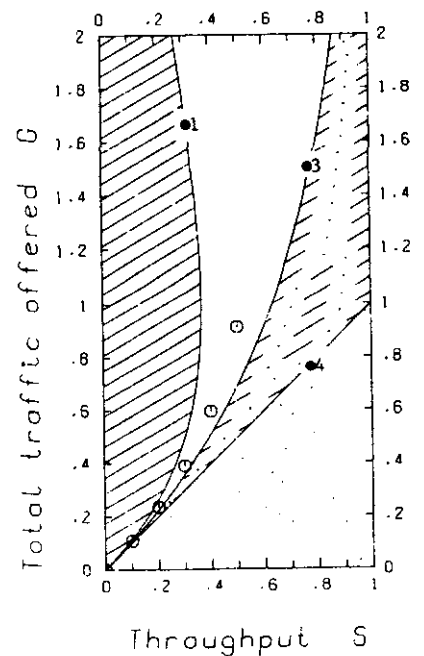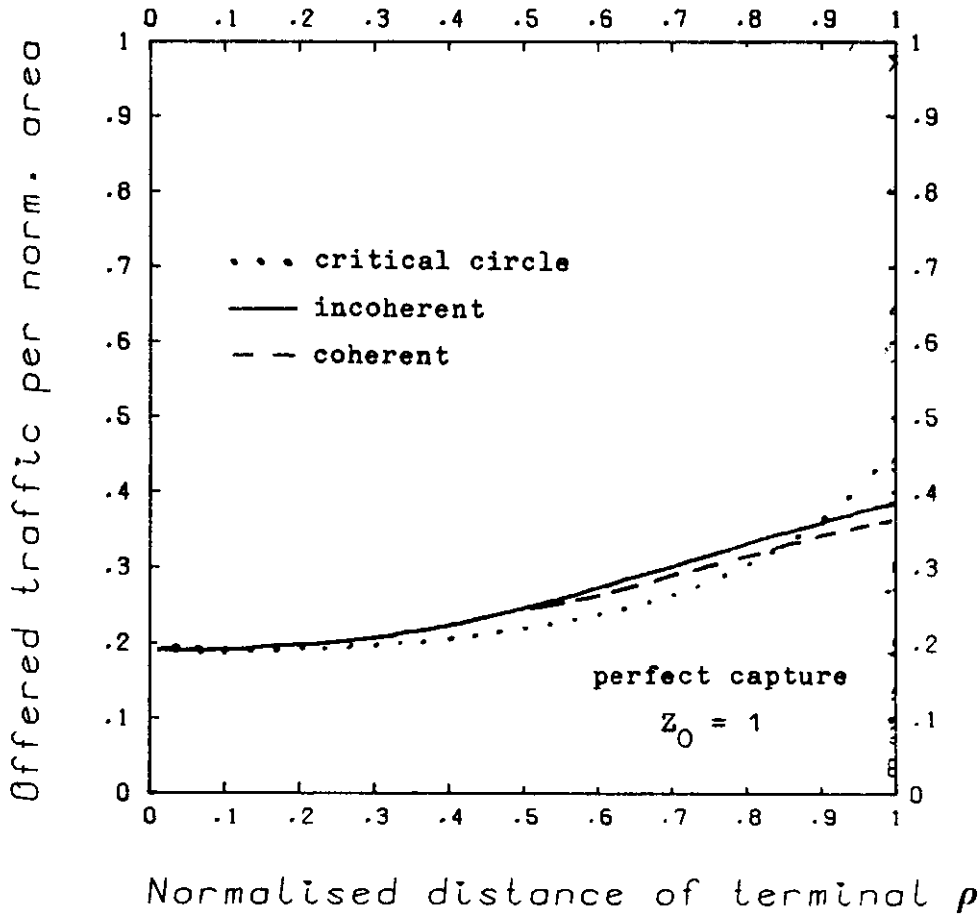
Figure 6.6: Synthesis for
various models in the event of
perfect capture. Comparison of
the traffic G(ρ) to be offered
to achieve the uniform
throughput

$$S(\rho) = 0.6/\pi \text{ ppspa,}$$

for, respectively,
••• the critical circle model,
—— the incoherent model,
– – the coherent model.

# 7   CONCLUSIONS AND RECOMMENDATIONS

The image-function approach has been shown very fertile in analysing the spatial distribution of packet traffic in a mobile cellular network. Analytic methods for analysis have been found. Extension to the synthesis problem is possible by iterative numerical computing.

In the incoherent case, general analytic results and many examples have been presented and explained. For coherently interfering signals, the analysis method obtained has been applied to a few examples. In this case, closed-form solutions are difficult to find, as integrals of exponents with complicated arguments are often involved. However, coherent transmission of the packets should be explored as the throughput will be larger than when incoherent interference is experienced. Even for heavy coherent traffic loads the theoretical limit of the throughput is non-zero. Stability of the channel is thus guaranteed.

Recommendations for further study have been given throughout this thesis, they are printed with dense characters. A summary of these recommendations is given below:

1) The introduction of a receiver threshold dependent on the number of interfering signals.

2) Derivation of coherent and incoherent analysis equations for more sophisticated propagation models, in particular with shadowing included.

3) Application of the expansion for Laplace integrals, for the incoherent analysis equation, to yield more insight in the behaviour under high traffic loads.

4) A more detailed study of the coherent addition channel. In particular:

5) Evaluation of the described coherent analysis methods using a typical offered traffic distribution. As an example, the image of the truly-constant distribution has been described in section 4.1.3. The Gauss-Laguerre method yields the throughput distribution in the $\rho$-domain. For various offered traffic loads G, this can be compared with the Taylor series (6.6) and Laurent series (6.25). Study of the convergence area of both expansions in the $\rho$ and G domain is recommended.

6) Implementation of the results in a channel control system. Packet retransmission protocols may be optimised using the developed knowledge of the behaviour of the ALOHA channel. The channel control system can measure the pdf of the received packets. This uniquely specifies the spatial distribution and the image functions. A synthesis technique is useful to gather information on the saturation of the channel and to predict congestion.

## ACKNOWLEDGEMENT

## APPENDIX A    PROPERTIES OF THE LAPLACE TRANSFORM

A.1    TABLE

| operation | image | original | |
|---|---|---|---|
| integration | $\frac{1}{v}\, h(v)$ | $\int_0^x f(\lambda)\, d\lambda$ | (A.1.1) |
| differentiation | $v\, h(v)$ | $f'(v) \overset{\Delta}{=} \frac{d}{dv}\, f(v)$ | (A.1.2) |
| convolution | $h_1(v)\, h_2(v)$ | $\int_0^x f_1(x-\lambda) f_2(\lambda)\, d\lambda$ | (A.1.3) |
| int of image | $\int_v^\infty h(\lambda)\, d\lambda$ | $\frac{1}{x}\, f(x)$ | (A.1.4) |
| diff of image | $\frac{d}{dv}\, h(v) \overset{\Delta}{=} h'(v)$ | $-xf(x)$ | (A.1.5) |
| translation | $e^{-\alpha v}\, h(v)$ | $f(x-\alpha)U(x-\alpha)\ \ \alpha>0$ | (A.1.6) |
| transl. of image | $h(v-\alpha)$ | $e^{\alpha x}\, f(x)$ | (A.1.7) |
| scaling | $h(\alpha v)$ | $\frac{1}{\alpha}\, f(\frac{x}{\alpha})$ | (A.1.8) |

## A.2 LEMMA

Assume two functions $f_1(x)$ and $f_2(w)$, with Laplace images, resp., $g_1(q)$ and $g_2(p)$, and given $f_1(x)$, $f_2(w)$ can be found from

$$f_2(w) = \int_0^\infty \frac{1}{x} \exp\left\{-\frac{w}{x}\right\} f_1(x)\, dx. \tag{A.2.1}$$

The Laplace image of $f_2(w)$ now becomes

$$g_2(p) = \frac{1}{p} \int_0^\infty \exp\left\{-\frac{q}{p}\right\} g_1(q)\, dq \tag{A.2.2}$$

A typical example of $f_1$ and $f_2$ is found in formulas concerning Rayleigh fading, e.g. (2.2). Note the different role of independent and dummy variables in (A.2.1) and (A.2.2).

**Proof:**

$$g_2(p) = \int_0^\infty \int_0^\infty \frac{1}{x} \exp\left\{-\frac{w}{x} - wp\right\} f_1(x)\, dx\, dw.$$

Integration over $w$ gives

$$g_2(p) = \int_0^\infty \frac{1}{x} \frac{f_1(x)}{p + 1/x}\, dx.$$

A temporary substitution of $y \stackrel{\Delta}{=} x + \frac{1}{p}$ gives

$$g_2(p) = \int_{1/p}^\infty \frac{1}{yp} f_1(y - \frac{1}{p})\, dy \ .$$

This can be written as a integral over $q$:

$$g_2(p) = \frac{1}{p} \int_0^\infty \int_{1/p}^\infty f_1(y - \frac{1}{p})\, e^{-yq}\, dy\, dq,$$

or $\quad g_2(p) = \frac{1}{p} \int_0^\infty \int_0^\infty f_1(x)\ \exp\left\{-q(x + \frac{1}{p})\right\} dx\, dq \tag{A.2.3}$

The integration over $q$ equals a Laplace transformation from $x$ to $p$ domain, so

$$g_2(p) = \frac{1}{p} \int_0^\infty \exp\left\{-\frac{q}{p}\right\} g_1(q)\, dq. \qquad \text{Q.E.D.}$$

## APPENDIX B: COMPUTER PROGRAMS FOR SYNTHESIS

```
100     FILE  2(TITLE="RESULTS",KIND=DISK,PROTECTION=SAVE,NEWFILE=TRUE)
200     FILE  6(KIND=REMOTE,MYUSE=OUT)
300     FILE  5(KIND=REMOTE,MYUSE=IN)
400     FILE  90(KIND=PREVIEWER)
500           BLOCK GLOBALS
600     $ INCLUDE "PLOTTER/FORTRAN/DECLARATION ON APPL"
700           END
800     $ INCLUDE "PLOTTER/FORTRAN/ALLSUBS ON APPL"
900
1000    C*************************************************************
1100    C                                                           C
1200    C          This program calculates the TRAFFIC OFFERED      C
1300    C             to an ALOHA mobile radio network              C
1400    C          which  gives a homogeneous throughput S0         C
1500    C                                                           C
1600    C*************************************************************C
1700    C                                                           C
1800    C                                                           C
1900    C       author: Jean-Paul Linnartz, may 1986                C
2000    C       Eindhoven University of Technology                  C
2100    C       Department of Electrical Engineering                C
2200    C       Telecommunications division                         C
2300    C                                                           C
2400    C*************************************************************C
2500    C                                                           C
2600    C In the incoherent case, the iteration equation for        C
2700    C synthesis of traffic to be offered is                     C
2800    C                          2 pi Z r**4                       C
2900    C G   (r)= S0  *  exp(+int(------------- 1 G (1) dl))        C
3000    C  I+1                      Z r**4 + 1**4    I               C
3100    C                                                           C
3200    C where the integral is taken from zero to one.             C
3300    C                                                           C
3400    C*************************************************************C
3500          REAL  IREAL,NREAL,WEIGHT,BOUND
3600          REAL  GT,ER,EROLD
3700          REAL  Z,S,PI,POINT,INT,L,A
3800          REAL  G,GNW,R,GABR
3900          REAL  GTOT,STOT,PURE,GAR,RING,PERF
4000          REAL  ABX,ABY
4100          DIMENSION  GTOT(11),STOT(11),GABR(1000)
4200          DIMENSION  ABX(3),ABY(3)
4300          DIMENSION  PURE(50),GAR(50),RING(50),PERF(50)
4400          DIMENSION  G(100),GNW(100),R(100)
4500          INTEGER M,N,I,II,III
4600          INTEGER K,KK,PR
4700          INTEGER OBJ1,OBJ2,OBJ3
4800          PI=3.141592
4900    C
5000          WRITE (6,100)
5100          WRITE (6,101)
5200          READ  (5,200) Z
5300          WRITE (6,104)
5400          READ  (5,210) M
5500          WRITE (6,106)
5600          READ  (5,210) N
5700           IF (N.GT.50) THEN N=50
5800           K=10
```

```
5900              IF (M.GT.30) THEN M=30
6000              WRITE (2,111) Z,K,M,N
6100              WRITE (6,150)
6200              READ  (5,151)
6300               NREAL=N*1.
6400      C
6500     100    FORMAT(" calculation of traffic offered to the channel",/)
6600     101    FORMAT("    receiver/modulation threshold Z0 =   ",/)
6700     102    FORMAT("    total traffic throughput S= ",/)
6800     103    FORMAT("     max number of curves in plot",/)
6900     104    FORMAT("    M, max number of iterations =    ",/)
7000     106    FORMAT("    N, number of samples in spatial distrib.=   ",/)
7100     111    FORMAT(" Z0= ",F10.5," K=   ",I3," M,N= ",2I3,/)
7200     110    FORMAT(" ")
7300     113    FORMAT("Fading and power add model")
7400     112    FORMAT("Critical surface model")
7500     150    FORMAT(" Do you want convergence info on terminal? Y=1",/)
7600     151    FORMAT(I1)
7700     200    FORMAT(F10.5)
7800     210    FORMAT(I3)
7900      C
8000      C*********************************************************
8100      C
8200             KK=0
8300             STOT(1)=0.
8400             GTOT(1)=0.
8500     3000   KK=KK+1
8600              EROLD=1000000
8700      C    new parameter S; new curve
8800             S=0.10 * KK/PI
8900             STOT(KK+1)=0.1*KK
9000             WRITE (2,113)
9100             WRITE (2,2010) KK,STOT(KK+1),S
9200      C
9300      C
9400             DO 400  III=1,N
9500             IREAL=III*1.
9600             R(III)=IREAL/N
9700     400    G(III)=S
9800      C
9900              I=0
10000    1000    I=I+1
10100            ER=0.
10200            GT=0.
10300     C
10400     C******** calculation of a new distibution of G(r) *************
10500     C
10600             DO 900  II=1,N
10700     C       per sample point we calculate the integral
10800             INT=0.
10900             A= Z * (R(II)**4)
11000     C
11100                DO 800  III=1,N-1
11200     C          N samples of integrand
11300                IREAL=III * 1.
11400                L=IREAL/N
11500                POINT= A*2.*PI*L*G(III)
11600                INT=INT+POINT/(A+L**4)
11700    800         CONTINUE
11800                INT = INT+A*PI*G(N)/(A+1)
11900     C
12000                INT= INT / N
```

```
12100                 IF (INT.GT.30) GOTO 3100
12200                 GNW(II) = S * EXP(INT)
12300        900       CONTINUE
12400     C
12500     C**********************************************************
12600     C
12700     C***** total traffic and convergence control ************
12800                 DO 950 II=1,N-1
12900                 IREAL=II * 1.
13000                 GT=GT+ (IREAL * G(II) / N)
13100                 ER=ER+ ABS( (GNW(II)-G(II))/G(II) )
13200        950       G(II) = GNW(II)
13300                 G(N) = GNW(N)
13400                 GT=2.*PI*GT/N
13500                 GT=GT+ PI*G(N)/N
13600                 GTOT(KK+1)=GT
13700                 ER=ER*100./N
13800                 IF(PR.EQ.1) WRITE(6,2005) I,ER,GT
13900                 WRITE(2,2005) I,ER,GT
14000     C          test on divergence:
14100                 IF(ER.GT.EROLD) GOTO 3100
14200                 EROLD=ER
14300     C
14400     C
14500                 IF (I.LT.M .AND. ER.GT.0.001) GOTO 1000
14600     C          make another iteration
14700                 IF (I.EQ.M) WRITE (2,2006)
14800                 IF(PR.EQ.1) WRITE(6,2001)
14900                 WRITE(2,2001)
15000     C
15100     C          **************** OUTPUT OF RESULTS ************
15200     C
15300       2000     FORMAT(2X,I5,1X,F10.5,1X,4F10.5)
15400       2001     FORMAT(" ")
15500       2005     FORMAT(" iteration ",I2," dev",F9.3," %  Gtot= ",F10.6)
15600       2006     FORMAT("  MAX NUMBER OF ITERATIONS !"  )
15700       2010     FORMAT("*** plot ",I3," with total traffic S= ",
15800           $    F6.3,", distributed ", F6.4," per area ***")
15900       2020     FORMAT(" ! Exponent overflow !   end of calculation")
16000     C
16100     C
16200                 CALL CURVDZ(90,0,0,15,15,1,N,R,G,
16300           $    10,0,1,10,0,1,.FALSE.,.FALSE.)
16400     C
16500                 IF (GT.LT.4  .AND. KK.LT.K)  GOTO 3000
16600     C          make another plot with higher traffic load
16700     C
16800     C********* the total traffic S-G curve  ******************
16900     C
17000       3100     IF (INT.GT.30) WRITE (2,2020)
17100     C
17200                 CALL CURVDZ(90,15,0,25,15,1,KK,STOT,GTOT,
17300           $    10,0.,1.,10,0.,2., .FALSE.,.FALSE.)
17400     C
17500     C*******************************************************************C
17600     C                                                                  C
17700     C     If fading and power addition are neglected, the              C
17800     C     traffic to be offered can be calculated from the             C
17900     C     critical surface model presented by Abramson.                C
18000     C                                                                  C
18100     C*******************************************************************C
18200     C                                                                  C
```

```
18300   C                                                              C
18400   C G    (r)= SO  *  exp(+int( 2 pi 1 G (1) d1))                 C
18500   C  I+1                                      I                  C
18600   C                                                              C
18700   C where the integral is taken from zero to a.                  C
18800   C                                                              C
18900   C********** CRITICAL SURFACE MODEL BY ABRAMSON *************C
19000   C
19100          WRITE (6,114)
19200          WRITE (2,114)
19300     114  FORMAT("*******************************************")
19400   C
19500          REAL GTOTA
19600          DIMENSION GTOTA(11)
19700          KK=0
19800          A=SQRT(SQRT(Z))
19900          GTOTA(1)=0.
20000     6000 KK=KK+1
20100          EROLD=1000000
20200   C      new parameter S; new curve
20300          S=0.10 * KK/PI
20400          WRITE (2,112)
20500          WRITE (2,2010) KK,STOT(KK+1),S
20600   C
20700   C
20800             DO 3400  III=1,N
20900             IREAL=III*1.
21000             R(III)=IREAL/NREAL
21100     3400    G(III)=S
21200   C
21300          I=0
21400     4000 I=I+1
21500          ER=0.
21600          GT=0.
21700   C
21800   C******* calculation of a new distibution of G(r) ************
21900   C
22000          DO 3900  II=1,N
22100   C      per sample point we calculate the integral
22200          BOUND= A*II
22300          IF(BOUND.GT.NREAL) BOUND=NREAL
22400   C      No traffic offered outside cell
22500          INT=0.
22600          III=1
22700          IREAL= III *1.
22800     3800    CONTINUE
22900   C        samples of integrand
23000            WEIGHT= BOUND - IREAL + 0.5
23100            IF(WEIGHT.GE.1.) WEIGHT = 1.
23200            IF(WEIGHT.LE.0.) GOTO 3850
23300            INT=INT+2.*PI*IREAL*G(III)*WEIGHT
23400            III=III+1
23500            IREAL=III *1.
23600            GOTO 3800
23700     3850    CONTINUE
23800   C
23900   C
24000   C
24100   C
24200          INT= INT /(NREAL**2)
24300          IF (INT.GT.30) GOTO 6100
24400          GNW(II) = S * EXP(INT)
```

```
24500      3900      CONTINUE
24600    C
24700    C
24800    C*******************************************************
24900    C
25000    C***** total traffic and convergence control *************
25100              DO 3950 II=1,N-1
25200              IREAL=II * 1.
25300              GT=GT+ (IREAL * G(II) /NREAL)
25400              ER=ER+ ABS( (GNW(II)-G(II))/G(II) )
25500      3950    G(II) = GNW(II)
25600              G(N) = GNW(N)
25700    C
25800              GT=2.*PI*GT/NREAL
25900              GT=GT+ PI*G(N)/NREAL
26000              GTOTA(KK+1)=GT
26100              ER=ER*100./NREAL
26200              IF(PR.EQ.1)WRITE(6,2005) I,ER,GT
26300              WRITE(2,2005) I,ER,GT
26400    C
26500              IF(ER.GT.EROLD) GOTO 6100
26600              EROLD=ER
26700    C
26800              IF (I.LT.M .AND. ER.GT.0.001) GOTO 4000
26900    C         make another iteration
27000              IF (I.EQ.M) WRITE (2,2006)
27100              IF(PR.EQ.1) WRITE(6,2001)
27200              WRITE(2,2001)
27300    C
27400    C         **************** OUTPUT OF RESULTS ************
27500              DO 3960 III = 1,N
27600      3960    GABR((KK-1)*N+III)=G(III)
27700    C
27800    C
27900              IF (GT.LT.4. .AND. KK.LT.K) GOTO 6000
28000    C         make another plot with higher traffic load
28100      6100    IF (INT.GT.30) WRITE (2,2020)
28200    C
28300              CALL MPNTDZ(90,0,0,15,15,1,N,1,KK*N,R,GABR,
28400         $    10,0.,1.,10,0.,1.,.FALSE.,.FALSE.)
28500    C
28600    C********* the total traffic S-G curve ******************
28700    C
28800              CALL NEWOBJ(OBJ3)
28900              CALL PNTSDZ(90,15,0,25,15,1,KK,STOT,GTOTA,
29000         $    10,0.,1.,10,0.,2., .FALSE.,.FALSE.)
29100    C
29200              DO 8888 II=1,21
29300              GT=(II-1.)/10.
29400              GAR(II)=2.5+5* GT
29500              GAR(21+II)=12.5-5.*GT
29600              PURE(II)=17.5+5.* GT*EXP(-1.*GT)
29700              PURE(21+II)=17.5
29800              PERF(II)=22.5 - 5.*EXP(-1.*GT)
29900              PERF(21+II)=22.5
30000              A=-1.*Z*GT/ (Z+1.)
30100              RING(II)=17.5+5.*GT*EXP(A)
30200              RING(43-II)=PURE(II)
30300      8888    CONTINUE
30400    C
30500                  ABX(1)=17.5
30600                  ABY(1)= 2.5
```

```
30700                     ABX(2)=22.5
30800                     ABY(2)= 7.5
30900                     ABX(3)=22.5
31000                     ABY(3)= 2.5
31100    C
31200                     A=10.*ALOG10(Z)
31300                     CALL FILPOL(OBJ3,1,42,PURE,GAR,"A",30,0.25)
31400                     CALL FILPOL(OBJ3,1,42,RING,GAR,"A",0.,0.35)
31500                     CALL FILPOL(OBJ3,1,32,PERF,GAR,"D",30,0.25)
31600                     CALL FILPOL(OBJ3,1,3,ABX,ABY,"B",30,0.25)
31700                     CALL POLYGN(OBJ3,1,42,PURE,GAR,1)
31800                     CALL POLYGN(OBJ3,1,21,PERF,GAR,1)
31900                     CALL POLYGN(OBJ3,1,2,ABX,ABY,1)
32000                     CALL POLYGN(OBJ3,1,42,RING,GAR,1)
32100                     CALL COTEXT(OBJ3,16.3,2.5,90,.35,5,
32200    $           "Total traffic offered  G")
32300                     CALL COTEXT(OBJ3,2.2,1. ,0.,,32,5,
32400    $           "Normalised distance of terminal")
32500                     CALL COTEXT(OBJ3,1, 2.2 ,90,.32,5,
32600    $           "Offered traffic per norm. area S( )")
32700                     CALL COTEXT(OBJ3,17.9,1.,0,.35,5,
32800    $           "Throughput   S")
32900                     CALL COTEXT(OBJ3,.5,15 ,0,0.8,0,
33000    $           "SYNTHESIS")
33100                     CALL COTEXT(OBJ3,.52 ,15 ,0,0.8,0,
33200    $           "SYNTHESIS")
33300                     CALL COTEXT(OBJ3,.5,14.4 ,0,.25,0,
33400    $           "Traffic G( ) to be offered to give a homogeneous")
33500                     CALL COTEXT(OBJ3,.5,14.0 ,0,.25,0,
33600    $           "spatial distribution of the traffic troughput S( )")
33700                     CALL COTEXT(OBJ3,14.5,14.7 ,0,.40,5,
33800    $           "Incoherent addition")
33900                     CALL COTEXT(OBJ3,14.5,14.0 ,0,.27,5,
34000    $           "receiver threshold:     (     dB)")
34100                     CALL CONNUM(OBJ3,19.6,14,0,0.27,5,"F4.1",DBLE(Z))
34200                     CALL CONNUM(OBJ3,21.4,14,0,0.27,5,"F4.1",DBLE(A))
34300                     CALL DRAWOB(90,OBJ3,0,0,25,20)
34400                     CALL DISPOB(OBJ3)
34500    C
34600                 CLOSE(2,DISP=CRUNCH)
34700                 STOP
34800                 END
34900    C********************************************************
```

```
100     FILE  2(TITLE="RESULTS",KIND=DISK,PROTECTION=SAVE,NEWFILE=TRUE)
200     FILE  6(KIND=REMOTE,MYUSE=OUT)
300     FILE  5(KIND=REMOTE,MYUSE=IN)
400     FILE  90(KIND=PREVIEWER)
500             BLOCK GLOBALS
600   $ INCLUDE "PLOTTER/FORTRAN/DECLARATION ON APPL"
700             END
800   $ INCLUDE "PLOTTER/FORTRAN/ALLSUBS ON APPL"
900
1000    C****************************************************************
1100    C                                                              C
1200    C         This program calculates the TRAFFIC OFFERED          C
1300    C            to an ALOHA mobile radio network                  C
1400    C         which  gives a homogenoous throughput SO             C
1500    C                                                              C
1600    C***************************************************************C
1700    C                                                              C
1800    C                                                              C
1900    C     author: Jean-Paul Linnartz, OCTOBER 1986                 C
2000    C     Eindhoven University of Technology                       C
2100    C     Department of Electrical Engineering                     C
2200    C     Telecommunications division                             C
2300    C                                                              C
2400    C***************************************************************C
2500    C                                                              C
2600    C In the COHERENT case, the iteration equation for             C
2700    C synthesis of traffic to be offered is obtained               C
2800    C from the Gauss-Laguerre numerical integration                C
2900    C method                                                       C
3000    C                                                              C
3100    C                                                              C
3200    C                                                              C
3300    C                                                              C
3400    C***************************************************************C
3500            REAL IREAL,IIIRL,IMAGE
3600            REAL GT,ER,EROLD,NREAL
3700            REAL Z,S,PI,POINT,INT,A, SAREA
3800            REAL G,GNW,R,GABR,TERM,SUM
3900            REAL GTOT,STOT,PURE,GAR,RING,PERF
4000            REAL ABX,ABY,X,W,ARG,GTNEW
4100            DIMENSION GTOT(11),STOT(11),GABR(1000)
4200            DIMENSION ABX(3),ABY(3)
4300            DIMENSION PURE(50),GAR(50),RING(50),PERF(50)
4400            DIMENSION G(100),GNW(100),R(100),X(20),W(20)
4500            INTEGER M,N,I,II,III,L,LL
4600            INTEGER K,KK,PR,NN
4700            INTEGER OBJ1,OBJ2,OBJ3
4800            PI=3.141592
4900    C
5000            WRITE (6,100)
5100            WRITE (6,101)
5200            READ  (5,200) Z
5300            WRITE (6,104)
5400            READ  (5,210) M
5500            WRITE (6,106)
5600            READ  (5,210) N
5700             IF (N.GT.50) THEN N=50
5800             K=10
```

```
5900                  IF (M.GT.30) THEN M=30
6000                  WRITE (2,111) Z,K,M,N
6100                  WRITE (6,150)
6200                  READ  (5,151) PR
6300                   IF(S.GT.1) S=1.
6400                 NREAL=N*1.
6500        C
6600                     NN=0
6700        100  FORMAT(" calculation of traffic offered to the channel",/)
6800        101  FORMAT("     receiver/modulation threshold ZO =  ",/)
6900        102  FORMAT("     total traffic throughput S= ",/)
7000        103  FORMAT("      max number of curves in plot",/)
7100        104  FORMAT("     M, max number of iterations =   ",/)
7200        106  FORMAT("     N, number of samples in spatial distrib.=   ",/)
7300        111  FORMAT(" ZO= ",F10.5," K=   ",I3," M,N= ",2I3,/)
7400        110  FORMAT(" ")
7500        113  FORMAT("COHERENT ADDITION     model")
7600        C112 FORMAT("")
7700        114  FORMAT("     S, TOTAL TRAFFIC THROUGHPUT =    ",/)
7800        150  FORMAT(" Do you want convergence info on terminal? Y=1",/)
7900        151  FORMAT(I1)
8000        200  FORMAT(F10.5)
8100        210  FORMAT(I3)
8200        220  FORMAT(F10.5)
8300        C
8400        C*************************************************
8500        C
8600        C
8700        C******** calculation of a new distibution of G(r) ************
8800                 X(1)=0.1702796323
8900                 X(2)=0.9037017767
9000                 X(3)=2.2510866298
9100                 X(4)=4.2667001702
9200                 X(5)=7.0459054023
9300                 X(6)=10.7585160101
9400                 X(7)=15.7406786412
9500                 X(8)=22.8631317368
9600                  W(1)=3.69188589342*.1**1
9700                  W(2)=4.18786780814*.1**1
9800                  W(3)=1.75794986637*.1**1
9900                  W(4)=3.33434922612*.1**2
10000                 W(5)=2.79453623523*.1**3
10100                 W(6)=9.07650877336*.1**5
10200                 W(7)=8.48574671627*.1**7
10300                 W(8)=1.04800117487*.1**9
10400       3000     NN=NN+1
10500       C
10600                STOT(1)=0.
10700                GTOT(1)=0.
10800                 S=NN*0.1
10900                 EROLD=1000000
11000       C      new parameter S; new curve
11100                SAREA=S/PI
11200                WRITE (2,113)
11300                WRITE (2,2010) NN,S,SAREA
11400                GTNEW=S
11500                 STOT(NN+1) = S
11600       C
11700                DO 400  III=1,N
11800                IREAL=III*1.
11900                R(III)=IREAL/NREAL
12000       400      G(III)=SAREA
```

```
12100     C
12200            KK=0
12300     1000   KK=KK+1
12400            ER=0.
12500     C      NEW ITERATION
12600          GT=GTNEW
12700          DO 600 I=1,N
12800     C    For every sample point
12900          IREAL=I*1.
13000          SUM=0.
13100            DO 700 II=1,8
13200     C      summing Gauss-Laguerre
13300            IMAGE=0.
13400              DO 800 III=1,N-1
13500     C        Calculate image function point
13600              IIIRL=III*1.
13700              ARG=-1.*Z * ((IREAL/IIIRL)**4) * X(II)
13800              IMAGE=IMAGE+2.*PI*IIIRL*G(III)*(EXP(ARG)-1.)
13900     800    CONTINUE
14000              ARG=-1.*Z*((IREAL/NREAL)**4)*X(II)
14100              IMAGE=IMAGE+PI*G(N)*(EXP(ARG)-1.)
14200              IMAGE=IMAGE/ (NREAL**2)
14300          TERM= W(II) * EXP(IMAGE)
14400          SUM= SUM + TERM
14500     700    CONTINUE
14600          GNW(I)= SAREA / SUM
14700     600  CONTINUE
14800     C
14900     C
15000     C**********************************************************
15100     C
15200     C***** total traffic and convergence control ************
15300     C
15400            GTNEW=0.
15500            DO 950 II=1,N-1
15600            IREAL=II * 1.
15700            GTNEW=GTNEW+ (IREAL * GNW(II) / NREAL)
15800            ER=ER+ ABS( (GNW(II)-G(II))/G(II) )
15900     950    G(II) = GNW(II)
16000            G(N)=GNW(N)
16100            GTNEW=2.*PI*GTNEW /NREAL
16200            GTNEW=GTNEW+PI*GNW(N)/(NREAL)
16300             GTOT(NN+1)=GTNEW
16400            ER=ER*100./NREAL
16500            IF(PR.EQ.1) WRITE(6,2005) KK,ER,GTNEW
16600            WRITE(2,2005) KK,ER,GTNEW
16700     C      test on divergence:
16800            IF(ER.GT.EROLD) GOTO 3100
16900            EROLD=ER
17000     C
17100     C
17200          IF(KK.LT.M.AND.ER.GT.0.001.AND.GTNEW.LT.30)GOTO 1000
17300     C      make another iteration
17400            IF (KK.EQ.M) WRITE (2,2006)
17500            IF(PR.EQ.1) WRITE(6,2001)
17600            WRITE(2,2001)
17700     C
17800     C      *************** OUTPUT OF RESULTS ************
17900     C
18000     2000   FORMAT(2X,I5,1X,F10.5,1X,4F10.5)
18100     2001   FORMAT(" ")
18200     2005   FORMAT(" iteration ",I2," dev",F9.3," % Gtot= ",F10.6)
```

```
18300      2006    FORMAT("  MAX NUMBER OF ITERATIONS !"  )
18400      2010    FORMAT("*** plot ",I3," with total traffic S= ",
18500        $     F6.3,", distributed ", F6.4," per area ***")
18600      2020    FORMAT(" ! Exponent overflow !   end of calculation")
18700      C
18800      C
18900              CALL CURVDZ(90,0,0,15,15,1,N,R,G,
19000        $     10,0,1,10,0,1,.FALSE.,.FALSE.)
19100      C
19200              IF(NN.LT.10.AND.GTNEW.LT.30.) GOTO 3000
19300      C       make another plot with higher traffic load
19400      C
19500      C********  the total traffic S-G curve  ******************
19600      C
19700      3100    IF (INT.GT.30) WRITE (2,2020)
19800      C
19900              CALL PNTSDZ(90,15,0,25,15,1,NN,STOT,GTOT,
20000        $     10,0.,1.,10,0.,2., .FALSE.,.FALSE.)
20100      C
20200      C
20300      C********  the total traffic S-G curve  ******************
20400      C
20500              CALL NEWOBJ(OBJ3)
20600      C
20700      C
20800      C
20900              DO 8888 II=1,21
21000              GT=(II-1.)/10.
21100              GAR(II)=2.5+5* GT
21200              GAR(21+II)=12.5-5.*GT
21300              PURE(II)=17.5+5.* GT*EXP(-1.*GT)
21400              PURE(21+II)=17.5
21500              PERF(II)=22.5 - 5.*EXP(-1.*GT)
21600              PERF(21+II)=22.5
21700      8888    CONTINUE
21800      C
21900              ABX(1)=17.5
22000              ABY(1)= 2.5
22100              ABX(2)=22.5
22200              ABY(2)= 7.5
22300              ABX(3)=22.5
22400              ABY(3)= 2.5
22500      C
22600              A=10.*ALOG10(Z)
22700              CALL FILPOL(OBJ3,1,42,PURE,GAR,"A",30,0.25)
22800              CALL FILPOL(OBJ3,1,42,RING,GAR,"A",0.,0.35)
22900              CALL FILPOL(OBJ3,1,32,PERF,GAR,"D",30,0.25)
23000              CALL FILPOL(OBJ3,1,3,ABX,ABY,"B",30,0.25)
23100              CALL POLYGN(OBJ3,1,42,PURE,GAR,1)
23200              CALL POLYGN(OBJ3,1,21,PERF,GAR,1)
23300              CALL POLYGN(OBJ3,1,2,ABX,ABY,1)
23400              CALL COTEXT(OBJ3,16.3,2.5,90,.35,5,
23500        $     "Total traffic offered  G")
23600              CALL COTEXT(OBJ3,2.5,1. ,0.,.34,5,
23700        $     "Normalised distance of terminal")
23800              CALL COTEXT(OBJ3,1, 2.4 ,90,.34,5,
23900        $     "Offered traffic per norm. area")
24000              CALL COTEXT(OBJ3,17.9,1.,0,.35,5,
24100        $     "Throughput  S")
24200              CALL COTEXT(OBJ3,.5,15 ,0,1.1,0,
24300        $     "SYNTHESIS")
24400              CALL COTEXT(OBJ3,.525,15 ,0,1.1,0,
```

```
24500          $    "SYNTHESIS")
24600               CALL COTEXT(OBJ3,.5,14.4 ,0,.25,0,
24700          $    "Traffic G(r) to be offered to give a homogeneous")
24800               CALL COTEXT(OBJ3,.5,14.0 ,0,.25,0,
24900          $    "spatial distribution of the traffic troughput S(r)")
25000               CALL COTEXT(OBJ3,14.5,14.7 ,0,.40,5,
25100          $    "coherent addition")
25200               CALL COTEXT(OBJ3,14.5,14.0 ,0,.27,5,
25300          $    "receiver threshold:     (    dB)")
25400               CALL CONNUM(OBJ3,19.6,14,0,0.27,5,"F4.1",DBLE(Z))
25500               CALL CONNUM(OBJ3,21.4,14,0,0.27,5,"F4.1",DBLE(A))
25600               CALL DRAWOB(90,OBJ3,0,0,25,20)
25700               CALL DISPOB(OBJ3)
25800     C
25900               CLOSE(2,DISP=CRUNCH)
26000               STOP
26100               END
26200     C*********************************************************
```

RESULTS
DATE & TIME PRINTED: TUESDAY, NOVEMBER 18, 1986 @ 11:04:48.

```
 100    ZO=    1.00000 K=    10 M,N=   30 30
 200
 300    Fading and power add model
 400    *** plot   1  with traffic S=  0.100, i.e. 0.0318 per area
 500       iteration  1  dev    3.464 %  Gtot=   0.100272
 600       iteration  2  dev    0.130 %  Gtot=   0.105167
 700       iteration  3  dev    0.005 %  Gtot=   0.105373
 800       iteration  4  dev    0.000 %  Gtot=   0.105381
 900
1000    Fading and power add model
1100    *** plot   2  with traffic S=  0.200, i.e. 0.0637 per area
1200       iteration  1  dev    7.120 %  Gtot=   0.201133
1300       iteration  2  dev    0.535 %  Gtot=   0.221372
1400       iteration  3  dev    0.044 %  Gtot=   0.223190
1500       iteration  4  dev    0.004 %  Gtot=   0.223344
1600       iteration  5  dev    0.000 %  Gtot=   0.223357
1700
1800    Fading and power add model
1900    *** plot   3  with traffic S=  0.300, i.e. 0.0955 per area
2000       iteration  1  dev   10.980 %  Gtot=   0.302656
2100       iteration  2  dev    1.245 %  Gtot=   0.349776
2200       iteration  3  dev    0.164 %  Gtot=   0.356560
2300       iteration  4  dev    0.022 %  Gtot=   0.357489
2400       iteration  5  dev    0.003 %  Gtot=   0.357614
2500       iteration  6  dev    0.000 %  Gtot=   0.357631
2600
2700    Fading and power add model
2800    *** plot   4  with traffic S=  0.400, i.e. 0.1273 per area
2900       iteration  1  dev   15.056 %  Gtot=   0.404919
3000       iteration  2  dev    2.297 %  Gtot=   0.491695
3100       iteration  3  dev    0.427 %  Gtot=   0.509563
3200       iteration  4  dev    0.083 %  Gtot=   0.513103
3300       iteration  5  dev    0.016 %  Gtot=   0.513797
3400       iteration  6  dev    0.003 %  Gtot=   0.513932
3500       iteration  7  dev    0.001 %  Gtot=   0.513959
3600
3700    Fading and power add model
3800    *** plot   5  with traffic S=  0.500, i.e. 0.1592 per area
3900       iteration  1  dev   19.362 %  Gtot=   0.508013
4000       iteration  2  dev    3.738 %  Gtot=   0.648636
4100       iteration  3  dev    0.925 %  Gtot=   0.687639
4200       iteration  4  dev    0.244 %  Gtot=   0.698231
4300       iteration  5  dev    0.065 %  Gtot=   0.701092
4400       iteration  6  dev    0.018 %  Gtot=   0.701863
4500       iteration  7  dev    0.005 %  Gtot=   0.702072
4600       iteration  8  dev    0.001 %  Gtot=   0.702128
4700       iteration  9  dev    0.000 %  Gtot=   0.702143
4800
4900    Fading and power add model
5000    *** plot   6  with traffic S=  0.600, i.e. 0.1910 per area
5100       iteration  1  dev   23.913 %  Gtot=   0.612034
5200       iteration  2  dev    5.629 %  Gtot=   0.822356
5300       iteration  3  dev    1.786 %  Gtot=   0.898176
5400       iteration  4  dev    0.623 %  Gtot=   0.925624
5500       iteration  5  dev    0.224 %  Gtot=   0.935621
5600       iteration  6  dev    0.082 %  Gtot=   0.939274
5700       iteration  7  dev    0.030 %  Gtot=   0.940612
5800       iteration  8  dev    0.011 %  Gtot=   0.941102
```

| 5900 | iteration | 9 | dev | 0.004 % | Gtot= | 0.941281 |
| 6000 | iteration | 10 | dev | 0.001 % | Gtot= | 0.941347 |
| 6100 | iteration | 11 | dev | 0.001 % | Gtot= | 0.941371 |
| 6200 | | | | | | |

6300 Fading and power add model
6400 *** plot   7  with traffic S=  0.700, i.e. 0.2228 per area

| 6500 | iteration | 1 | dev | 28.724 % | Gtot= | 0.717092 |
| 6600 | iteration | 2 | dev | 8.049 % | Gtot= | 1.014928 |
| 6700 | iteration | 3 | dev | 3.203 % | Gtot= | 1.151445 |
| 6800 | iteration | 4 | dev | 1.455 % | Gtot= | 1.216557 |
| 6900 | iteration | 5 | dev | 0.701 % | Gtot= | 1.248495 |
| 7000 | iteration | 6 | dev | 0.347 % | Gtot= | 1.264422 |
| 7100 | iteration | 7 | dev | 0.174 % | Gtot= | 1.272434 |
| 7200 | iteration | 8 | dev | 0.088 % | Gtot= | 1.276483 |
| 7300 | iteration | 9 | dev | 0.044 % | Gtot= | 1.278535 |
| 7400 | iteration | 10 | dev | 0.022 % | Gtot= | 1.279575 |
| 7500 | iteration | 11 | dev | 0.011 % | Gtot= | 1.280103 |
| 7600 | iteration | 12 | dev | 0.006 % | Gtot= | 1.280371 |
| 7700 | iteration | 13 | dev | 0.003 % | Gtot= | 1.280507 |
| 7800 | iteration | 14 | dev | 0.001 % | Gtot= | 1.280576 |
| 7900 | iteration | 15 | dev | 0.001 % | Gtot= | 1.280611 |
| 8000 | | | | | | |

8100 Fading and power add model
8200 *** plot   8  with traffic S=  0.800, i.e. 0.2546 per area

| 8300 | iteration | 1 | dev | 33.812 % | Gtot= | 0.823308 |
| 8400 | iteration | 2 | dev | 11.100 % | Gtot= | 1.228858 |
| 8500 | iteration | 3 | dev | 5.471 % | Gtot= | 1.462178 |
| 8600 | iteration | 4 | dev | 3.240 % | Gtot= | 1.608971 |
| 8700 | iteration | 5 | dev | 2.122 % | Gtot= | 1.707961 |
| 8800 | iteration | 6 | dev | 1.479 % | Gtot= | 1.778146 |
| 8900 | iteration | 7 | dev | 1.075 % | Gtot= | 1.829732 |
| 9000 | iteration | 8 | dev | 0.805 % | Gtot= | 1.868661 |
| 9100 | iteration | 9 | dev | 0.616 % | Gtot= | 1.898626 |
| 9200 | iteration | 10 | dev | 0.479 % | Gtot= | 1.922042 |
| 9300 | iteration | 11 | dev | 0.378 % | Gtot= | 1.940557 |
| 9400 | iteration | 12 | dev | 0.301 % | Gtot= | 1.955334 |
| 9500 | iteration | 13 | dev | 0.241 % | Gtot= | 1.967214 |
| 9600 | iteration | 14 | dev | 0.195 % | Gtot= | 1.976822 |
| 9700 | iteration | 15 | dev | 0.158 % | Gtot= | 1.984629 |
| 9800 | iteration | 16 | dev | 0.129 % | Gtot= | 1.990998 |
| 9900 | iteration | 17 | dev | 0.105 % | Gtot= | 1.996210 |
| 10000 | iteration | 18 | dev | 0.086 % | Gtot= | 2.000486 |
| 10100 | iteration | 19 | dev | 0.071 % | Gtot= | 2.004002 |
| 10200 | iteration | 20 | dev | 0.058 % | Gtot= | 2.006898 |
| 10300 | iteration | 21 | dev | 0.048 % | Gtot= | 2.009286 |
| 10400 | iteration | 22 | dev | 0.040 % | Gtot= | 2.011258 |
| 10500 | iteration | 23 | dev | 0.033 % | Gtot= | 2.012888 |
| 10600 | iteration | 24 | dev | 0.027 % | Gtot= | 2.014237 |
| 10700 | iteration | 25 | dev | 0.023 % | Gtot= | 2.015353 |
| 10800 | iteration | 26 | dev | 0.019 % | Gtot= | 2.016277 |
| 10900 | iteration | 27 | dev | 0.015 % | Gtot= | 2.017043 |
| 11000 | iteration | 28 | dev | 0.013 % | Gtot= | 2.017678 |
| 11100 | iteration | 29 | dev | 0.011 % | Gtot= | 2.018205 |
| 11200 | iteration | 30 | dev | 0.009 % | Gtot= | 2.018642 |
| 11300 | MAX NUMBER OF ITERATIONS ! | | | | | |
| 11400 | | | | | | |

11500 Fading and power add model
11600 *** plot   9  with traffic S=  0.900, i.e. 0.2865 per area

| 11700 | iteration | 1 | dev | 39.195 % | Gtot= | 0.930813 |
| 11800 | iteration | 2 | dev | 14.917 % | Gtot= | 1.467247 |
| 11900 | iteration | 3 | dev | 9.076 % | Gtot= | 1.852430 |
| 12000 | iteration | 4 | dev | 7.119 % | Gtot= | 2.177232 |

```
12100          iteration  5   dev    6.689 %  Gtot=   2.495494
12200          iteration  6   dev    7.366 %  Gtot=   2.856995
12300          *********************************************
12400     Critical surface model
12500     *** plot    1  with traffic S=  0.100, i.e. 0.0318 per area
12600          iteration  1   dev    3.263 %  Gtot=   0.100351
12700          iteration  2   dev    0.094 %  Gtot=   0.105196
12800          iteration  3   dev    0.002 %  Gtot=   0.105363
12900          iteration  4   dev    0.000 %  Gtot=   0.105367
13000
13100     Critical surface model
13200     *** plot    2  with traffic S=  0.200, i.e. 0.0637 per area
13300          iteration  1   dev    6.722 %  Gtot=   0.201476
13400          iteration  2   dev    0.388 %  Gtot=   0.221605
13500          iteration  3   dev    0.020 %  Gtot=   0.223094
13600          iteration  4   dev    0.001 %  Gtot=   0.223176
13700
13800     Critical surface model
13900     *** plot    3  with traffic S=  0.300, i.e. 0.0955 per area
14000          iteration  1   dev   10.393 %  Gtot=   0.303499
14100          iteration  2   dev    0.900 %  Gtot=   0.350614
14200          iteration  3   dev    0.073 %  Gtot=   0.356241
14300          iteration  4   dev    0.005 %  Gtot=   0.356745
14400          iteration  5   dev    0.000 %  Gtot=   0.356781
14500
14600     Critical surface model
14700     *** plot    4  with traffic S=  0.400, i.e. 0.1273 per area
14800          iteration  1   dev   14.290 %  Gtot=   0.406558
14900          iteration  2   dev    1.658 %  Gtot=   0.493865
15000          iteration  3   dev    0.189 %  Gtot=   0.508914
15100          iteration  4   dev    0.018 %  Gtot=   0.510872
15200          iteration  5   dev    0.002 %  Gtot=   0.511073
15300          iteration  6   dev    0.000 %  Gtot=   0.511091
15400
15500     Critical surface model
15600     *** plot    5  with traffic S=  0.500, i.e. 0.1592 per area
15700          iteration  1   dev   18.430 %  Gtot=   0.510812
15800          iteration  2   dev    2.694 %  Gtot=   0.653347
15900          iteration  3   dev    0.406 %  Gtot=   0.686791
16000          iteration  4   dev    0.053 %  Gtot=   0.692798
16100          iteration  5   dev    0.006 %  Gtot=   0.693650
16200          iteration  6   dev    0.001 %  Gtot=   0.693750
16300
16400     Critical surface model
16500     *** plot    6  with traffic S=  0.600, i.e. 0.1910 per area
16600          iteration  1   dev   22.831 %  Gtot=   0.616442
16700          iteration  2   dev    4.054 %  Gtot=   0.831532
16800          iteration  3   dev    0.778 %  Gtot=   0.897994
16900          iteration  4   dev    0.134 %  Gtot=   0.914074
17000          iteration  5   dev    0.020 %  Gtot=   0.917151
17100          iteration  6   dev    0.003 %  Gtot=   0.917634
17200          iteration  7   dev    0.000 %  Gtot=   0.917699
17300
17400     Critical surface model
17500     *** plot    7  with traffic S=  0.700, i.e. 0.2228 per area
17600          iteration  1   dev   27.512 %  Gtot=   0.723654
17700          iteration  2   dev    5.797 %  Gtot=   1.031599
17800          iteration  3   dev    1.382 %  Gtot=   1.154696
17900          iteration  4   dev    0.306 %  Gtot=   1.194556
18000          iteration  5   dev    0.060 %  Gtot=   1.204865
18100          iteration  6   dev    0.010 %  Gtot=   1.207048
18200          iteration  7   dev    0.002 %  Gtot=   1.207440
```

```
18300        iteration  8  dev    0.000 %  Gtot=   1.207501
18400
18500   Critical surface model
18600   *** plot    8  with traffic S=  0.800, i.e. 0.2546 per area
18700        iteration  1  dev   32.494 %  Gtot=   0.832681
18800        iteration  2  dev    8.003 %  Gtot=   1.257793
18900        iteration  3  dev    2.339 %  Gtot=   1.476384
19000        iteration  4  dev    0.663 %  Gtot=   1.572337
19100        iteration  5  dev    0.170 %  Gtot=   1.606849
19200        iteration  6  dev    0.039 %  Gtot=   1.617073
19300        iteration  7  dev    0.008 %  Gtot=   1.619635
19400        iteration  8  dev    0.001 %  Gtot=   1.620195
19500        iteration  9  dev    0.000 %  Gtot=   1.620305
19600
19700   Critical surface model
19800   *** plot    9  with traffic S=  0.900, i.e. 0.2865 per area
19900        iteration  1  dev   37.799 %  Gtot=   0.943788
20000        iteration  2  dev   10.778 %  Gtot=   1.516050
20100        iteration  3  dev    3.847 %  Gtot=   1.897526
20200        iteration  4  dev    1.406 %  Gtot=   2.134865
20300        iteration  5  dev    0.490 %  Gtot=   2.264832
20400        iteration  6  dev    0.158 %  Gtot=   2.326285
20500        iteration  7  dev    0.046 %  Gtot=   2.351645
20600        iteration  8  dev    0.012 %  Gtot=   2.361034
20700        iteration  9  dev    0.003 %  Gtot=   2.364253
20800        iteration 10  dev    0.001 %  Gtot=   2.365305
20900
21000   Critical surface model
21100   *** plot   10  with traffic S=  0.000, i.e. 0.3183 per area
21200        iteration  1  dev   43.452 %  Gtot=   1.057276
21300        iteration  2  dev   14.270 %  Gtot=   1.815075
21400        iteration  3  dev    6.255 %  Gtot=   2.488961
21500        iteration  4  dev    3.040 %  Gtot=   3.164621
21600        iteration  5  dev    1.546 %  Gtot=   3.967802
21700        iteration  6  dev    0.808 %  Gtot=   5.354789
21800        iteration  7  dev    0.433 %  Gtot=  11.621261
21900        iteration  8  dev    0.239 %  Gtot= **********
22000   ! Exponent overflow !   end of calculation
```

RESULTS
DATE & TIME PRINTED: TUESDAY, NOVEMBER 18, 1986 @ 11:17:27.

```
 100     Z0=    1.00000 K=    10 M,N=   30 30
 200
 300     COHERENT ADDITION     model
 400     *** plot   1  with traffic S=  0.100, i.e. 0.0318 per area
 500        iteration  1   dev    3.439 %  Gtot=   0.105108
 600        iteration  2   dev    0.125 %  Gtot=   0.105319
 700        iteration  3   dev    0.005 %  Gtot=   0.105327
 800        iteration  4   dev    0.000 %  Gtot=   0.105327
 900
1000     COHERENT ADDITION     model
1100     *** plot   2  with traffic S=  0.200, i.e. 0.0637 per area
1200        iteration  1   dev    7.046 %  Gtot=   0.220999
1300        iteration  2   dev    0.509 %  Gtot=   0.222827
1400        iteration  3   dev    0.040 %  Gtot=   0.222974
1500        iteration  4   dev    0.003 %  Gtot=   0.222986
1600        iteration  5   dev    0.000 %  Gtot=   0.222987
1700
1800     COHERENT ADDITION     model
1900     *** plot   3  with traffic S=  0.300, i.e. 0.0955 per area
2000        iteration  1   dev   10.828 %  Gtot=   0.348569
2100        iteration  2   dev    1.169 %  Gtot=   0.355270
2200        iteration  3   dev    0.144 %  Gtot=   0.356130
2300        iteration  4   dev    0.018 %  Gtot=   0.356238
2400        iteration  5   dev    0.002 %  Gtot=   0.356252
2500        iteration  6   dev    0.000 %  Gtot=   0.356254
2600
2700     COHERENT ADDITION     model
2800     *** plot   4  with traffic S=  0.400, i.e. 0.1273 per area
2900        iteration  1   dev   14.795 %  Gtot=   0.488777
3000        iteration  2   dev    2.123 %  Gtot=   0.506078
3100        iteration  3   dev    0.363 %  Gtot=   0.509229
3200        iteration  4   dev    0.064 %  Gtot=   0.509791
3300        iteration  5   dev    0.011 %  Gtot=   0.509891
3400        iteration  6   dev    0.002 %  Gtot=   0.509909
3500        iteration  7   dev    0.000 %  Gtot=   0.509912
3600
3700     COHERENT ADDITION     model
3800     *** plot   5  with traffic S=  0.500, i.e. 0.1592 per area
3900        iteration  1   dev   18.956 %  Gtot=   0.642650
4000        iteration  2   dev    3.396 %  Gtot=   0.679548
4100        iteration  3   dev    0.757 %  Gtot=   0.688541
4200        iteration  4   dev    0.177 %  Gtot=   0.690693
4300        iteration  5   dev    0.042 %  Gtot=   0.691205
4400        iteration  6   dev    0.010 %  Gtot=   0.691327
4500        iteration  7   dev    0.002 %  Gtot=   0.691356
4600        iteration  8   dev    0.001 %  Gtot=   0.691362
4700
4800     COHERENT ADDITION     model
4900     *** plot   6  with traffic S=  0.600, i.e. 0.1910 per area
5000        iteration  1   dev   23.319 %  Gtot=   0.811287
5100        iteration  2   dev    5.019 %  Gtot=   0.881096
5200        iteration  3   dev    1.398 %  Gtot=   0.903097
5300        iteration  4   dev    0.418 %  Gtot=   0.909928
5400        iteration  5   dev    0.128 %  Gtot=   0.912041
5500        iteration  6   dev    0.039 %  Gtot=   0.912694
5600        iteration  7   dev    0.012 %  Gtot=   0.912896
5700        iteration  8   dev    0.004 %  Gtot=   0.912958
5800        iteration  9   dev    0.001 %  Gtot=   0.912977
```

```
5900          iteration 10   dev     0.000 %   Gtot=   0.912983
6000
6100     COHERENT ADDITION      model
6200     *** plot    7  with traffic S=  0.700, i.e. 0.2228 per area
6300          iteration   1   dev    27.895 %   Gtot=   0.995863
6400          iteration   2   dev     7.026 %   Gtot=   1.117571
6500          iteration   3   dev     2.378 %   Gtot=   1.166145
6600          iteration   4   dev     0.888 %   Gtot=   1.185379
6700          iteration   5   dev     0.344 %   Gtot=   1.192990
6800          iteration   6   dev     0.135 %   Gtot=   1.196003
6900          iteration   7   dev     0.053 %   Gtot=   1.197196
7000          iteration   8   dev     0.021 %   Gtot=   1.197669
7100          iteration   9   dev     0.008 %   Gtot=   1.197856
7200          iteration 10   dev     0.003 %   Gtot=   1.197930
7300          iteration 11   dev     0.001 %   Gtot=   1.197960
7400          iteration 12   dev     0.001 %   Gtot=   1.197971
7500
7600     COHERENT ADDITION      model
7700     *** plot    8  with traffic S=  0.800, i.e. 0.2546 per area
7800          iteration   1   dev    32.695 %   Gtot=   1.197634
7900          iteration   2   dev     9.461 %   Gtot=   1.397677
8000          iteration   3   dev     3.813 %   Gtot=   1.497506
8100          iteration   4   dev     1.744 %   Gtot=   1.547551
8200          iteration   5   dev     0.844 %   Gtot=   1.572799
8300          iteration   6   dev     0.419 %   Gtot=   1.585591
8400          iteration   7   dev     0.211 %   Gtot=   1.592087
8500          iteration   8   dev     0.107 %   Gtot=   1.595391
8600          iteration   9   dev     0.054 %   Gtot=   1.597072
8700          iteration 10   dev     0.027 %   Gtot=   1.597928
8800          iteration 11   dev     0.014 %   Gtot=   1.598364
8900          iteration 12   dev     0.007 %   Gtot=   1.598586
9000          iteration 13   dev     0.004 %   Gtot=   1.598699
9100          iteration 14   dev     0.002 %   Gtot=   1.598756
9200          iteration 15   dev     0.001 %   Gtot=   1.598785
9300
9400     COHERENT ADDITION      model
9500     *** plot    9  with traffic S=  0.900, i.e. 0.2865 per area
9600          iteration   1   dev    37.728 %   Gtot=   1.417942
9700          iteration   2   dev    12.374 %   Gtot=   1.732506
9800          iteration   3   dev     5.849 %   Gtot=   1.927448
9900          iteration   4   dev     3.237 %   Gtot=   2.051208
10000         iteration   5   dev     1.941 %   Gtot=   2.131409
10100         iteration   6   dev     1.218 %   Gtot=   2.184148
10200         iteration   7   dev     0.785 %   Gtot=   2.219172
10300         iteration   8   dev     0.515 %   Gtot=   2.242584
10400         iteration   9   dev     0.341 %   Gtot=   2.258304
10500         iteration 10   dev     0.228 %   Gtot=   2.268889
10600         iteration 11   dev     0.153 %   Gtot=   2.276031
10700         iteration 12   dev     0.103 %   Gtot=   2.280856
10800         iteration 13   dev     0.069 %   Gtot=   2.284119
10900         iteration 14   dev     0.047 %   Gtot=   2.286327
11000         iteration 15   dev     0.032 %   Gtot=   2.287821
11100         iteration 16   dev     0.021 %   Gtot=   2.288833
11200         iteration 17   dev     0.015 %   Gtot=   2.289519
11300         iteration 18   dev     0.010 %   Gtot=   2.289983
11400         iteration 19   dev     0.007 %   Gtot=   2.290297
11500         iteration 20   dev     0.005 %   Gtot=   2.290510
11600         iteration 21   dev     0.003 %   Gtot=   2.290654
11700         iteration 22   dev     0.002 %   Gtot=   2.290752
11800         iteration 23   dev     0.001 %   Gtot=   2.290818
11900         iteration 24   dev     0.001 %   Gtot=   2.290863
12000
```

```
12100     COHERENT ADDITION     model
12200     *** plot  10  with traffic S=  1.000, i.e. 0.3183 per area
12300       iteration  1  dev   43.006 %  Gtot=   1.658219
12400       iteration  2  dev   15.825 %  Gtot=   2.136255
12500       iteration  3  dev    8.674 %  Gtot=   2.503141
12600       iteration  4  dev    5.748 %  Gtot=   2.800184
12700       iteration  5  dev    4.254 %  Gtot=   3.052267
12800       iteration  6  dev    3.387 %  Gtot=   3.274786
12900       iteration  7  dev    2.844 %  Gtot=   3.477861
13000       iteration  8  dev    2.489 %  Gtot=   3.668657
13100       iteration  9  dev    2.255 %  Gtot=   3.852674
13200       iteration 10  dev    2.105 %  Gtot=   4.034522
13300       iteration 11  dev    2.018 %  Gtot=   4.218452
13400       iteration 12  dev    1.983 %  Gtot=   4.408773
13500       iteration 13  dev    1.994 %  Gtot=   4.610267
```

Appendix C <u>ALTERNATIVE DERIVATIONS OF EXPRESSIONS OBTAINED DURING</u>
<u>THE PREPARATION OF THIS THESIS</u>

Although not of great additional value, appendix C has a historical
value to the author as it describes the (roundabout) way the
results of this thesis have been derived.

The image-function approach to find spatial distributions stems
from an attempt to formally prove that any spatial distribution of
traffic yields a higher throughput than a $\delta$-distribution, for which
all packets have the same area mean power. This proof was intended
to give the observation that increasing the differences in received
packet power increases capacity of the multiple access channel a
more formal basis. A proof was not found, but it soon appeared that
Laplace transformation provides a very useful method to analyse the
spatial distribution of traffic.

One of the first results was the derivation of the probability of
loss $F_{z,n}$ in the coherent case, later followed by an analogous
expression for $I_{z,n}$. Both original calculations are in appendix C.
They start off with expressions used by Arnbak and Van Blitterswijk
in [1]. Their model of propagation, spatial traffic distribution
and interference signal addition plays a key role in this thesis.
The ring and quasi-constant distributions described have been used
as verification of equations derived in this paper.

The neat form of the coherent analysis equation giving the relation
between images of traffic offered and throughput was surprising.
However, despite many efforts to solve the equation, general
solutions have not been found. Professor R. Prasad proposed the
Gauss-Laguerre numerical integration method which can be used for
analysis (find $S(\rho)$, given $G(\rho)$). Eventually its possibility to
support iterative computing for synthesis was recognised.

With coherent addition, simple analytic solutions are not likely to
be found in both analysis and synthesis, as even simple examples
usually result in non-standard integrals. It must, however, be said
that a lot of time was lost in trying to solve integrals having a
singularity in the point $v=0$.

Only after comparing Laplace transforms with characteristic functions, the background of this problem was understood.

Compared with coherent addition, the incoherent case was more straightforward to derive and image functions could easily be removed in the results. Many examples have been included.

The very neat universal expression found for the conditional probability of loss $I_{z,n}$, containing an image function sampled in a point $v=Z_0\rho^\beta$, explained the succes of using image functions. These appear to be useful to resolve the problem of convolutions in the power domain. The mathematical way of modelling Rayleigh fading by an exponential pdf yields equations which can be transformed quite easily.

Only a few weeks before finishing this thesis, the asymptotic expansion for high traffic loads was found. The derivation has been carried out, but application of the results is left as a recommendation.

In the following sections the relation with $[1]$ is indicated as the expressions were originally derived from $[1,(28)]$ and $[1,(40)]$.

## C.1   Incoherent addition

$I_{z,n}(\rho)$ can be expressed in terms of the image function $\phi(v)$ by Laplace transformation from the w to v domain. The variable z will not be transformed. We start off with the relation (4.47) describing the joint interference power pdf and its image

$$\phi^n(v) \qquad \overset{L_I^I}{\leftarrow} \qquad f_{P_n}^i(w). \qquad\qquad (C.1)$$

Translation by $z\rho^\beta$ in the v domain gives

$$\phi^n(v+z\rho^\beta) \qquad \overset{L_I^I}{\leftarrow} \qquad f_{P_n}^i(w)\, e^{-zw\rho^\beta}. \qquad\qquad (C.2)$$

Multiplication by w of the original, corresponds to a $\left(\frac{-d}{dv}\right)$-differentiation of the image (A.1.5)

$$-\frac{d}{dv}\,\rho^{\beta}\,\phi^{n}(v+z\rho^{\beta}) \quad \leftarrow L_I^I \quad \rightarrow \quad w\rho^{\beta}\,f_{P_n}^i(w)e^{-zw\rho^{\beta}} \qquad (C.3)$$

$$-n\rho^{\beta}\phi^{n-1}(v+z\rho^{\beta})\,\phi'(v+z\rho^{\beta}) \quad \leftarrow L_I^I \quad \rightarrow \quad w\rho^{\beta}\,f_{P_n}^i(w)e^{-zw\rho^{\beta}} \qquad (C.4)$$

Integration over z of both original and image gives

$$-\phi^{n}(v+z\rho^{\beta})\,\Big|_{z=0}^{Z_0} \quad \leftarrow L \quad \rightarrow \quad \int_0^{Z_0}dz\;w\rho^{\beta}\,f_{P_n}^i(w)\;e^{-zw\rho^{\beta}} \qquad (C.5)$$

Integration of the original from zero to infinity over w now yields $I_{z,n}(\rho)$, as this integration equals the definition (4.3) of Laplace transforms for v=0

$$I_{z,n}(\rho) = 1 - \phi^{n}(Z_0\rho^{\beta}), \qquad \text{which equals (5.1).}$$

## C.2 Coherent addition

We assume coherent addition of interfering packets. This means that the random phase terms of the signals hardly vary during the capture time $t_w$, so wideband phase modulation or large Doppler frequency shifts are not incorporated in the model.
As Arnbak and van Blitterswijk have shown, for a channel with uncorrelated Rayleigh fading for all packets, the conditional probability of loss for a packet in the presence of n other packets is [1(28)]

$$F_{z,n} = \text{Prob}\{\text{loss}|n,Z_0\} = \int\limits_0^{\infty}\!\!\int\limits_0^{\infty} f_{\bar{P}_n}(\bar{P}_n)f_{\bar{P}_s}(\bar{P}_s)\,\frac{Z_0\bar{P}_n}{Z_0\bar{P}_n+\bar{P}_s}d\bar{P}_n d\bar{P}_s \;. \qquad (C.6)$$

Given a normalised receiver distance $\rho$ at which the test packet is transmitted with n contenders in the same timeslot, $I_{z,n}(\rho)$ gives the probability that the packet will not capture the common receiver, with threshold $Z_0$. Equation [1,(40)] indicates that for a noiseless channel with uncorrelated Rayleigh fading for the n+1 packets, in the coherent case [1,(40)]

$$\text{Prob}\{\text{loss}|n,Z_0,\rho\} \triangleq I_{z,n}(\rho) = \int_0^{\infty} f_{\bar{P}_n}(\bar{P}_n)\frac{Z_0\bar{P}_n}{Z_0\bar{P}_n+\rho^{-\beta}}\,d\bar{P}_n. \qquad (C.7)$$

## C.2.1 Channel throughput in the coherent case

We now concentrate on the calculation of $F_{z,n}$. The double integral in $[1,(28)]$ equals a two-dimensional Laplace transform considered in the origin of the image variables $(u,v)=(0,0)$. The $L^{II}$-image of the integrand can be written in terms of the image $g(v)$ of the pdf of $\bar{P}_s$. In the two-dimensional plane we consider operations imposed upon the Laplace pair

$$g^n(u)\,g(v) \quad \xleftarrow{L^{II}_I}\rightarrow \quad f_{\bar{P}_s}(y)\,f_{\bar{P}_n}(x). \qquad (C.8)$$

Starting with scaling of the $(u{\rightarrow}x)$ variable pair

$$g^n(Z_0 u)g(v) \quad \xleftarrow{L^{II}_I}\rightarrow \quad \frac{1}{Z_0}\,f_{\bar{P}_n}(\frac{x}{Z_0})f_{\bar{P}_s}(y). \qquad (C.9)$$

Voelker and Doetsch $[4,(46)$ at page $159]$ give the correspondence

$$\int_u^\infty g^n(Z_0\lambda)g(v+\lambda+u)d\lambda \quad \xleftarrow{L^{II}_I}\rightarrow \quad \frac{1}{x+y}\frac{1}{Z_0}\,f_{\bar{P}_n}(\frac{x}{Z_0})f_{\bar{P}_s}(y). \qquad (C.10)$$

Here x can again be scaled to $Z_0 x$

$$Z_0\int_{u/Z_0}^\infty g^n(Z_0\lambda)g(v+\lambda-\frac{u}{Z_0})d\lambda \quad \xleftarrow{L^{II}_I}\rightarrow \quad \frac{Z_0}{Z_0 x+y}f_{\bar{P}_n}(x)f_{\bar{P}_s}(y). \qquad (C.11)$$

A $(\frac{-\partial}{\partial u})$ differentiation in the convergence area of the image corresponds to multiplication $(A.1.5)$ by the variable x of the original. First we differentiate the lower limit of the integral; a second term is generated by differentiating the integrand itself.

$$-g^n(u)g(v) + \int_{u/Z_0}^\infty g^n(Z_0\lambda)g'(v+\lambda\frac{-u}{Z_0})d\lambda \quad \xleftarrow{L^{II}_I}\rightarrow \quad \frac{Z_0 x}{Z_0 x+y}f_{\bar{P}_n}f_{\bar{P}_s}. \qquad (C.12)$$

At this moment $F_{z,n}$ equals the original integrated over the first quadrant. As can be seen from the definition of Laplace transformation, it also equals the image with $(u,v)=(0,0)$ substituted. After applying (4.4) we find

$$F_{z,n} \quad = \quad 1 \; + \; \int_0^\infty g^n(Z_0\lambda)g'(\lambda)d\lambda \qquad\qquad \text{(C.13a)}$$

or, after partial integration,

$$F_{z,n} = \quad -nZ_0 \int_0^\infty g(\lambda)g'(Z_0\lambda)g^{n-1}(Z_0\lambda)d\lambda \qquad\qquad \text{(C.13b)}$$

From this equation it was first noted that the probability $F_{z,n}$ of a destroying collision, given a receiver threshold $Z_0$ and a number of n interferers, can be stated purely in terms of the Laplace transform $g(.)$ of the mean packet power pdf $f_{\bar{P}_s}$.

● special case $Z_0=1$

For the receiver with perfect capture ($Z_0 =1$), $F_{z,n}$ can be calculated quite easily.

$$F_{z,n} = \quad -n \int_0^\infty g^n(\lambda)g'(\lambda)d\lambda \quad = \quad \frac{n}{n+1} \qquad\qquad \text{(C.14)}$$

In this case $F_{z,n}$ and therefore the average capture probability are independent of the power classification of the individual transmitters, e.g. spatial distribution will not increase channel throughput.

The average throughput of packets equals $1/_{n+1}$, which is just the probability for a test packet to be selected at random from a set with n other contenders.

With (C.13) we can find the total channel throughput S by using the series expansion of the exponential function after interchanging integration and summation.

$$S= G\left[1- \sum_{n=1}^\infty R_n F_{z,n}\right]= -G \; e^{-G} \int_0^\infty g'(\lambda)\exp\left\{Gg(Z_0\lambda)\right\} \, d\lambda \qquad\qquad \text{(C.15)}$$

• Extreme of the throughput curve (channel capacity)

The top of the throughput $S(G)$ curve can be found from

$$\frac{dS}{dG} = e^{-G} \int_0^\infty g'(\lambda) \exp\{Gg(Z_0\lambda)\}[G-1-Gg(Z_0\lambda)]d\lambda = 0 \qquad (C.16)$$

Attempts with examples have not led to an explicit expression
for $G_{top}$.

## C2.1.1    Mellin transforms

To consider alternative possibilities to evaluate the throughput
equations, we now return to equation (4.56):

$$F_{z,n} = \int_0^{Z_n} dz \int_0^\infty f_{P_s}(zw) f_{P_n}^a(w) wdw \qquad (=4.56)$$

The Mellin transformation yields image functions defined as

$$M_X(p) \triangleq \int_0^\infty x^{p-1} f(x) dx. \qquad (C.18)$$

Thus, if p a natural number and f(x) a pdf of a positive random
variable, then

$$M_X(p+1) = \mu_p. \qquad (C.19)$$

The integral over w of (4.56) can be written as a convolution [12,
par.12 (37)], in the Mellin transform domain.

$$M_{P_s}(p) \ M_{P_n}(2-p) \quad \xleftarrow{M} \quad \int_0^\infty f_{P_n}^a(zw) f_{P_s}(w) wdw, \qquad (C.20)$$

where $M_{P_s}$ and $M_{P_n}$ are the Mellin transforms of $f_{P_s}$ resp. $f_{P_n}$.

Integrating the original, with upper limit $Z_n$ gives the transform
pair (from $Z_n$ to p domain)

$$-\frac{1}{p} M_{P_s}(1+p) \ M_{P_n}(1-p) \quad \xleftarrow{M} \quad F_{z,n} \qquad (C.21)$$

C.2.2  Spatial distribution in the coherent case

For $I_{z,n}(\rho)$, an expression can be found, containing the Laplace transform $g^n(\cdot)$ of the pdf of $\bar{P}_n$. The aim of the next section is to start off with this $L^I_{I \text{ or } II}$ correspondence and again use mathematical operations upon the original pdf which lead to the integral $I_{z,n}(\rho)$ in $[1,(40)]$.

First the variable x is to be scaled to $x/Z_0$

$$g^n(Z_0 u) \qquad \xleftarrow{L^I_{I \text{ or } II}} \qquad \frac{1}{Z_0} f_{\bar{P}_n}(\frac{x}{Z_0}). \qquad (C.22)$$

The original can be translated over a distance $\rho^{-\beta}$. This correspondence can be derived from a $q=y-\rho^{-\beta}$ substitution of the dummy variable in definition (4.3). With this substitution the lower and upper limits are also translated, so the next correspondence is only valid for a two-sided transform where we integrate from $-\infty$ to $\infty$.

$$\exp\{-\rho^{-\beta}u\} \, g^n(Z_0 u) \qquad \xleftarrow{L^I_{II}} \qquad \frac{1}{Z_0} f_{\bar{P}_n}(\frac{x-\rho^{-\beta}}{Z_0}). \qquad (C.23)$$

At this point we integrate the image

$$\int_u^\infty \exp\{-\rho^{-\beta}\lambda\} \, g^n(Z_0 \lambda)d\lambda \qquad \xleftarrow{L^I_{II}} \qquad \frac{1}{Z_0 x} f_{\bar{P}_n}(\frac{x-\rho^{-\beta}}{Z_0}). \qquad (C.24)$$

The denominator $x+\rho^{-\beta}$ appears after a translation over $(-\rho^{-\beta})$

$$\exp\{\rho^{-\beta}u\} \int_u^\infty \exp\{-\rho^{-\beta}\lambda\}g^n(Z_0\lambda)d\lambda \qquad \xleftarrow{L^I_{I \text{ or } II}} \qquad \frac{1}{Z_0(x+\rho^{-\beta})} f_{\bar{P}_n}(\frac{x}{Z_0})$$

As the pdf of $\bar{P}_n$ is different from zero only for positive mean interference powers, the correspondence is again valid for both one- and two-sided transforms.

A $\left(-\frac{d}{dv}\right)$ differentiation of the image, using the product rule yields

$$e^0 g^n(Z_0 u) \quad -\rho^{-\beta} \int_u^\infty \exp\{\rho^{-\beta}(u-\lambda)\} g^n(Z_0\lambda) d\lambda \quad \overset{I}{\underset{\leftarrow I,II}{\rightarrow}} \quad \frac{x/Z_0}{x+\rho^{-\beta}} f_{\bar{P}_n}\left(\frac{x}{Z_0}\right)$$

Now by rescaling the variable x, we recover the integrand of $I_{z,n}(\rho)$ according to $[1,(40)]$

$$g^n(u) - \rho^{-\beta} \int_{u/Z_0}^\infty \exp\{\rho^{-\beta}(\frac{u}{Z_0}-\lambda)\} g^n(Z_0\lambda) d\lambda \quad \overset{I}{\underset{\leftarrow I,II}{\rightarrow}} \quad \frac{Z_0 x}{Z_0 x+\rho^{-\beta}} f_{\bar{P}_n}(x)$$

Taking the value at u=0 of the image gives $I_{z,n}(\rho)$ of (C.7) after applying (4.4) and (4.6)

$$I_{z,n}(\rho) \quad = \quad 1 \quad - \quad \rho^{-\beta} \int_0^\infty \exp\{-\rho^{-\beta}\lambda\} g^n(Z_0\lambda) d\lambda \qquad (C.25)$$

For practical calculation, a more often convenient form is

$$I_{z,n}(\rho) \quad = \quad 1 - \int_0^\infty e^{-\nu} g^n(Z_0\nu\rho^\beta) d\nu, \qquad (C.26)$$

where we have substituted $\lambda=\nu\rho^\beta$. This form can for instance be used with Gauss-Laguerre numerical integration.

Appendix D    ANOTHER EXAMPLE OF A SPATIAL DISTRIBUTION

A study by Joanna Fronczak [17] is interesting because the differences in mean power introduced here by spatial distribution are the same as the power differences by Rayleigh fading in the ring model. See section 4.2.1 example 4. Furthermore, this distribution is a valuable addition to the sections 6.7 and 6.8. As distinct from the ring model, in this example packets are received with different mean power, but the moments of the pdf remain bounded. The area mean power has a pdf

$$f_{\bar{P}_s}(\bar{p}_s) = h \ \exp\{-h\bar{p}_s\}. \tag{=4.16}$$

Using (1.14) this corresponds to

$$G(\rho) = \frac{G}{2\pi} \frac{4h}{\rho^6} \ \exp\{-h\rho^{-4}\} \tag{=4.17}$$

As shown in example 3 of chapter 4, the Laplace image of the mean packet power pdf is

$$g(v) = \frac{h}{v+h} \tag{=4.18}$$

The unconditional mean received power $\mu_1$ equals h. In section 4.1.3 we have chosen h=1.

D.1   Capture probability

We will initially discuss the throughput without assuming G to be large. $F_{z,n}$ can be found by using (4.57)

$$F_{z,n} = 1 - \frac{h^{n+2}}{z_0^n} \ \int_0^\infty \left(x + \frac{h}{z_0}\right)^{-n} \left(x + h\right)^{-2} dx$$

A Gaussian hypergeometric solution of this integral is given by [8, (3.197) on p 286]. We may calculate the total traffic throughput as given by (6.26)

$$S = G \exp\{-G\} \int_0^\infty \frac{h}{(\lambda+h)^2} \exp\{\frac{hG}{Z_0\lambda+h}\} \, d\lambda.$$

We substitute the inverse function $x \overset{\Delta}{=} g^+(v)$:

$$S = Z_0 G \exp\{-G\} \int_0^1 \frac{\exp\{Gx\} \, dx}{(1+(Z_0-1)x)^2}$$

$$= -Ge^{-G} \int_0^1 e^{Gx} \frac{d}{dx} \left(\frac{1}{1+(Z_0-1)x}\right) \frac{Z_0 dx}{Z_0-1}$$

After partial integration and applying [8,(3.352.1)] we find

$$S = \frac{Z_0 G}{Z_0-1} \left[ e^{-G} - \frac{1}{Z_0} + G \frac{\exp\{\frac{-GZ_0}{Z_0-1}\}}{Z_0-1} \left[ \mathrm{Ei}\left(\frac{Z_0 G}{Z_0-1}\right) - \mathrm{Ei}\left(\frac{G}{Z_0-1}\right) \right] \right] ,$$

with the exponential integral $\mathrm{Ei}(x) \overset{\Delta}{=} -\int_{-x}^\infty e^{-t} t^{-1} dt.$

The total traffic throughput can be written as the series expansion

$$S = G - G^2 Z_0 \left[\frac{Z_0-1-\ln Z_0}{(Z_0-1)^2}\right] + G^3 \left[\frac{Z_0}{Z_0-1}\right] \left(\frac{1}{2} - \frac{\ln Z_0 - Z_0 + 1}{(Z_0-1)^2}\right) - \cdots$$

The limit $S = 1 - e^{-G}$ can be derived by expansion of $\ln\{1+(Z_0-1)\}$ or by using l'Hôpital's rule.

## D.2 Conditional capture probability

The integral

$$I_{z,n}(\rho) = 1 - \int_0^\infty e^{-\lambda}\, h^4 (Z_0\rho^4\lambda + h)^{-n}\, d\lambda$$

is solved by using [8,(3.353.2) on p311]:

$$\int_0^\infty \frac{e^{-x}\, dx}{\left(x + \frac{h}{Z_0\rho^4}\right)^n} = \frac{1}{(n-1)!} \sum_{k=1}^{n-1} (k-1)!\,(-)^{n-k-1}\left(\frac{h}{Z_0\rho^4}\right)^k - \frac{(-)^{n-1}}{(n-1)!} e^{\frac{h}{Z_0\rho^4}}\, \mathrm{Ei}\left(\frac{-h}{Z_0\rho^4}\right)$$

with n>2.

With unity written as the n-th term of the summing we find

$$I_{z,n}(\rho) = \frac{h^n}{(n-1)!}\quad \left[ -\left(\frac{-1}{Z_0\rho^4}\right)^n \exp\left\{\frac{h}{Z_0\rho^4}\right\}\, \mathrm{Ei}\left\{\frac{-h}{Z_0\rho^4}\right\}\right.$$

$$\left. + \sum_{k=1}^{n} (k-1)!\left(\frac{-1}{Z_0\rho^4}\right)^{n-k} h^{-k}\right]$$

which has been derived by Fronczak [17,(13)].

## D.3 Spatial distribution of the traffic throughput

The throughput per normalised unit area is found directly from (6.3)

$$S(\rho) = Ge^{-G}\, e^{-h\rho^{-4}}\, \frac{2h}{\pi\, \rho^{10}} \int_0^\infty \exp\left\{-s\rho^{-4} + \frac{hG}{Z_0\left(s + \frac{h}{Z_0}\right)}\right\}\, ds.$$

A closed-form solution has not been found.

Appendix E

## ASYMPTOTIC EXPANSION BY PARTIAL INTEGRATION FOR LAPLACE INTEGRALS

For ease of notation we write:

$$\xi_n^m \overset{\Delta}{=} \{g^{(n)}(\lambda+v)\}^m$$

$$\zeta_n^m \overset{\Delta}{=} \{g^{(n)}(Z_0\lambda)\}^m$$

$$\chi \overset{\Delta}{=} \exp\{Gg(Z_0\lambda) - G\}$$

The coherent analysis equation (6.14) becomes

$$s(v) = \frac{-1}{Z_0} \int_{\lambda=0}^{\infty} \frac{\xi_1}{\zeta_1} \, d\chi .$$

Three steps of partial integration yield

$$s(v) = -\frac{\chi}{Z_0} \frac{\xi_1}{\zeta_1} \Big|_0^{\infty} + \frac{-1}{Z_0} \int_0^{\infty} \chi \frac{d}{d\lambda} \frac{\xi_1}{\zeta_1} \, d\lambda$$

$$= \frac{1}{Z_0} \frac{g'(v)}{g'(0)} + \int_0^{\infty} \frac{\xi_2\zeta_1 - Z_0\xi_1\zeta_2}{G \, Z_0^2 \, \zeta_1^3} \, d\chi$$

$$= \frac{-g'(v)}{Z_0\mu_1} + \chi \frac{\xi_2\zeta_1 - Z_0\xi_1\zeta_2}{G \, Z_0^2 \, \zeta_1^3} \Big|_0^{\infty} - \frac{1}{G^2Z_0^2} \int_0^{\infty} \frac{d}{d\lambda}\Big[\frac{\xi_2}{Z_0\zeta_1^2} + \frac{\xi_1\zeta_2}{\zeta_1^3}\Big] \frac{1}{\zeta_1} d\chi$$

$$= \frac{-g'(v)}{Z_0\mu_1} - \frac{g''(v)}{GZ_0^2\mu_1^2} - \frac{g'(v)}{GZ_0} \frac{\mu_2}{\mu_1^3}$$

$$\quad - \frac{1}{G^2Z_0^2} \int_0^{\infty} \Big[\frac{\xi_3\zeta_1^2 - 2Z_0\xi_2\zeta_1\zeta_2}{Z_0\zeta_1^5} + \frac{\xi_2\zeta_2\zeta_1^3 + Z_0\xi_1\zeta_3\zeta_1^3}{\zeta_1^7} - \frac{3Z_0\xi_1\zeta_2^2\zeta_1^2}{\zeta_1^7}\Big]d\chi$$

$$= -\frac{g'(v)}{Z_0\mu_1} - \frac{g''(v)}{GZ_0^2\mu_1^2} - \frac{g'(v)}{G\,Z_0}\frac{\mu_2}{\mu_1^3} - \frac{g'''(v)}{G^2Z_0^3\mu_1^3} - \frac{g''(v)}{G^2Z_0^2}\frac{\mu_2}{\mu_1^4} - \frac{g'(v)}{G^2Z_0}\frac{\mu_3}{\mu_1^4}$$

$$\quad + 3\frac{g'(v)}{G^2Z_0}\frac{\mu_2^2}{\mu_1^5} + \int_0^{\infty} \ldots\ldots \, d\chi$$

which is used in (6.24)

## REFERENCES

[1] Arnbak, J.C. and W. van Blitterswijk
CAPACITY OF SLOTTED ALOHA IN RAYLEIGH FADING CHANNELS.
IEEE J. Sel. Areas Commun., Vol. SAC-5(1987), to be published.

[2] Metzner, J.J.
ON IMPROVING UTILIZATION IN ALOHA NETWORKS.
IEEE Trans. Commun., Vol. COM-24(1976), p. 447-448.

[3] Abramson, N.
THE THROUGHPUT OF PACKET BROADCASTING CHANNELS.
IEEE Trans. Commun., Vol. COM-25(1977), p. 117-128.

[4] Voelker, D. und G. Doetsch
DIE ZWEIDIMENSIONALE LAPLACE-TRANSFORMATION: Eine Einführung in ihre
Anwendung zur Lösung von Randwertproblemen nebst Tabellen von Korrespondenzen.
Basel: Birkhäuser, 1950.
Lehrbücher und Monographien aus dem Gebiete der exakten Wissenschaften:
Mathematische Reihe, Band 12.

[5] Doetsch, G.
HANDBUCH DER LAPLACE-TRANSFORMATION. Band 1: Theorie der Laplace-Transformation.
Basel: Birkhäuser, 1950.
Lehrbücher eun Monographien aus dem Gebiete der exakten Wissenschaften:
Mathematische Reihe, Band 14.

[6] Doetsch, G.
EINFÜHRUNG IN THEORIE UND ANWENDUNG DER LAPLACE-TRANSFORMATION: Ein Lehrbuch
für Studierende der Mathematik, Physik und Ingenieurwissenschaft. 2. Aufl.
Basel: Birkhäuser, 1970.
Lehrbücher und Monographien aus dem Gebiete der exakten Wissenschaften:
Mathematische Reihe, Band 24.

[7] HANDBOOK OF MATHEMATICAL FUNCTIONS. Ed. by M. Abramowitz and I.A. Stegun.
New York: Dover, 1965.

[8] Gradshteyn, I.S. and I.M. Ryzhik
TABLE OF INTEGRALS, SERIES AND PRODUCTS. 4th ed.
New York: Academic Press, 1965.

[9] TABLES OF INTEGRAL TRANSFORMS, Vol. 1. Based, in part, on notes left by
H. Bateman. Ed. by A. Erdélyi et al.
New York: McGraw-Hill, 1954.
California Institute of Technology Bateman Manuscript Project

[10] Hansen, F. and F.I. Meno
MOBILE FADING - RAYLEIGH AND LOGNORMAL SUPERIMPOSED.
IEEE Trans. Veh. Technol., Vol. VT-26(1977), p. 332-335.

[11] MICROWAVE MOBILE COMMUNICATIONS. Ed. by W.C. Jakes.
New York: Wiley, 1974.

[12] Davies, B.
INTEGRAL TRANSFORMS AND THEIR APPLICATIONS.
New York: Springer, 1978.
Applied mathematical sciences, Vol. 25.

[13] Verhulst, D. and M. Mouly, J. Szpirglas
SLOW FREQUENCY HOPPING MULTIPLE ACCESS FOR DIGITAL CELLULAR RADIOTELEPHONE.
IEEE J. Sel. Areas Commun., Vol. SAC-2(1984), p. 563-574.

[14] Boomars, J.L.M.
THE DISTRIBUTION FUNCTION OF INTERFERENCE AND BLOCKING CHANCES IN A CELLULAR
RADIO SYSTEM.
In: Proc. 2nd Int. Conf. on Radio Spectrum Conservation Techniques,
Birmingham, 6-8 Sept. 1983.
London: Institution of Electrical Engineers, 1983.
IEE Conference Publication, No. 224. P. 80-84.

[15] Menges, G.
GRUNDRISS DER STATISTIK. Teil 1: Theorie.
Köln und Opladen: Westdeutscher Verlag, 1968. P. 225.

[16]     Loève, M.
         PROBABILITY THEORY I. 4th ed.
         Berlin: Springer, 1977.
         Graduate texts in mathematics, Vol. 45.

[17]     Fronczak, J.
         DATA COMMUNICATIONS IN THE MOBILE RADIO CHANNEL.
         Department of Electrical Engineering, Eindhoven University of Technology, 1983.
         EUT Report 83-E-142

[18]     Colombo, S. et J. Lavoine
         TRANSFORMATIONS DE LAPLACE ET DE MELLIN: Formulaires. Mode d'utilisation.
         Paris: Gauthier-Villars, 1972.
         Mémorial des sciences mathématiques, fascicule 169.

[19]     Whitehead, J.F.
         CELLULAR SYSTEM DESIGN: An emerging engineering discipline.
         IEEE Commun. Mag., Vol. 24, No. 2(Febr. 1986), p. 8-15.

[20]     Preller, H.G. and W. Koch
         MATS-E: An advanced 900 MHz cellular radio telephone system. Description,
         performance, evaluation, and field measurements.
         IEEE Commun. Mag., Vol. 24, No. 2(Febr. 1984), p. 30-39.

[21]     Cohen, P. and H.-H. Hoang, D. Haccoun
         TRAFFIC CHARACTERIZATION AND CLASSIFICATION OF USERS OF LAND MOBILE
         COMMUNICATION CHANNELS.
         IEEE Trans. Veh. Technol., Vol. VT-33(1984), p. 276-284.

[22]     Sinha, R. and S.C. Gupta
         MOBILE PACKET RADIO NETWORKS: State-of-the-art.
         IEEE Commun. Mag., Vol. 23, No. 3(March 1985), p. 53-61.
         (Reprinted from GLOBECOM 1983).

[23]     Gosling, W.
         PROTECTION RATIO AND ECONOMY OF SPECTRUM USE IN LAND MOBILE RADIO.
         IEE Proc. F, Vol. 127(1980), p. 174-178.

[24]     Namislo, C.
         ANALYSIS OF MOBILE RADIO SLOTTED ALOHA NETWORKS.
         IEEE J. Sel. Areas Commun., Vol. SAC-2(1984), p. 583-588.

[25]     Daikoku, K. and H. Ohdate
         OPTIMAL DESIGN FOR CELLULAR MOBILE SYSTEMS.
         IEEE Trans. Veh. Technol., Vol. VT-34(1985), p. 3-12.

[26]     Oetting, J.
         CELLULAR MOBILE RADIO: An emerging technology.
         IEEE Commun. Mag., Vol. 21, No. 8(Nov. 1983), p. 10-15.

[27]     French, R.C.
         THE MOBILE RADIO DATA CHANNEL.
         In: Proc. 6th Int. Zurich Seminar on Digital Communications: Digital
         transmission in wireless systems, Zürich, 4-6 March 1980.
         Zürich: Institut für Fernmeldetechnik, ETH, 1980. Paper D1.

[28]     Stocker, A.C.
         SMALL-CELL MOBILE PHONE SYSTEMS.
         IEEE Trans. Veh. Technol., Vol. VT-33(1984), p. 269-275

[29]     Gamst, A. and R. Beck, R. Simon, E.-G. Zinn
         AN INTEGRATED APPROACH TO CELLULAR RADIO NETWORK PLANNING.
         In: Proc. 35th IEEE Vehicular Technology Conf., Boulder, Colo.,
         21-23 May 1985.
         New York: IEEE, 1985. P. 21-25.

[30]     Halpern, S.W.
         REUSE PARTITIONING IN CELLULAR SYSTEMS.
         In: Proc. 33rd IEEE Vehicular Technology Conf., Toronto, Ont.,
         25-27 May 1983.
         New York: IEEE, 1983. P. 322-327.

[ 31]   Lorenz, R.W.
        FREQUENCY PLANNING OF CELLULAR RADIO BY THE USE OF A TOPOGRAPHICAL DATA
        BASE.
        In: Proc. 35th IEEE Vehicular Technology Conf., Boulder, Colo.,
        21-23 May 1985.
        New York: IEEE, 1985. P. 1-5

[ 32]   Henry, P.S. and B.S. Glance
        A NEW APPROACH TO HIGH-CAPACITY DIGITAL MOBILE RADIO.
        Bell Syst. Tech. J., Vol. 60(1981), p. 1891-1904.

[ 33]   Bomy, D. and K. Mouline
        GESTION DE FLOTTES DE VEHICULES PAR RADIOTELEPHONE.
        Onde Electr., Vol. 64, No. 3(Mai-Juin 1984), p. 47-53.

[ 34]   DaSilva, J.S. and H.M. Hafez, S.A. Mahmoud
        OPTIMAL PACKET LENGTH FOR FADING LAND MOBILE DATA CHANNELS.
        In: ICC'80 Conf. Record, 16th Int. Conf. on Communications, Seattle, Wash.,
        8-12 June 1980.
        New York: IEEE, 1980. Paper 61.3.

[ 35]   Kuperus, F. and J.C. Arnbak
        PACKET RADIO IN A RAYLEIGH FADING CHANNEL.
        Electron. Lett., Vol. 18(1982), p. 506-507.

[ 36]   Montgomery, G.F.
        A COMPARISON OF AMPLITUDE AND ANGLE MODULATION FOR NARROW-BAND
        COMMUNICATION FOR BINARY-CODED MESSAGES IN FLUCTUATION NOISE.
        Proc. IRE, Vol. 42(1954), p. 447-454.

[ 37]   French, R.C.
        ERROR RATE PREDICTIONS AND MEASUREMENTS IN THE MOBILE RADIO DATA CHANNEL.
        IEEE Trans. Veh. Technol., Vol. VT-27(1978), p. 110-116.

[ 38]   Bender, C.M. and S.A. Orszag
        ADVANCED MATHEMATICAL METHODS FOR SCIENTISTS AND ENGINEERS.
        New York: McGraw-Hill, 1978.
        International series in pure and applied mathematics. Chapter 6.3.

[ 39]   LAND MOBILE RADIO SYSTEMS. Ed. by R.J. Holbeche.
        London: Peter Peregrinus, 1985.
        IEE telecommunications series, Vol. 14.

[ 40]   Oetting, J.D.
        A COMPARISON OF MODULATION TECHNIQUES FOR DIGITAL RADIO.
        IEEE Trans. Commun., Vol. COM-27(1979), p. 1752-1762.

[ 41]   Guttman, I. and S.S. Wilks, J.S. Hunter
        INTRODUCTORY ENGINEERING STATISTICS. 3rd ed.
        New York: Wiley, 1982. Wiley series in probability and mathematical statistics.

[ 42]   MOBIELE COMMUNICATIE, KIVI Leergang, Eindhoven, 6-7 april 1983.
        's-Gravenhage: Koninklijk Instituut van Ingenieurs, 1983.

[ 43]   Kleinrock, L.
        QUEUEING SYSTEMS. Vol. 1: Theory.
        New York: Wiley, 1975.

[ 44]   Kleinrock, L.
        QUEUEING SYSTEMS. Vol. 2: Computer applications.
        New York: Wiley, 1976. P. 362-365.

(149) Beeckman, P.A.
MILLIMETER-WAVE ANTENNA MEASUREMENTS WITH THE HP8510 NETWORK ANALYZER.
EUT Report 85-E-149. 1985. ISBN 90-6144-149-8

(150) Meer, A.C.P. van
EXAMENRESULTATEN IN CONTEXT MBA.
EUT Report 85-E-150. 1985. ISBN 90-6144-150-1

(151) Ramakrishnan, S. and W.M.C. van den Heuvel
SHORT-CIRCUIT CURRENT INTERRUPTION IN A LOW-VOLTAGE FUSE WITH ABLATING WALLS.
EUT Report 85-E-151. 1985. ISBN 90-6144-151-X

(152) Stefanov, B. and L. Zarkova, A. Veefkind
DEVIATION FROM LOCAL THERMODYNAMIC EQUILIBRIUM IN A CESIUM-SEEDED ARGON PLASMA.
EUT Report 85-E-152. 1985. ISBN 90-6144-152-8

(153) Hof, P.M.J. Van den and P.H.M. Janssen
SOME ASYMPTOTIC PROPERTIES OF MULTIVARIABLE MODELS IDENTIFIED BY EQUATION ERROR TECHNIQUES.
EUT Report 85-E-153. 1985. ISBN 90-6144-153-6

(154) Geerlings, J.H.T.
LIMIT CYCLES IN DIGITAL FILTERS: A bibliography 1975-1984.
EUT Report 85-E-154. 1985. ISBN 90-6144-154-4

(155) Groot, J.F.G. de
THE INFLUENCE OF A HIGH-INDEX MICRO-LENS IN A LASER-TAPER COUPLING.
EUT Report 85-E-155. 1985. ISBN 90-6144-155-2

(156) Amelsfort, A.M.J. van and Th. Scharten
A THEORETICAL STUDY OF THE ELECTROMAGNETIC FIELD IN A LIMB, EXCITED BY ARTIFICIAL SOURCES.
EUT Report 86-E-156. 1986. ISBN 90-6144-156-0

(157) Lodder, A. and M.T. van Stiphout, J.T.J. van Eijndhoven
ESCHER: Eindhoven SCHematic EditoR reference manual.
EUT Report 86-E-157. 1986. ISBN 90-6144-157-9

(158) Arnbak, J.C.
DEVELOPMENT OF TRANSMISSION FACILITIES FOR ELECTRONIC MEDIA IN THE NETHERLANDS.
EUT Report 86-E-158. 1986. ISBN 90-6144-158-7

(159) Wang Jingshan
HARMONIC AND RECTANGULAR PULSE REPRODUCTION THROUGH CURRENT TRANSFORMERS.
EUT Report 86-E-159. 1986. ISBN 90-6144-159-5

(160) Wolzak, G.G. and A.M.F.J. van de Laar, E.F. Steennis
PARTIAL DISCHARGES AND THE ELECTRICAL AGING OF XLPE CABLE INSULATION.
EUT Report 86-E-160. 1986. ISBN 90-6144-160-9

(161) Veenstra, P.K.
RANDOM ACCESS MEMORY TESTING: Theory and practice. The gains of fault modelling.
EUT Report 86-E-161. 1986. ISBN 90-6144-161-7

(162) Meer, A.C.P. van
TMS32010 EVALUATION MODULE CONTROLLER.
EUT Report 86-E-162. 1986. ISBN 90-6144-162-5

(163) Stok, L. and R. van den Born, G.L.J.M. Janssen
HIGHER LEVELS OF A SILICON COMPILER.
EUT Report 86-E-163. 1986. ISBN 90-6144-163-3

(164) Engelshoven, R.J. van and J.F.M. Theeuwen
GENERATING LAYOUTS FOR RANDOM LOGIC: Cell generation schemes.
EUT Report 86-E-164. 1986. ISBN 90-6144-164-1

(165) Lippens, P.E.R. and A.G.J. Slenter
GADL: A Gate Array Description Language.
EUT Report 87-E-165. 1987. ISBN 90-6144-165-X

(166) Dielen, M. and J.F.M. Theeuwen
AN OPTIMAL CMOS STRUCTURE FOR THE DESIGN OF A CELL LIBRARY.
EUT Report 87-E-166. 1987. ISBN 90-6144-166-8

(167) Oerlemans, C.A.M. and J.F.M. Theeuwen
ESKISS: A program for optimal state assignment.
EUT Report 87-E-167. 1987. ISBN 90-6144-167-6

(168) Linnartz, J.P.M.G.
SPATIAL DISTRIBUTION OF TRAFFIC IN A CELLULAR MOBILE DATA NETWORK.
EUT Report 87-E-168. 1987. ISBN 90-6144-168-4

(169) Vinck, A.J. and J. Pineda de Gyvez, K.A. Post
IMPLEMENTATION AND EVALUATION OF A COMBINED TEST-ERROR CORRECTION PROCEDURE FOR MEMORIES WITH DEFECTS.
EUT Report 87-E-169. 1987. ISBN 90-6144-169-2